

Hidden Group Time Profiles: Heterogeneous Drawdown Behaviours in Retirement

Igor Balnozan^{*†}, Denzil G. Fiebig^{*}, Anthony Asher^{*}, Robert Kohn^{*}, Scott A. Sisson^{*}

Version: 7 December 2021

Abstract

This article investigates retirement decumulation behaviours using the Grouped Fixed-Effects (GFE) estimator applied to Australian panel data on drawdowns from phased withdrawal retirement income products. Behaviours exhibited by the distinct latent groups identified suggest that retirees may adopt simple heuristics determining how they draw down their accumulated wealth. Two extensions to the original GFE methodology are proposed: a latent group label-matching procedure which broadens bootstrap inference to include the time profile estimates, and a modified estimation procedure for models with time-invariant additive fixed effects estimated using unbalanced data.

Keywords

Panel data, discrete heterogeneity, microeconomics, retirement

JEL codes

C51, D14, G40

Acknowledgements

Balnozan is grateful for the support provided by the Commonwealth Government of Australia through the provision of an Australian Government Research Training Program Scholarship, and to State Super for provision of the State Super Academic Scholarship. Balnozan, Kohn and Sisson are partially supported by the Australian Research Council through the Australian Centre of Excellence in Mathematical and Statistical Frontiers (ACEMS; CE140100049). We thank Plan For Life, Actuaries & Researchers, who collected, cleaned and allowed us to analyse the data used in this research; this data capture forms one part of a broader survey into retirement incomes, commissioned by the Institute of Actuaries of Australia. This research includes computations using the computational cluster Katana supported by Research Technology Services at UNSW Sydney. Katana DOI: 10.26190/669x-a286

Conflict of interest statement

The authors have no conflict of interest to declare.

^{*}University of New South Wales, UNSW Sydney, NSW 2052, Australia.

[†]Correspondence: i.balnozan@unsw.edu.au / West Lobby Level 4, UNSW Business School Building, UNSW Sydney, NSW 2052, Australia.

1 Introduction

The importance and prevalence of preference heterogeneity is a pervasive feature of microeconomic modelling. Such heterogeneity is usually unobserved, remaining unexplained after controlling for the observable characteristics of individuals. Where the effects of unobservables have clear economic interpretations, methods of identifying latent groups of individuals that share common behaviours can provide insights into economic phenomena.

There is a need to improve understanding of the behaviours of retirees who fund their consumption by drawing down savings accumulated in personal Defined Contribution accounts. Such understanding can inform appropriate financial advice and product development. Existing theoretical work by [Bateman and Thorp \(2008\)](#) gives reason to expect distinct behavioural groups, where group behaviours correspond to strategies that individuals employ when accessing their retirement savings using phased withdrawal products.

This article investigates drawdown behaviours in phased withdrawal retirement income products by studying latent time profiles estimated using the Grouped Fixed-Effects (GFE) estimator of [Bonhomme and Manresa \(2015\)](#). Of primary interest is testing for the presence of multiple behavioural groups in the data, and characterising any groups found. Furthermore, in this application, using the GFE estimator also allows testing whether retirees were heterogeneous in their responses to the Global Financial Crisis and retirement incomes policy changes, demonstrating the value of the GFE estimator to such event studies.

In the presence of group-level time-varying unobservable heterogeneity, using the standard two-way fixed-effects (2WFE) model, defined in Section 4, generally gives biased covariate effect estimates and unrepresentative time effect estimates. This is what the present study finds: estimates for the time effects in the standard 2WFE model, which allows for only one set of time effects, obscure the different latent group-level effects which suggest retirees may adopt simple, distinct heuristics when determining how they draw down their accumulated wealth during retirement. The importance of this comparison with the 2WFE model results motivates our modification to the GFE estimator, described in Section 4.

A key novelty in this application of the GFE estimator is the focus on performing statistical inference on the estimated effects of the latent heterogeneity. To robustify the GFE estimator in this scenario, this article proposes an extension to the bootstrap method outlined in the Online Supplement to [Bonhomme and Manresa \(2015\)](#). While these authors describe a procedure for using the bootstrap to obtain standard errors for covariate effects, a group label switching problem prevents finding standard errors for the effects of group-level time-varying unobservable heterogeneity. A method to match group labels across independent GFE estimations is required so that the bootstrap can also explore uncertainty in the latent heterogeneity effect estimates.

Related to this, the fixed- T variance estimate formula given in the supplement to [Bonhomme and Manresa \(2015\)](#) provides an alternative approach to performing inference on the effects

of the latent heterogeneity, where T is the maximum number of observations on each unit in the sample. The proposed label-matching method also allows studying the properties of the standard errors for the latent group effects derived from this analytical formula, by observing their distribution across a large number of simulated datasets. This is useful in determining the potential applicability of the analytical formula for obtaining standard errors of the latent group effects in finite samples, explored in the Online Supplement to this article.

The rest of the paper is organised as follows. Section 2 summarises the literature to which this article contributes. Section 3 describes the available data for our application to retirement decumulation behaviours. Section 4 outlines the GFE estimator from [Bonhomme and Manresa \(2015\)](#), and explains our proposed extensions. Section 5 presents the main results from applying the GFE estimator to the available data. Section 6 concludes by examining the implications for retirement incomes research and policy. This article has an Online Supplement which provides robustness checks, a simulation exercise, descriptive analysis of the data, and further details on the second proposed methodological extension.

2 Related literature

2.1 Drawdown behaviours in phased withdrawal retirement income products

Recent work studying drawdown behaviours builds on [Horneff, Maurer, Mitchell, and Dus \(2008\)](#). These authors compare three rate-based drawdown strategies against a level guaranteed lifetime annuity, using a model of retiree utility that incorporates stochastic interest returns and retiree lifetimes. The first strategy draws a fixed proportion of the account balance each year; the second determines a terminal time horizon T and draws a proportion $1/T$ of the account balance in the first year, $1/(T - 1)$ in the second year, and so on, continuing until the T^{th} year of the plan when all the remaining funds are drawn down; the third draws a proportion of the balance that updates each year based on the surviving retiree’s expected remaining lifetime.

[Bateman and Thorp \(2008\)](#) extend [Horneff et al. \(2008\)](#), motivated by newly legislated minimum annual drawdown rates for a phased withdrawal retirement income product in Australia known as the account-based pension. Table 1 details these age-based rates, which start at 4% of the account balance for retirees under age 65, and increase as a step function of age to a maximum of 14% for retirees aged 95 or above; these are specified in Schedule 7 of the Superannuation Industry (Supervision) Regulations 1994. The rates, when applied to a retiree’s account balance at the start of the relevant financial year, give the dollar amount the retiree must draw down from their account during that financial year.

Table 1: Minimum drawdown rates by age for account-based pensions, effective 1 July 2007.

Age at financial year start	<65	65–74	75–79	80–84	85–89	90–94	95+
Minimum drawdown rate	0.04	0.05	0.06	0.07	0.09	0.11	0.14

Bateman and Thorp (2008) use a stochastic lifecycle model to compare five drawdown strategies. Three are based on Horneff et al. (2008); the remaining two are based on legislated minimum drawdown rates in Australia: always drawing at the newly legislated minimum drawdown rates effective from 1 July 2007;¹ and drawing at the minima previously in effect. Bateman and Thorp (2008) also use their model to derive the implied optimal drawdown plan, and examine the sensitivity of these results to changes in the model assumptions. The fixed-rate strategy they consider draws a fixed proportion of the remaining account balance each year, where this fixed proportion is the annuity payout rate the retiree would have received in the market at the time of writing by purchasing a guaranteed lifetime annuity using their account balance at retirement. The authors find that while the newly legislated minima outperform the second and third rate-based strategies of Horneff et al. (2008) described earlier, in most cases, simulated utility is increased by initially drawing at a fixed rate higher than the minimum, then switching to the new minimum drawdown schedule once the minimum rate rises higher than the fixed rate.

Based on this theoretical literature alone, researchers can expect, *a priori*, that analysing drawdowns data will reveal groups of retirees exhibiting distinct drawdown behaviours based on simple rules, or heuristics. The present article uses recent advances in panel data methods to empirically investigate whether such groups exist, and if so, what behaviours they display. Section 2.2 summarises recent methodological progress in panel data econometrics.

2.2 Capturing time-varying unobserved heterogeneity

Bonhomme and Manresa (2015) present the Grouped Fixed-Effects (GFE) estimator and apply it to a linear panel data model that allows for group-level time-varying unobserved heterogeneity and unknown group membership. Importantly, their method allows for correlation between the latent group effects and the observed regressors. Being able to control for, and estimate, the varying latent group time profiles is the key advantage of using this model over the traditional fixed-effects model, which captures only time-constant unit-level unobservable heterogeneity.

Factor-model approaches to capturing unobserved heterogeneity (e.g., Bai, 2009; Su & Ju, 2018) provide more flexible specifications for the individual-specific heterogeneity. These models assume the presence of common, but unobserved, time-varying factors to which individuals respond heterogeneously. Bonhomme and Manresa (2015) show that their linear panel model, to which they apply the GFE estimator, is a special type of latent-factor model, where the latent factors are group-specific time effects and the factor loadings are group membership indicator variables. In applications where group time profiles are of economic interest, having this interpretation of the time-varying unobservable heterogeneity is an advantage of using the GFE estimator over a factor-model approach. Furthermore, compared to competing latent-factor model methods, the GFE estimator converges faster to the true parameter values with T , and so has better finite-sample performance (Bonhomme & Manresa, 2015). This makes

¹Superannuation Industry (Supervision) Amendment Regulations 2007 (No. 1) Schedule 3.

GFE the preferred estimator when analysing a typical microeconomic panel, which may have a large number of units N , but rarely more than a moderate length T .

A related research area concerns finite mixture models, which can incorporate unobservable heterogeneity when the heterogeneity is constant over time. Finite mixture models are parsimonious solutions to modelling unobserved heterogeneity in populations, wherein data from latent subpopulations can be drawn from different distributions, and the true allocation of specific individuals to subpopulations is unobserved. [Deb and Trivedi \(2013\)](#) develop finite mixture models with time-constant fixed effects. Critically, these models cannot specify the likelihood of being in a particular group as a function of the covariates. By contrast, one of the primary advantages of using the GFE estimator over a standard 2WFE model estimator is the ability to control for correlation between latent group effects and the included covariates. Mixture-of-experts models (e.g., [Jacobs, Jordan, Nowlan, & Hinton, 1991](#); [Jordan & Jacobs, 1994](#)) generalise mixture models by parametrically specifying a link between group identity and covariate values; however, these models do not control for unit-level fixed effects in panel data.

The discussion above suggests that the GFE estimator is the most appropriate for the present application, because: the available dataset only has a moderate panel length T ; a review of the theoretical drawdowns literature suggests that there may be a finite number of distinct behavioural groups in the population, consistent with the GFE assumption that there are a finite number of latent group time profiles; the time profiles recovered by the GFE estimator are likely to have economically meaningful interpretations.

3 Data on superannuation drawdowns

The available superannuation dataset contains information on drawdowns from account-based pensions (ABPs), a phased withdrawal retirement income product in Australia. Using ABPs, retirees generate personal income streams or receive lump-sum payments by drawing down their accumulated savings during retirement. Throughout, the balance remains invested in financial markets based on each retiree’s chosen combination of safe and risky exposures.

Following the Global Financial Crisis (GFC), the Australian government introduced temporary minimum drawdown rate reductions as per Schedule 7 of the Superannuation Industry (Supervision) Regulations 1994. These resulted in ‘concessional’ minimum drawdown rates, which came into effect for the financial year ended 30 June 2009. For financial years 2009–2011 inclusive, the reduction was 50%, so that any retiree’s minimum drawdown rate over this period was halved relative to the standard schedule in [Table 1](#). For financial years 2012 and 2013, the reduction decreased to 25%, meaning the minimum drawdown rates were three-quarters of those given in the table. For subsequent financial years, the rates returned to their nominal values.

To generate an income stream from an ABP, retirees can elect a payment amount and a frequency, for example \$1000 monthly, which the superannuation fund follows in paying the re-

tiree from their account balance. This type of drawdown, which is specified by the beginning of a given financial year, is referred to here as a ‘regular’ drawdown, and is the primary object of interest in this study. These regular drawdowns are distinct from ‘ad-hoc’ drawdowns, referring to any additional lump-sum payments requested by the retiree during the financial year. A rigorous analysis of ad-hoc drawdowns is crucial in understanding retirees’ needs for flexibility and insurance, but is not the focus of this paper.

The dependent variable studied here is $y_{it} := \ln DR_{it}$; DR_{it} is the rate of drawdown for retiree i over financial year t , which is a ratio of the regular drawdown amount over the account balance: $DR_{it} := DA_{it}/AB_{it}$. The dependent variable is the logarithm of this rate because the raw rate variable is strictly positive and right-skewed. Appendix A gives further details on the relationship between the drawdown rate and the account balance, as well as histograms of the dependent variable and the raw rate variable.

Qualitatively, one interpretation of the drawdown rate is the speed at which retirees deplete their accumulated savings throughout retirement. In ABPs, retirees are exposed to the risk of outliving their savings and their retirement income becoming reliant on non-superannuation assets or taxpayer-funded transfer payments known as the age pension. Policy and product design should support retiree needs for regular income, and so understanding the drawdown behaviours that manifest in this flexible withdrawal product has the potential to inform policymakers, financial advisors and superannuation fund trustees.

The superannuation dataset contains $N = 9516$ individuals, combining source data from multiple large industry and retail superannuation funds. Due to the small number of funds in the sample whose data permitted determining the regular drawdown rate, the economic results in this paper may not be representative of the Australian superannuation system as a whole.

The data capture window spans the financial years 2004 to 2015 inclusive, for $T = 12$ annual observations. The main results use a balanced subset of each superannuation fund’s data, removing individuals with missing observations. However, as the data capture window is not the same for each fund, when combining these balanced subsets, the resulting dataset is unbalanced. The Online Supplement shows that the results are robust to using a fully balanced subsample of all the available data.

Individuals recorded as dying during the sample observation period do not appear in the data analysed. For some records, obtaining regular and ad-hoc drawdown amounts requires inputting these as estimates based on observed total drawdown amounts using a method which, in periods where the retiree makes an ad-hoc drawdown, may underestimate the amount of the ad-hoc drawdown; this affects fewer than 2.4% of the records in the sample.

The superannuation dataset is derived from administrative data, and so has limited demographic information on members. Table 2 provides summary statistics for characteristics that vary across individuals but not time; Table 3 summarises the time-varying variables in the dataset. The two covariates considered are the minimum drawdown rate for each individ-

ual at each time point, and their account balance at the beginning of the respective financial year, both on the log scale. Thus the model, with regular drawdown rate on the log scale as the dependent variable, estimates the elasticity of the regular drawdown rate with respect to the minima and account balances. The remainder of the variation in log regular drawdown rates is attributed to the latent group effects estimated by the GFE procedure, and residual noise.

The lack of demographic information, particularly health and marital status, is also a data-based motivation for using GFE as an estimation procedure. These unobserved characteristics are a potential source of omitted variable bias; they are possibly correlated with the dependent variable as well as the included covariates. Because relevant characteristics such as health and marital status may vary over time, controlling for time-constant unobserved heterogeneity by using a standard fixed-effects model may not remove the biasing effect of all relevant unobservables. For this reason, a model allowing for sources of time-varying unobserved heterogeneity, such as the linear panel model to which the GFE estimator is applied, may be more appropriate; the results in Section 5.1 provide evidence for this proposition.

4 Methodology

4.1 The Grouped Fixed-Effects (GFE) Estimator

The GFE estimator introduced by [Bonhomme and Manresa \(2015\)](#) considers a linear model of the form

$$y_{it} = x'_{it}\theta + \alpha_{g_{it}} + v_{it}; \tag{1}$$

in our application $i = 1, 2, \dots, N$ indexes individual retirees; $t = 1, 2, \dots, T$ indexes financial years; y_{it} is the dependent variable; x_{it} is a vector of covariates; θ are the partial effects of covariates on the dependent variable after controlling for group-level time profiles; $g_i = 1, 2, \dots, G$ identifies the group membership for unit i , where G is the chosen number of latent groups in the sample; $\alpha_{g_{it}}$ is a term representing time-varying, group-specific unobserved heterogeneity—these are time-varying model intercepts that can differ across individuals, depending on the value of the individual’s group identifier, g_i ; v_{it} represents the residual effect of all other unobserved determinants of the dependent variable.

For the estimator consistency and asymptotic Normality results of [Bonhomme and Manresa \(2015\)](#) to apply, the distribution of the errors, v_{it} , must have finite fourth moment and be uncorrelated with the covariates, x_{it} ; errors can be correlated across cross-sectional units if there is a finite limit on the magnitude of the correlation; the unit-level time-sequences of errors can be autocorrelated if the sequences are strongly mixing processes; the tails of the error distribution must exhibit a faster-than-polynomial decay rate. The time profile values, $\alpha_{g_{it}}$, may be correlated with x_{it} but not v_{it} . For the complete list of assumptions required for the GFE estimator, see [Bonhomme and Manresa \(2015\)](#), pp. 1156–1159.

The linear model in (1) can be extended to include time-constant, individual-specific fixed

Table 2: Summary statistics – Time-invariant variables.

	Age at 31 December 2015	Age at Account Open	Sex: Male	Risk Appetite
mean	79.4	63.57	0.56	0.41
SD	5.22	4.17	0.5	0.21
median	79.78	64.23	1	0.46
Q1	76.37	60.9	0	0.25
Q3	83.03	65.39	1	0.54
min	60.66	48.48	0	0
max	101.46	85.44	1	1.88
count	9516	9516	9516	9507

The age at 31 December 2015 represents the individual’s cohort, equivalent to measuring a year-of-birth variable. The age at account opening is the age when the retiree initiates a phased withdrawal product and begins drawing down from the account. The sex indicator variable equals 1 if the retiree is male, and 0 otherwise. The risk appetite variable is a proxy for the returns in the account relative to the reference S&P/ASX 200 index; see Online Supplement for details. SD refers to the sample standard deviation of the variable. Q1 and Q3 refer to the empirical 25th and 75th percentiles, respectively.

Table 3: Summary statistics – Time-varying variables.

	Regular Drawdown Rate	Regular Drawdown Amount	Ad-hoc Drawdown Indicator	Ad-hoc Drawdown Rate	Ad-hoc Drawdown Amount	Account Balance
mean	0.12	6435.91	0.07	0.15	10,216.56	72,686.55
SD	0.12	6121.76	0.25	0.21	24,672.68	78,721.39
median	0.09	4800	0	0.07	4655.9	52,063
Q1	0.07	2992	0	0.02	1132.33	30,532.5
Q3	0.12	7728	0	0.18	10,000	87,427
min	0	1	0	0	1	1
max	2	166,695	1	0.9	600,000	2,427,083
count	107,935	107,975	108,717	7450	7454	108,635

The regular drawdown rate is the dependent variable of interest. The account balance is defined as the position at the start of the relevant financial year; this is the denominator for the rate computations. The ad-hoc drawdown indicator variable equals 1 if the retiree made an ad-hoc withdrawal from their account during a given financial year. SD refers to the sample standard deviation of the variable. Q1 and Q3 refer to the empirical 25th and 75th percentiles, respectively.

effects, c_i , so that

$$y_{it} = x'_{it}\theta + c_i + \alpha_{g_it} + v_{it}, \quad (2)$$

because applying the within transformation (centering the variables around individual-specific means) reduces (2) to the form of (1). To see this, for any variable z_{it} , define $\dot{z}_{it} := z_{it} - \bar{z}_i$, where $\bar{z}_i := T^{-1} \sum_{t=1}^T z_{it}$; then,

$$\dot{y}_{it} = \dot{x}'_{it}\theta + \dot{\alpha}_{g_it} + \dot{v}_{it}, \quad (3)$$

which has the same form as (1). In (3), the time profiles, $\dot{\alpha}_{g_it}$, have a different economic interpretation to the α_{g_it} from (1); Section 4.2 explains the treatment and interpretation of the group time profile estimators in the transformed model (3).

Throughout this paper, ‘GFE model’ refers to (2). A useful way to consider the GFE model is as a generalisation of the 2WFE model,

$$y_{it} = x'_{it}\theta + c_i + \alpha_t + v_{it}, \quad (4)$$

where the GFE model allows distinct time profiles for G groups, with group membership unobserved.

[Bonhomme and Manresa \(2015\)](#) state the assumptions needed for large- N , large- T consistency and asymptotic normality of the GFE estimator, in models both with, and without, time-invariant fixed effects. Moreover, the asymptotics show that the estimator converges in distribution even when T grows substantially more slowly than N . For any fixed value of T , however, the θ and α estimators are root- N consistent not for the true population parameters, but for ‘pseudo-true’ parameter values, and although these pseudo-true values may differ from the true population values for any fixed T , any difference vanishes rapidly as T increases. Specifically, the pseudo-true and true values may differ when group classification is imperfect; because of this possibility, the authors derive a fixed- T consistent variance estimate formula which takes into account potential group misclassification, providing a practical alternative to the large- T variance estimate formula ([Bonhomme & Manresa, 2015](#), p. 1161). To examine the finite- T properties of the GFE estimator, [Bonhomme and Manresa \(2015\)](#) use a Monte Carlo exercise with simulated datasets that match the $N = 90$, $T = 7$ panel used in their empirical application. In the present study, the superannuation dataset has large $N = 9516$ but moderate $T = 12$; the Online Supplement finds that the GFE estimator and the fixed- T consistent variance estimator perform well on simulated datasets of this size.

When using the standard 2WFE model, if there is group-level time-varying unobservable heterogeneity, α_{g_it} , correlated with observable characteristics, x_{it} , two problems arise: first, estimates of the covariate effects, θ , may suffer from omitted variable bias; second, the group time profiles, which in many applications have interesting economic interpretations, remain uncovered. The 2WFE model is a special case of the GFE model with $G = 1$; hence, the GFE model is an appealing alternative to the 2WFE model in applications where there is the possibility of unobservable time-varying heterogeneity in addition to time-invariant unobservable

heterogeneity. While determining the precise number of groups, G , lacks a general solution, estimating the GFE model can provide evidence for whether only controlling for one set of time effects, as in the 2WFE model, is adequate; Section 5.1 discusses this issue.

The GFE estimator for (1) minimises the sum of squared residuals, giving

$$(\hat{\theta}, \hat{\alpha}, \hat{\gamma}) = \arg \min_{(\theta, \alpha, \gamma) \in \Theta \times \mathcal{A}^{GT} \times \Gamma_G} \sum_{i=1}^N \sum_{t=1}^T (y_{it} - x'_{it}\theta - \alpha_{g_{it}})^2, \quad (5)$$

where the vector $\gamma = (g_1, g_2, \dots, g_N)$ defines the grouping of each of the N units into one of the G groups; Γ_G is the set of all possible groupings of N units into G or fewer groups; Θ is a subset of \mathbb{R}^k , the k -dimensional real space, where k is the number of covariates or equivalently the dimension of x_{it} ; \mathcal{A} is a subset of \mathbb{R} ; the α_{gt} parameters belong to \mathcal{A}^{GT} .

Bonhomme and Manresa (2015) present an iterative algorithm for estimating (5). The algorithm initialises values for the grouping vector γ and the model parameters (θ, α) ; it then alternates between the following two steps until convergence: 1) a grouping update step, which allocates each unit to the group minimising the sum of squared residuals given the most recent estimate of the model parameters θ and α ; 2) a parameter update step, which estimates the parameters (θ, α) conditioning on the most recent estimate of the grouping vector γ .

Estimating the GFE model does not require a balanced panel; the algorithm can be adjusted to run even when the sample contains unit–period combinations with missing data. However, when considering the relationship between the 2WFE model (4) and the GFE model (2) with $G = 1$, the unbalanced data case presents subtleties requiring further discussion.

The original GFE estimator for (2) with $G = 1$ gives the same estimates as applying the within transformation to the data and running a least-squares regression on the time-demeaned data, including T time dummy variables and no constant term. In balanced samples, this returns the same numerical results as standard implementations of the 2WFE model: for example `Stata's xtreg` command with the `fe` option and time dummy variables as covariates. However, in unbalanced panels, the results differ.

With unbalanced data, obtaining the results from standard implementations of the 2WFE model requires time-demeaning the time dummy variables at the unit level. Hence, this article proposes and utilises a modified GFE estimation procedure having the following property: when $G = 1$, it recovers precisely the same estimates as a standard implementation of the 2WFE model even when the data is unbalanced and the model includes time-invariant unit-level unobservable heterogeneity. Section 4.5 describes this alternative estimation procedure. When the panel is balanced, or when there are no time-invariant unit-level unobservables, the results from this method are identical to the unmodified GFE estimation procedure results. However, panel data models in microeconomic applications generally control for time-invariant unit-level unobservable heterogeneity. Hence, this is a useful extension when applying the GFE estimator to microeconomic applications more broadly. To examine the sensi-

tivity of the present results to using the modified algorithm, the Online Supplement provides a robustness check using the unmodified GFE estimation procedure in place of the proposed modified algorithm.

[Bonhomme and Manresa \(2015\)](#) explain that in the absence of covariates, their algorithm outlined above reduces to k -means clustering. Similarly to standard implementations of k -means clustering algorithms, the results depend on the starting values. Running the algorithm multiple times with randomly generated starting values increases the likelihood of finding solutions corresponding to smaller values of the objective function in (5).

In the present study, the algorithm is initialised by drawing starting values for each covariate effect from independent Gaussian distributions, centred at the coefficient estimates from a 2WFE regression fit to the data, and with standard deviations equal to the magnitude of these coefficient estimates. Results for the application take the most optimal solution across 1000 independent runs of the algorithm using randomly drawn starting values to initialise the parameters. The Online Supplement also tests the sensitivity of the results to the number of starting values used.

To facilitate inference on the group time profiles, this study implements the fixed- T variance estimate formula in the Online Supplement to [Bonhomme and Manresa \(2015\)](#), as well as an extension to their non-parametric bootstrap method. Notably, approximating the variability in time profile estimates using the non-parametric bootstrap method described by [Bonhomme and Manresa \(2015\)](#) requires solving a label-switching problem. Section 4.4 explains this problem and proposes an extension to the bootstrap procedure which matches group labels across replications to allow for bootstrap inference on the time profiles.

4.2 Time profiles in the transformed model

Within-transforming the data to remove the effect of any time-constant unobservable heterogeneity results in time-demeaned group time profiles, $\dot{\alpha}_{gt}$. As the $\dot{\alpha}_{gt}$ contain only information about changes in the group effects over time relative to their mean, and no information about the absolute level of the effect, the estimates of the $\dot{\alpha}_{gt}$ are modified in order to obtain the desired economic interpretations. All estimated time profiles are shifted to begin at a value of 0 at $t = 1$, so that the interpretations of the values are as changes relative to the first time period. This is analogous to estimating a set of $T - 1$ coefficients for the time effects in the standard 2WFE model, where each estimate is interpreted as a change relative to the omitted reference period.

This study uses two methods to estimate the uncertainty in the shifted time-demeaned group time profiles, defined as $\tilde{\alpha}_{gt} := \dot{\alpha}_{gt} - \dot{\alpha}_{g,1}$, for all g and t . First, Normal-approximation 95% confidence intervals are constructed for the $\tilde{\alpha}_{gt}$, using variance estimates which are computed from the variance-covariance matrix components for the time-demeaned time profiles, $Var(\dot{\alpha}_{gt})$, $Var(\dot{\alpha}_{g,1})$ and $Cov(\dot{\alpha}_{gt}, \dot{\alpha}_{g,1})$; these objects are obtained by applying the fixed- T variance estimate formula after estimating the GFE model on the within-transformed data.

Second, these confidence intervals are compared to the corresponding intervals obtained from the bootstrap, using the proposed extension for matching group labels across bootstrap replications.

A comparison of the time profile standard errors derived from the fixed- T variance estimate formula versus simulated standard errors from a Monte Carlo exercise shows that the fixed- T variance estimate formula performs well on simulated data calibrated to the superannuation dataset; the Online Supplement provides details of this comparison. Moreover, in the present study, confidence intervals constructed from the bootstrap procedure results are broadly similar to those derived from the fixed- T variance estimate formula, implying practically equivalent inference on the estimated parameters. For smaller datasets, where asymptotic results are less likely to provide accurate standard errors, and where the computational cost of running the bootstrap is lower, it may be preferable to use the bootstrap. However, the results suggest that in larger datasets, using the fixed- T variance estimate formula may be sufficiently accurate while keeping the computational burden low compared to using the bootstrap.

4.3 Selecting G

Bonhomme and Manresa (2015) propose an information criterion that correctly selects the number of groups when N and T are both large and similar in magnitude; however, for large- N moderate- T panels, like the superannuation dataset, this criterion may overestimate the true value of G (Bonhomme & Manresa, 2015). An alternative method to choose the number of groups, which Bonhomme and Manresa (2015) employ in their empirical application, uses the fact that underestimating G leads to a type of omitted-variable bias in the θ parameters, to the extent that the unobserved effects are correlated with the included covariates. Conversely, overestimating G does not bias the θ estimates, although it does increase the number of parameters to estimate and the parameter space of possible groupings, resulting in noisier estimates for all model parameters.

Taken together, these properties suggest that observing a plot of how the coefficient estimates change as G increases can reveal the point at which the coefficients have been de-biased relative to the $G = 1$ case. Visually, the coefficients might vary significantly between $G = 1$ and some higher value, G^* , after which they may appear to stabilise, albeit becoming noisier as G continues to increase. One can then select G^* as the number of groups suggested by the data.² This is how Bonhomme and Manresa (2015) decide on $G = 4$ in their application, rather than $G = 10$ as suggested by the information criterion—which, given the dimensions of their panel, may overestimate the true number of groups.

For applications that focus only on estimating unbiased effects of the covariates, the above suggests choosing the number of groups by selecting the smallest value of G that places the covariate effect estimates close to their stable values. However, the present application takes a unique interest in the time profiles for all latent groups in the sample. It is possible that stop-

²This method would not apply to a model with group-specific covariate effects.

ping at the first value of G that seems to successfully de-bias the regression coefficients will result in at least one estimated group whose time profile is an average over distinct time profiles of constituent subgroups. For the purposes of obtaining unbiased regression coefficients alone, separating out these mixed groups by further increasing G may unnecessarily increase the complexity of the model. However, identifying all distinct behavioural groups with economically meaningful interpretations may require searching beyond the smallest G that de-biases the regression coefficients.

On the other hand, overestimating G can result in the separation of a particular time profile into multiple biased representations of itself, where the difference between the representations is spuriously driven by noise (Bonhomme & Manresa, 2015). This means that the more similar a pair of time profiles appear, the more sceptical the researcher should be in regarding them as distinct effects.

Hence, this study posits a selection rule that picks the greater of two values of G : the smallest G that appears to result in unbiased estimates of the regression coefficients; or the last value of G for which the marginal change from $G - 1$ to G groups finds an economically important behaviour, sufficiently distinct from all others and exhibited by a non-trivial portion of the sample. Section 5 discusses this selection process alongside the main results.

4.4 Extension 1: Bootstrapping time profile estimates

Bonhomme and Manresa (2015) address how to obtain bootstrap standard errors for the covariate effects, but not the time profiles. As the covariate effects are unambiguously labelled across multiple runs of the GFE procedure, estimating their standard errors by comparing estimates across a large number of bootstrap replications requires no special consideration. By contrast, group-level results from the procedure are unique only up to a relabelling of the groups, and the group labels are determined at random during estimation. This means that the same economic group may receive different labels across multiple independent estimation runs, e.g., when performing the bootstrap. Hence, estimating the standard errors of group-level time effects by comparing time profile estimates across bootstrap replications requires a method to match labels across runs.

The bootstrap procedure outlined in the Online Supplement to Bonhomme and Manresa (2015) involves running the GFE procedure B times, each time on a different bootstrap replicate dataset. To create the bootstrap replicate datasets, all N units in the original data are sampled with replacement N times, taking all observations corresponding to a given unit into the replicate dataset when that unit is sampled. Each of the B model runs produces a set of coefficient estimates for the model covariates, as well as an estimated grouping and a set of time profiles for each group.

To match group labels across replications, this article proposes the following label-matching procedure, similar to the solution Hofmans, Ceulemans, Steinley, and Van Mechelen (2015) use for the analogous problem in k -means clustering.

1. Fix the labelling generated by the GFE model estimation completed on the original sample. These labels act as the reference labels to which all subsequent estimates will align their group labels. Define the initial time profile estimates labelled using the reference labels as $\hat{\alpha}_g^r := \left(\hat{\alpha}_{g,1}^r, \hat{\alpha}_{g,2}^r, \dots, \hat{\alpha}_{g,T}^r \right)'$ for $g = 1, 2, \dots, G$.
2. For $b = 1, 2, \dots, B$, find the permutation of group labels for the b^{th} bootstrap run which minimises the sum of Euclidean distances, aggregated across all G time profiles, between the time profiles estimated in the b^{th} bootstrap run and the original sample estimates as identified by the reference labels; i.e., for $b = 1, 2, \dots, B$, do:
 - 2.1. Using the unmodified labels generated by the b^{th} bootstrap run, define the estimated time profiles from the b^{th} bootstrap run with these labels as the length- T vectors $\hat{\alpha}_g^{b,0}$ for $g = 1, 2, \dots, G$.
 - 2.2. Index the $G!$ permutations of the label sequence $(1, 2, \dots, G)$ by $p = 1, 2, \dots, G!$. Each permutation p for the b^{th} bootstrap run defines a permuted set of time profiles, $\hat{\alpha}_g^{b,p}$, for $g = 1, 2, \dots, G$, and a corresponding mapping function, $m_p : \{1, 2, \dots, G\} \rightarrow \{1, 2, \dots, G\}$, such that $m_p(g)$ is the g^{th} element of the p^{th} permuted label sequence, and $\hat{\alpha}_g^{b,p} = \hat{\alpha}_{m_p(g)}^{b,0}$.
 - 2.3. For $p = 1, 2, \dots, G!$, do:³
 - 2.3.1. For $g = 1, 2, \dots, G$, compute the Euclidean distance between the length- T vectors $\hat{\alpha}_g^{b,p}$ and $\hat{\alpha}_g^r$, given by $\|\hat{\alpha}_g^{b,p} - \hat{\alpha}_g^r\|$; here $\|\cdot\|$ is the L_2 norm.
 - 2.3.2. Sum all G Euclidean distances to compute an aggregate distance metric for that permutation, $\sum_{g=1}^G \|\hat{\alpha}_g^{b,p} - \hat{\alpha}_g^r\|$.
 - 2.4. Select the permutation, p^* , with the smallest aggregate distance metric:

$$p^* = \arg \min_{p \in \{1, 2, \dots, G!\}} \sum_{g=1}^G \|\hat{\alpha}_g^{b,p} - \hat{\alpha}_g^r\|. \quad (6)$$

Relabel the G groups in the b^{th} bootstrap run using the labelling given by the selected permutation.

This method matches time profiles across different bootstrap replications in the main results presented in Section 5, as well as across different simulated datasets and bootstrap replications in the simulation exercise reported in the Online Supplement. In general, it could be seen as an issue that time profile bootstrap results are contingent on some method to match labels, because, in principle, the bootstrap results could prove sensitive to the choice of label-matching method. The results from the present paper, which use the procedure described here, show that in this application, the bootstrap and analytical formula results are similar, and so little is gained by using the bootstrap over the analytical formula. Thus, we did not pursue this question further, but this general problem may be of interest to future research.

Deriving standard errors for the shifted time-demeaned group time profiles, $\tilde{\alpha}_{gt}$, using the fixed- T variance estimate formula requires first estimating variance-covariance matrix compo-

³If $G!$ is too large to check each permutation in an acceptable amount of time, an alternative is to use the more computationally efficient approach given in Munkres (1957) and used by Hofmans et al. (2015).

nents for the time-demeaned time profile estimators, $\hat{\alpha}_{gt}$, then using these variance–covariance matrix components to estimate standard errors for the shifted time profiles to construct Normal-approximation element-wise confidence intervals. By contrast, the bootstrap results directly estimate the variability of the shifted time profile estimators, by matching shifted time profiles across the B bootstrap replications, then using the empirical distribution of the matched time profile estimates to obtain bootstrap intervals.

4.5 Extension 2: Alternative estimation method for unbalanced data

Consider the model in (4), which, after time-demeaning, has the form

$$\dot{y}_{it} = \dot{x}'_{it}\theta + \dot{\alpha}_t + \dot{v}_{it}. \quad (7)$$

The primary estimands of interest are the $T - 1$ relative effects $\tilde{\alpha}_t = \dot{\alpha}_t - \dot{\alpha}_1$ for $t = 2, 3, \dots, T$. Since $\dot{\alpha}_t := \alpha_t - \bar{\alpha}$, where $\bar{\alpha} = T^{-1} \sum_{t=1}^T \alpha_t$, the set of T values of $\dot{\alpha}_t$ satisfy $\sum_{t=1}^T \dot{\alpha}_t = 0$.

In balanced panels, the following three methods obtain identical estimates for the $\tilde{\alpha}_t$:⁴

1. regress \dot{y}_{it} on \dot{x}_{it} and T time dummy variables with no constant term to estimate all T values for $\dot{\alpha}_t$ as the coefficients of the time dummies; then compute $\tilde{\alpha}_t = \dot{\alpha}_t - \dot{\alpha}_1$ for $t = 2, 3, \dots, T$;
2. regress \dot{y}_{it} on \dot{x}_{it} and $T - 1$ time dummy variables excluding the dummy variable for the first time period, including a constant term, after which the $T - 1$ desired estimates of $\tilde{\alpha}_t$ are the estimated coefficients of the included $T - 1$ time dummy variables;
3. first, time-demean the time dummy variables corresponding to periods $2, 3, \dots, T$; then, regress \dot{y}_{it} on \dot{x}_{it} and the $T - 1$ time-demeaned time dummy variables, not including a constant term, after which the $T - 1$ desired estimates of $\tilde{\alpha}_t$ are the estimated coefficients of the included $T - 1$ time dummy variables.

When the panel is unbalanced, the choice of estimation strategy requires further consideration. With unbalanced data, methods 1 and 2 described above for obtaining estimates of $\tilde{\alpha}_t$ no longer guarantee that the corresponding values of $\dot{\alpha}_t$ sum to zero; a nonzero sum contradicts a property of the model given by (7). Conversely, method 3 obtains the desired estimates while ensuring that the T estimates of $\dot{\alpha}_t$, derived from the $T - 1$ estimates for $\tilde{\alpha}_t$, sum to 0, consistent with the model.

Using the GFE estimator implementation provided by [Bonhomme and Manresa \(2015\)](#) with $G = 1$ on unbalanced data gives estimates for the time effects in line with those produced by methods 1 and 2, whereas standard implementations of the 2WFE model give the same estimates as method 3. This motivates our modification to the GFE methodology, which aligns the $G = 1$ results with the standard 2WFE model estimates, regardless of whether the panel is balanced or not: in the modified procedure’s parameter update step, the algorithm interacts the group identity variables with $T - 1$ time-demeaned time dummy variables, analogous

⁴This claim is justified in the Online Supplement.

to using method 3 for $G = 1$.⁵

5 Main results

5.1 Covariate effects

Figure 1 plots the covariate effect estimates versus G for the GFE model fitted to the superannuation drawdowns dataset. The values of G on the horizontal axis correspond to the number of latent groups specified; the vertical axis denotes partial effect values for the two included covariates: log minimum drawdown rate and log account balance. The lines connect covariate effect estimates, while the shaded regions around these correspond to 95% confidence intervals constructed using standard errors derived from the fixed- T variance estimate formula in the Online Supplement to [Bonhomme and Manresa \(2015\)](#).

As the dependent variable and covariates are on the log scale, the covariate estimates represent the elasticity of regular drawdown rates to changes in account balances and the minimum drawdown rates. Section 5.2 provides the economic interpretation for the corresponding estimates after choosing the value of G .

A critical feature of Figure 1 is that as G increases, changes in the log account balance covariate effect estimates are large relative to the confidence intervals for the first few values of G . After $G = 7$, the point estimates become more stable and successive 95% confidence intervals show significant overlap. This suggests that from $G = 7$, the GFE procedure removes the bias arising from correlation between group-level latent time effects and the included covariates.

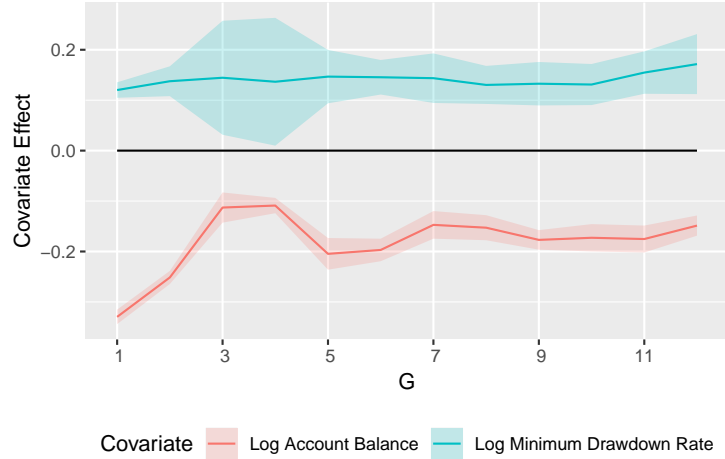
Using the proposed modified GFE model estimation procedure, the point estimates corresponding to $G = 1$ are identical to the results from a standard 2WFE estimation on the drawdowns dataset. Hence, Figure 1 implies that the estimators using a more traditional analysis including only one time profile are biased compared to the estimators in the GFE model for $G \geq 7$. The Online Supplement shows that this result holds in the fully balanced case, where both the modified and unmodified GFE procedures give results identical to the 2WFE model when $G = 1$.

5.2 Choice of G

Figure 2 shows plots of the time profiles estimated for $G = 4, 5, \dots, 9$, all shifted to begin at a y -axis value of 0, and omitting confidence interval bounds for clarity. This figure suggests that while increases in G initially produce new and economically distinct time profiles, at $G = 7$, incremental moves to a larger value of G split existing time profiles into highly similar representations of the same trajectory. This is consistent with a theoretical result from [Bonhomme and Manresa \(2015\)](#) that implies overestimating G can create spurious copies of the true time profiles, differing by random noise. Hence, the number of latent groups to use in

⁵The Online Supplement provides further details of this modification, as well as results using the unmodified GFE estimation procedure to compare with the results presented here.

Figure 1: Point estimates and 95% confidence intervals for partial effects of log minimum drawdown rate and log account balance covariates on log regular drawdown rate, controlling for group-level time-varying unobservable heterogeneity for a range of values of G . Shaded regions denote 95% confidence intervals constructed using standard errors derived from fixed- T variance estimate formula in the Online Supplement to [Bonhomme and Manresa \(2015\)](#).



the model is set to $G = 7$. Section 5.3 explains in detail the economic interpretations of the resulting time profile estimates.

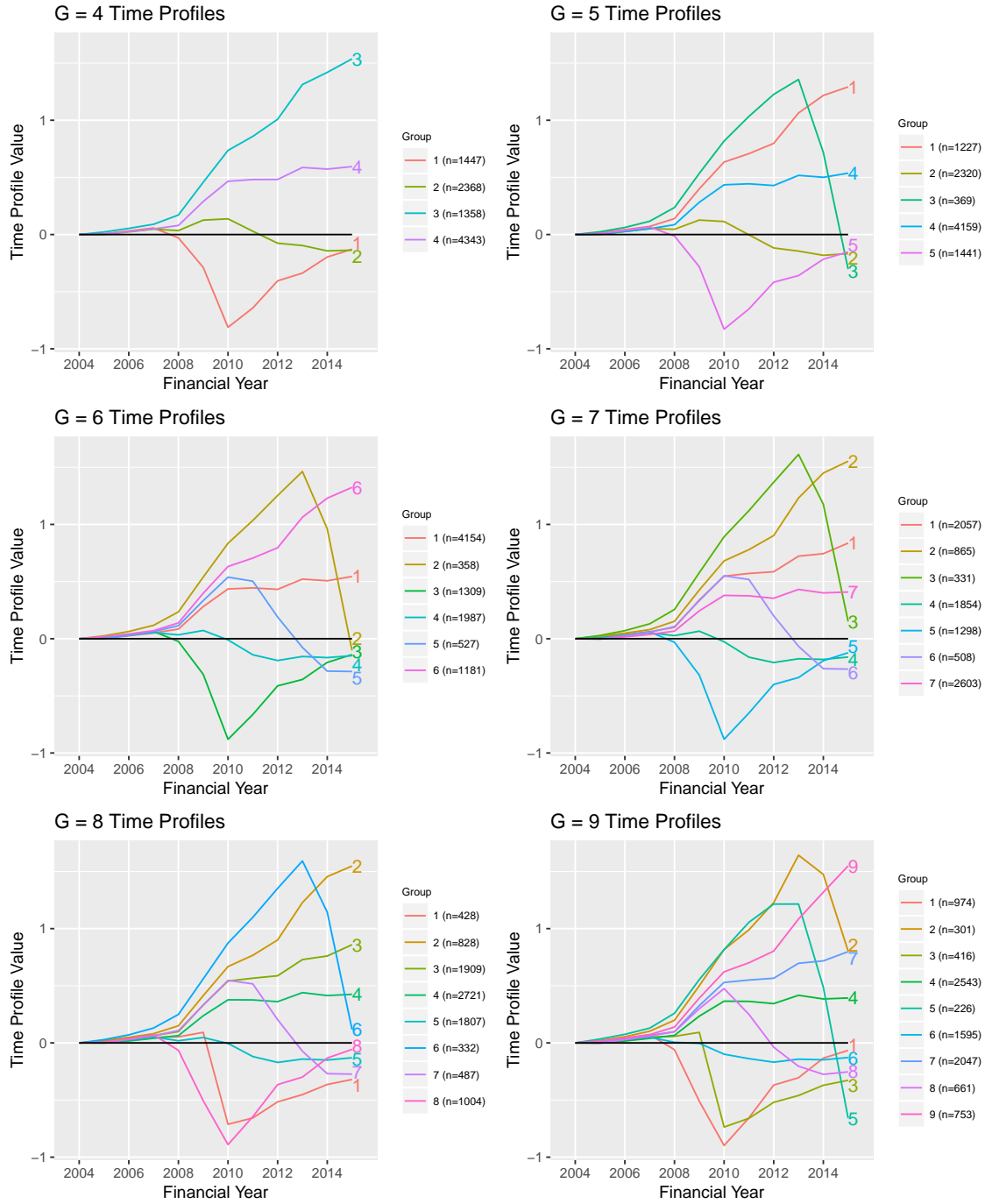
Selecting $G = 7$ groups corresponds to estimated covariate effects of 0.144 and -0.147 for the log minimum drawdown rate and log account balance, respectively. These are statistically significant at the usual levels, e.g. 5%, with respective standard errors of 0.0251 and 0.0140. As the dependent variable and covariates are on the log scale, the covariate effects represent partial elasticities of the regular drawdown rate with respect to the minimum drawdown rate and account balances. For example, consider an increase of 0.1 in the log minimum drawdown rate, which translates to a proportional increase in the level of the minimum drawdown rate of approximately 10.5%. This increase in the log minimum drawdown rate is expected to raise regular drawdown rates proportionally by an estimated $e^{0.0144} - 1 = 1.45\%$ on average, holding account balance equal and controlling for group-level time-varying heterogeneity. A similar proportional increase in a retiree’s account balance is expected to effect a proportional decrease of 1.46% ($1 - e^{-0.0147}$) in their regular drawdown rate on average, holding the minimum drawdown rate constant and controlling for group effects.

5.3 Time profiles

Figure 3 shows the time profiles estimated using the selected value of $G = 7$ with element-wise confidence interval bounds constructed using standard errors derived from the fixed- T variance estimate formula. Figure 4 presents the equivalent plot with confidence interval bounds computed from the empirical 2.5 and 97.5 percentiles of the time profile estimates from 1000 bootstrap replications.⁶ While qualitatively similar overall to the intervals con-

⁶Each bootstrap replication uses distinct sets of randomly generated starting values for the estimation algorithm.

Figure 2: Point estimates for effects of group-level time-varying unobservable heterogeneity on log regular drawdown rates assuming $G = 4, 5, \dots, 9$. Estimated time-demeaned group time profiles shifted to begin at 0 on the vertical axis.



structured using standard errors derived from the fixed- T variance estimate formula, a comparison highlights some differences. In particular, the intervals are wider around financial years 2011–2013 for group 6; the interval is wider for financial year 2010 for group 4; the intervals are tighter for group 5 throughout; the interval is wider in the terminal financial year for group 3; and the point estimates from the original sample tend towards the lower end of the 95% bootstrap confidence intervals for groups 1, 2 and 7. However, due to the estimated effect magnitudes, these numerical differences in the sets of confidence intervals do not meaningfully change inferential conclusions regarding the estimates or their economic interpretations.

The values of the time profiles represent behavioural effects on the proportional changes in a retiree’s regular drawdown rate, relative to their own rate of drawdown in 2004. As the dependent variable is on the log scale, a value of, say, 0.5 on the y -axis represents a proportional change in the regular drawdown rate of $e^{0.5} \approx 1.65$, or roughly a 65% increase in the drawdown rate, relative to 2004 levels.

Figure 5 shows the time profile estimates for the $G = 1$ model estimated using the modified GFE procedure, with the y -axis scale set to the same scale used for the $G = 7$ model group time profile plot (Figure 3). Comparing these shows that a model controlling for only one set of time effects fails to capture the shape and magnitude of any of the time profiles in the seven-group model. Visually, the resulting single time profile appears to ‘average over’ the seven markedly distinct time profiles. Hence, not only are the covariate effect estimates biased when $G = 1$, but the single time profile is entirely unrepresentative of the latent group-level time profiles.

5.4 Behavioural interpretations

The following refers to the group time profiles in Figure 3. All the time profiles exhibit similar, slowly rising trajectories until the financial year ended 30 June 2008, after which they diverge in statistically and economically significant ways.

Consider group 5, whose time profile describes a rapid reduction in drawdown rates between financial years 2008 and 2010, and then a gradual return towards pre-reduction levels. The timing of these movements follows closely the progression of concessional minimum drawdown rates (see Section 3). This implies that members of group 5 were the most responsive to the changing minimum drawdown rates over this period, compared to the rest of the sample. Figure 6 confirms that many individuals in group 5 show a step-like pattern in their log regular drawdown rate series during the second half of the observation period. This pattern is suggestive of the new step-function schedule for minimum drawdown rates which came into effect 1 July 2007.

Groups 1 and 2 display time profiles rising steadily following financial year 2008 for the remainder of the sample. Group 7 follows a similar rising trend with a reduced magnitude for the first few financial years after 2008, before stabilising for the remainder of the observation

Figure 3: Point estimates and 95% confidence intervals from analytical formula for effects of group-level time-varying unobservable heterogeneity on log regular drawdown rates assuming $G = 7$. Shaded regions denote 95% element-wise confidence intervals constructed using standard errors derived from fixed- T variance estimate formula in the Online Supplement to [Bonhomme and Manresa \(2015\)](#). Time-demeaned group time profiles shifted to begin at 0 on the vertical axis.

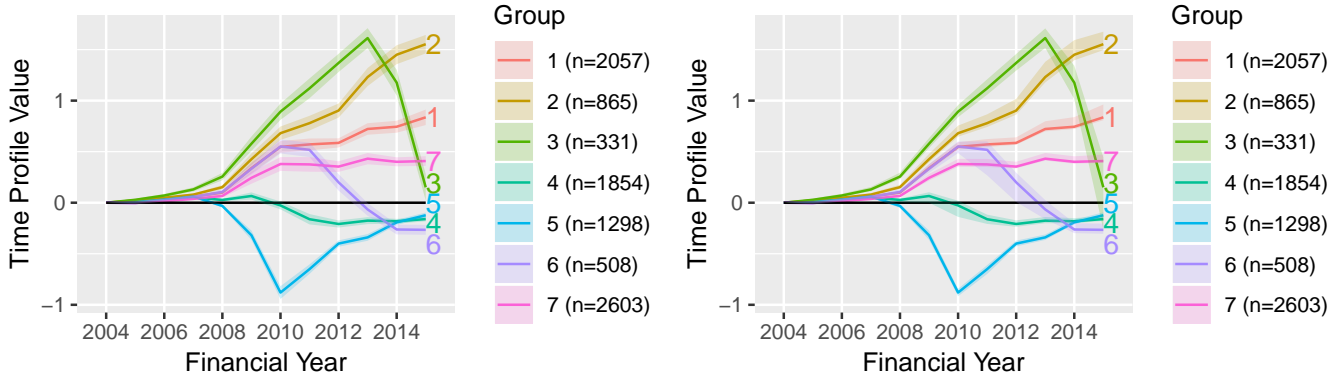


Figure 4: Point estimates and 95% bootstrap confidence intervals for effects of group-level time-varying unobservable heterogeneity on log regular drawdown rates assuming $G = 7$. Shaded regions denote 95% element-wise confidence intervals computed from empirical percentiles across 1000 bootstrap replications. Time-demeaned group time profiles shifted to begin at 0 on the vertical axis.

Figure 5: Point estimates and 95% confidence intervals for effects of group-level time-varying unobservable heterogeneity on log regular drawdown rates assuming $G = 1$. Shaded regions (indistinguishable from point estimates in plot) denote 95% element-wise confidence intervals constructed using standard errors derived from fixed- T variance estimate formula in the Online Supplement to [Bonhomme and Manresa \(2015\)](#). Time-demeaned time profile shifted to begin at 0 on the vertical axis. Owing to the modification of the GFE model estimation algorithm, point estimates here are identical to those recovered from estimating a standard 2WFE model on the data. The Online Supplement gives the corresponding results using the unmodified GFE model estimation procedure as a comparison.

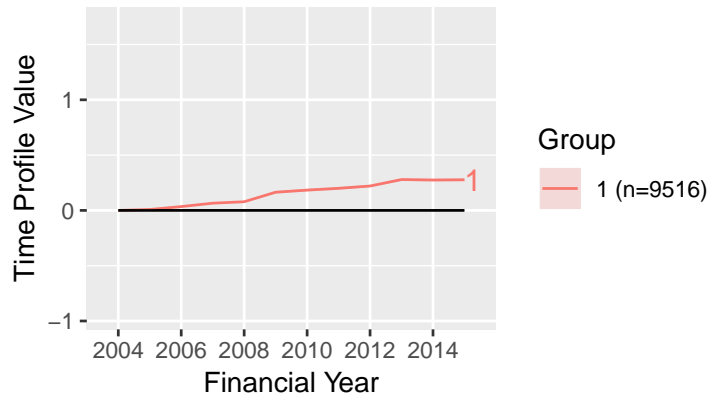
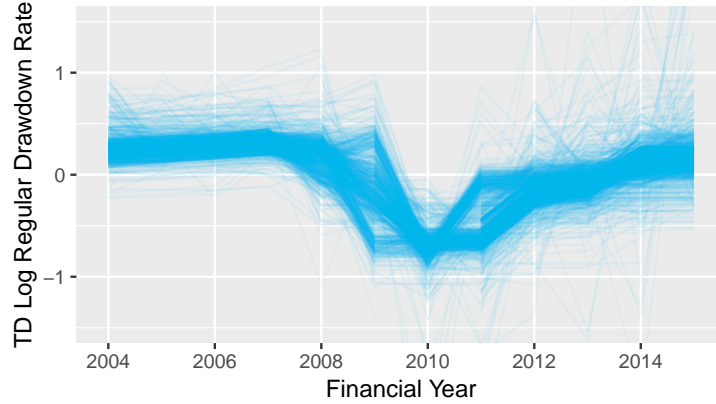


Figure 6: Panel plot showing all individual time series for group 5 of the time-demeaned (TD) log regular drawdown rate variable vs. financial year.



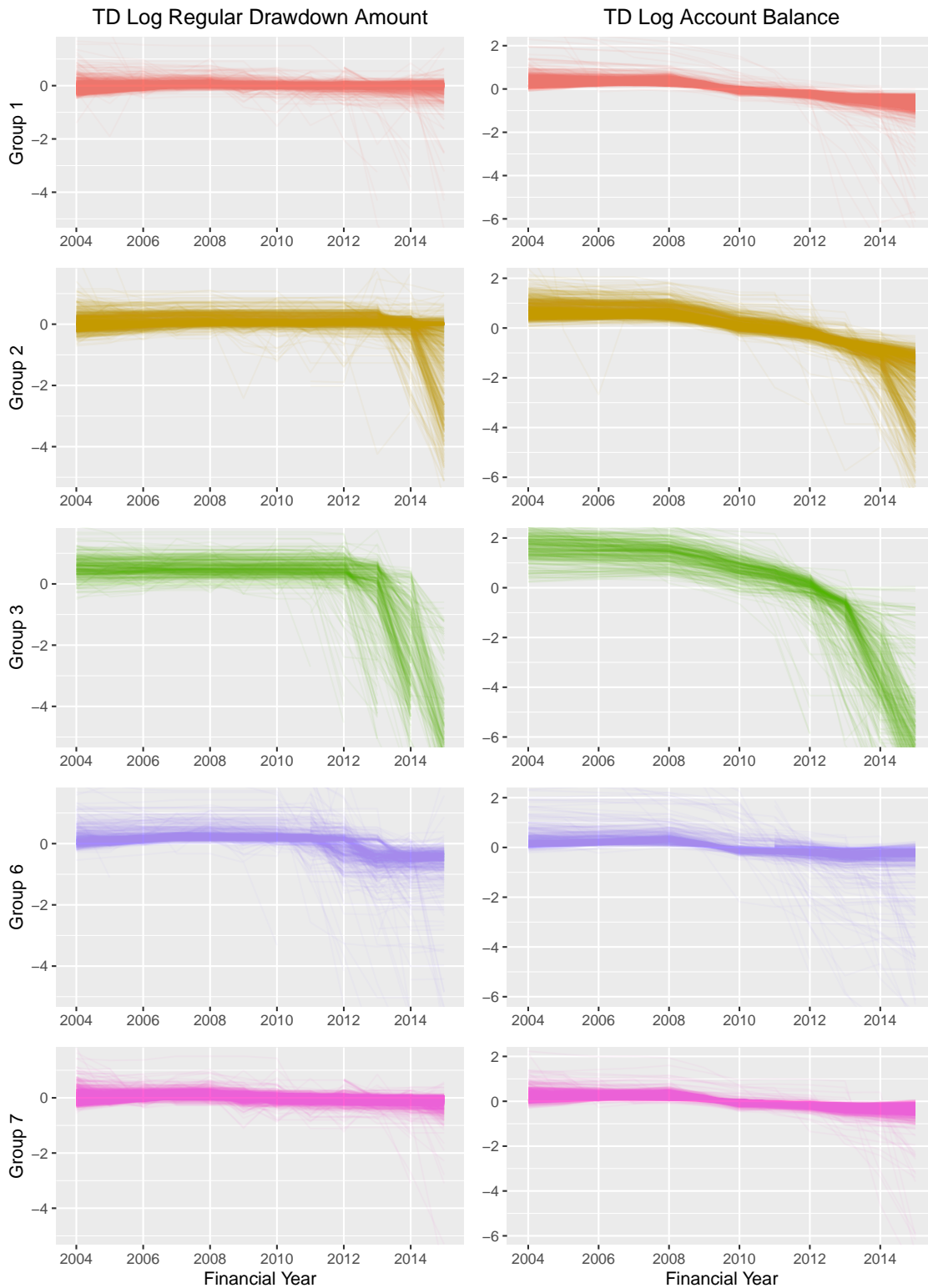
window. The panel plots in Figure 7 suggest a tendency for individuals in these groups to draw constant dollar amounts, while their account balances gradually decline over time. The corresponding plots for group 3 show a similar preference for constant dollar amounts, but after financial year 2013, individuals in this group suffer a rapid decline in both the amounts drawn down and account balances. Many members of group 6 undergo a similar evolution, characterised by mostly constant drawdowns initially and a subsequent reduction in the level in later years. The magnitudes of the downwards revisions appear smaller for this group, and occur earlier for many retirees. Moreover, while group 3 members continue to revise down over successive financial years, it appears that many individuals in group 6 revise down once and then continue to draw at the new, reduced level. The group 7 plots show gradual downward revisions in the amounts year on year.

Thus, groups 1, 2, 3, 6 and 7 appear to be similar in that members draw mostly constant dollar amounts over time; however, these groups seem to differ in how many members make a downwards revision in the level of their drawdown amounts, and whether this revision is once-off or the beginning of a downward trend. Crucially, the timing of downwards revisions often appears to align with periods where account balances begin falling at an accelerated rate. Hence, the heuristic of drawing constant amounts over time may be adversely impacting retiree financial security by contributing to a premature exhaustion of account balances.

Figure 3 shows that the time profile for group 4 closely follows the zero line before financial year 2011. A time profile with all values near zero would suggest the model for the group's data is well approximated by $y_{it} = x'_{it}\theta + c_i + v_{it}$. Correspondingly, a possible interpretation for group 4's behaviour is that before financial year 2011, they were constantly tuning their drawdown rates as they progressively faced higher minimum drawdown rates and as their account balances changed. This can potentially represent a group of 'engaged' retirees, who regularly occupy themselves with determining their desired rate of drawdown; however, it is not possible to further investigate this hypothesis using this dataset.

Group 4's time profile drops significantly below 0 after financial year 2010. These movements,

Figure 7: Panel plots showing all individual time series for groups 1, 2, 3, 6 and 7 (top to bottom) of the time-demeaned (TD) log regular drawdown amount (left column) and TD log account balance (right column) variables on the vertical axes vs. financial year on the horizontal axes. Plots in each column maintain same y -axis scale for comparability.



while of a smaller magnitude compared to the time profile values of other groups, are still economically significant; they suggest a behavioural response, after netting out the effect of covariates, of reducing drawdown rates relative to earlier levels from 2011 onwards.

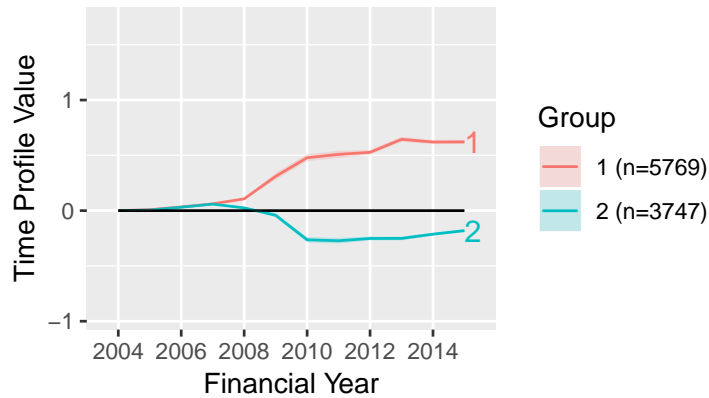
The Online Supplement provides summary statistics and descriptive plots for all seven groups. Based on these, some of the ways in which the groups differ in terms of observable characteristics are: the proportion of males in groups 1 to 3 are 62%, 62% and 69% respectively, while the sample on aggregate is 56% male; the members of groups 1 and 3 tend to be older, with median retirees aged 81 at 31 Dec 2015; members in groups 4, 5 and 6 have the youngest median retirees, aged 78 at 31 Dec 2015; group 5 members have the highest median risk appetite, a variable defined in the Online Supplement as a summary measure of the relative sizes of derived equity returns within individual accounts compared to the S&P/ASX 200 market index; group 7 members have the lowest median risk appetite; group 7 members make ad-hoc drawdowns least frequently, in roughly 3% of person-years observed, followed by group 1, for 5% of person-years observed—for all other groups this frequency was 9–11%; in years where they make ad-hoc drawdowns, group 3 members tend to draw down the largest proportions of their account balance using ad-hoc drawdowns over the course of a year—on average, these ad-hoc drawdowns over the year amount to 35% of their account balance at the start of the respective financial year.

5.5 Prior expectations

Section 1 presents this study’s prior expectations for finding at least two types of strategies in the data: drawing constant dollar amounts; following closely the minimum drawdown rates. Most of the group behaviours found under the seven-group assumption can be interpreted as cases of these two hypothesised behaviours. Moreover, a restricted model assuming only two groups already begins to show evidence for the existence of both of these groups. Figure 8 shows the time profiles for the two-group model. As in Figure 5, the y -axis scale allows for direct comparison of the estimated magnitudes with the $G = 7$ model results. The time profile of the first group appears similar to those for the groups in the seven-group model that seem to target constant dollar amounts for the regular drawdowns; the second profile shows a dip comparable to the group that seems to follow the minimum drawdown rate.

The Online Supplement also provides descriptive panel plots for these two groups. These plots are broadly consistent with the interpretation that the first group often attempts to hold drawdown amounts constant, although with downward revisions in the amount common, as well as rapid declines in account balance towards the end of the period; the second group mainly makes decisions regarding their drawdown rate. This analysis, alongside the observation that moving to a two-group model already removes much of the bias in the covariate effect estimates, suggests that accounting for both rate-based and amount-based strategies seems to be the most important step in controlling for unobservable heterogeneity in the data.

Figure 8: Point estimates and 95% confidence intervals from analytical formula for effects of group-level time-varying unobservable heterogeneity on log regular drawdown rates assuming $G = 2$. Shaded regions (indistinguishable from point estimates in plot) denote 95% element-wise confidence intervals constructed using standard errors derived from fixed- T variance estimate formula in the Online Supplement to [Bonhomme and Manresa \(2015\)](#). Time-demeaned group time profiles shifted to begin at 0 on the vertical axis.



6 Discussion

6.1 Retirement incomes

A key implication for retirement incomes research and policy is that there is now a statistical basis for empirical results that indicate different behavioural stances explain much of the variation in the drawdowns from phased withdrawal retirement income products. The significant change in covariate effect estimates and the emergence of distinct time profiles, as the number of groups assumed by the GFE estimator increases, is evidence for the presence of multiple behavioural groups in the data. The magnitudes of the estimated group time profile values suggest a sizeable contribution of this behavioural component to the observed drawdowns.

Retirees need to trade-off current against future consumption in the face of investment, longevity and other, background, risks that include inflation rates and health expenditure ([Yang & Huang, 2009](#)). Retirement fund trustees and financial advisors could use the findings from this research when aiding retirees who are navigating the trade-offs in apportioning their accumulated retirement savings between consumption, income-generating assets and precautionary assets. The results do not find clear evidence for a group following the optimal heuristic strategy from [Bateman and Thorp \(2008\)](#), which is to initially draw at a fixed rate until the rising minima require drawing larger proportions. Two-thirds of the sample belong to the groups exhibiting a preference for drawing down a constant dollar amount over time. We do not have evidence as to whether the initial level was optimal, but two of the groups targeting level income streams had their account balances begin a rapid decline following the GFC; retirees with this preference who are unable to respond to periods of low or negative investment returns by curtailing their income streams may be at risk of prematurely depleting their account balances. 14% of the sample belong to the group who most closely follow the next-most optimal heuristic strategy, which is to always draw at the legislated minimum rates.

Those providing financial advice may wish to convey these findings to retirees in the form of cautionary tales, or as part of a standard set of recommendations presented to retirees. Practitioners and policymakers may also wish to consider these findings when designing retirement income products and policy to align with the Comprehensive Income Products for Retirement framework, which places an emphasis on generating income streams without compromising the ability to retain superannuation savings until late into retirement by including some life annuity products ([The Australian Government the Treasury, 2016](#)). Financial advisors may benefit retirees by predicting their individual needs for income and precautionary savings later in life, monitoring their actual experience relative to this forecast, and recommending a reduction in expenditure before poorer experience exhausts their accounts.

The present study makes clear how a robust behavioural analysis of drawdowns data is vital for informing the various stakeholders in the retirement incomes space, including retirees, the government, and the financial services industry. However, [Section 3](#) notes that despite having data from multiple superannuation funds, due to the small number of funds in the estimation sample, the results may not describe the population of Australian retirees in general. In particular, using the current dataset may overlook behavioural patterns present in funds not included in the sample.

6.2 GFE in behavioural microeconomics and event studies

We believe that the GFE model is valuable for research in behavioural microeconomics and event studies. While the present paper’s focus is on the behavioural interpretations of the latent group effects, the superannuation data covers a period in which multiple common macroeconomic and policy shocks affect all members in the sample. Hence, the superannuation application also invites an event-study interpretation, although it is impossible to disentangle the effects of several common shocks which occur in close proximity. These include the Global Financial Crisis, the introduction of a new schedule of minimum drawdown rates for account-based pensions, and temporary tweaks made to the minimum drawdown rates. Taken together, however, the time profile plots presented in [Figure 3](#) clearly show how otherwise homogeneous-looking trends diverge radically, plausibly driven by one or more of these shocks. Hence, the results broadly show how researchers can utilise the same methodology in an event-study framework.

In the superannuation application, the GFE assumption of a group structure to the time-varying unobservable heterogeneity is tenable because it was *a priori* expected that an important source of heterogeneity in the drawdowns arises from the latent motivations that drive individuals to choose one of a finite number of drawdown strategies. In general, other behavioural economics studies with panel data may have analogous motivations to assume that there is some true, finite number of groups in the population, which the GFE estimator will attempt to characterise. This prior assumption may be important as it is not known precisely how the estimator behaves when a group structure only approximates, rather than accurately captures, the nature of the unobservable heterogeneity. For a discussion on approximating more general forms of heterogeneity, see e.g. [Bonhomme, Lamadon, and Manresa \(2021\)](#).

A Appendix: Account balance decomposition

The ABP account balance at 1 July of calendar year $t+1$ for an arbitrary retiree (i subscripts omitted) is given by

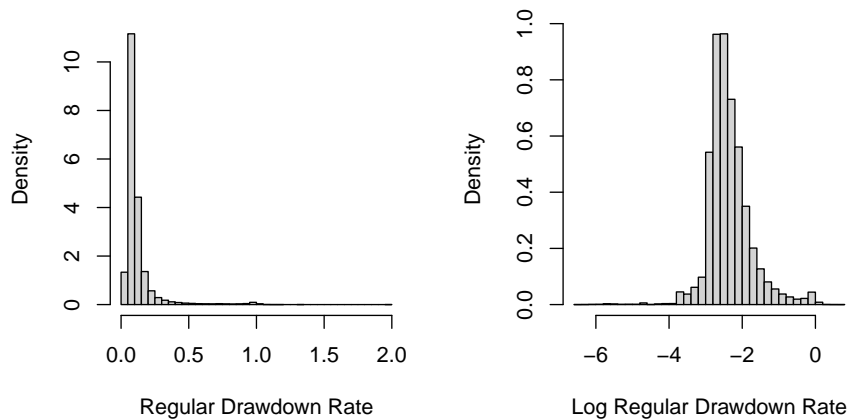
$$AB_{t+1} = AB_t - DA_t - ADA_t + NIRA_t - AF_t + NT_t,$$

where:

- t indexes financial years;
- AB_t is account balance at start of financial year t ;
- DA_t is the regular drawdown amount. This is the total dollar amount, determined in advance of the financial year, received over the course of the financial year as regular payments. E.g., the retiree nominates, before a financial year starts, to receive \$1000, once a month, each month, giving $DA_t = 12,000$;
- ADA_t is the ad-hoc drawdown amount. This is the total dollar value of any lump-sum commutations made throughout the year, not including the regular payment stream nominated;
- $NIRA_t$ are net investment returns, in dollars, over financial year t ;
- AF_t are account fees deducted;
- NT_t are net transfers, e.g., rollover amount from another super fund, or receipt of spouse's death benefit.

The dependent variable in the model estimated is $y_{it} := \ln DR_{it}$, where $DR_{it} = DA_{it}/AB_{it}$; $DA_{it} \neq AB_{it} - AB_{i,t+1}$. Figure 9 shows histograms of DR_{it} and $\ln DR_{it}$ for all non-missing unit-time combinations in the superannuation data.

Figure 9: Histograms of regular drawdown rate variable and its logarithm in superannuation data.



References

- Bai, J. (2009). Panel data models with interactive fixed effects. *Econometrica*, *77*, 1229–1279. doi:[10.3982/ECTA6135](https://doi.org/10.3982/ECTA6135)
- Bateman, H., & Thorp, S. (2008). Choices and constraints over retirement income streams: Comparing rules and regulations. *Economic Record*, *84*, S17–S31. doi:[10.1111/j.1475-4932.2008.00480.x](https://doi.org/10.1111/j.1475-4932.2008.00480.x)
- Bonhomme, S., Lamadon, T., & Manresa, E. (2021). Discretizing unobserved heterogeneity. *Econometrica*, to appear.
- Bonhomme, S., & Manresa, E. (2015). Grouped patterns of heterogeneity in panel data. *Econometrica*, *83*, 1147–1184. doi:[10.3982/ECTA11319](https://doi.org/10.3982/ECTA11319)
- Deb, P., & Trivedi, P. K. (2013). Finite mixture for panels with fixed effects. *Journal of Econometric Methods*, *2*, 35–51. doi:[10.1515/jem-2012-0018](https://doi.org/10.1515/jem-2012-0018)
- Hofmans, J., Ceulemans, E., Steinley, D., & Van Mechelen, I. (2015). On the added value of bootstrap analysis for k-means clustering. *Journal of Classification*, *32*, 268–284. doi:[10.1007/s00357-015-9178-y](https://doi.org/10.1007/s00357-015-9178-y)
- Horneff, W. J., Maurer, R. H., Mitchell, O. S., & Dus, I. (2008). Following the rules: Integrating asset allocation and annuitization in retirement portfolios. *Insurance: Mathematics and Economics*, *42*, 396–408. doi:[10.1016/j.insmatheco.2007.04.004](https://doi.org/10.1016/j.insmatheco.2007.04.004)
- Jacobs, R. A., Jordan, M. I., Nowlan, S. J., & Hinton, G. E. (1991). Adaptive mixtures of local experts. *Neural Computation*, *3*, 79–87. doi:[10.1162/neco.1991.3.1.79](https://doi.org/10.1162/neco.1991.3.1.79)
- Jordan, M. I., & Jacobs, R. A. (1994). Hierarchical mixtures of experts and the EM algorithm. *Neural Computation*, *6*, 181–214. doi:[10.1162/neco.1994.6.2.181](https://doi.org/10.1162/neco.1994.6.2.181)
- Munkres, J. (1957). Algorithms for the assignment and transportation problems. *Journal of the Society for Industrial and Applied Mathematics*, *5*, 32–38. doi:[10.1137/0105003](https://doi.org/10.1137/0105003)
- Su, L., & Ju, G. (2018). Identifying latent grouped patterns in panel data models with interactive fixed effects. *Journal of Econometrics*, *206*, 554–573. doi:[10.1016/j.jeconom.2018.06.014](https://doi.org/10.1016/j.jeconom.2018.06.014)
- The Australian Government the Treasury. (2016). *Development of the framework for comprehensive income products for retirement* (Discussion Paper). Retrieved from https://consult.treasury.gov.au/retirement-income-policy-division/comprehensive-income-products-for-retirement/supporting_documents/CIPRs_Discussion_Paper_1702.pdf
- Yang, S. S., & Huang, H.-C. (2009). The impact of longevity risk on the optimal contribution rate and asset allocation for defined contribution pension plans. *The Geneva Papers on Risk and Insurance - Issues and Practice*, *34*, 660–681. doi:[10.1057/gpp.2009.18](https://doi.org/10.1057/gpp.2009.18)

Online Supplement for
'Hidden Group Time Profiles: Heterogeneous Drawdown
Behaviours in Retirement'

Igor Balnozan*[†], Denzil G. Fiebig*, Anthony Asher*, Robert Kohn*, Scott A. Sisson*

Version: 7 December 2021

Abstract

This material supplements the paper with: robustness checks to examine the sensitivity of the main results to changes in the dataset and estimation strategy; a simulation exercise to compare simulated standard errors with those estimated from the analytical formula and the bootstrap; additional details on the superannuation drawdowns dataset; further details on the proposed modification to the estimation algorithm for unbalanced data; additional descriptive results for the seven-group model; and panel plots for the two-group model.

Keywords

Panel data, discrete heterogeneity, microeconomics, retirement

JEL codes

C51, D14, G40

Acknowledgements

Balnozan is grateful for the support provided by the Commonwealth Government of Australia through the provision of an Australian Government Research Training Program Scholarship, and to State Super for provision of the State Super Academic Scholarship. Balnozan, Kohn and Sisson are partially supported by the Australian Research Council through the Australian Centre of Excellence in Mathematical and Statistical Frontiers (ACEMS; CE140100049). We thank Plan For Life, Actuaries & Researchers, who collected, cleaned and allowed us to analyse the data used in this research; this data capture forms one part of a broader survey into retirement incomes, commissioned by the Institute of Actuaries of Australia. This research includes computations using the computational cluster Katana supported by Research Technology Services at UNSW Sydney. Katana DOI: 10.26190/669x-a286

Conflict of interest statement

The authors have no conflict of interest to declare.

*University of New South Wales, UNSW Sydney, NSW 2052, Australia

[†]Correspondence: i.balnozan@unsw.edu.au / West Lobby Level 4, UNSW Business School Building, UNSW Sydney, NSW 2052, Australia.

1 More details on ‘Extension 2: Alternative estimation method for unbalanced data’

We now justify the claims made in Section 4.5 of the paper about the relationship between the three methods for estimating time profiles with balanced and unbalanced data.

Lemma 1. Methods 1–3 estimate the same time profiles in the balanced data case.

Proof. The regression equation being estimated by method 3 (no constant term; $T-1$ time-demeaned time dummy variables, $\dot{\delta}_s$) is

$$\dot{y}_{it} = \dot{x}'_{it}\theta + \sum_{s=2}^T \tilde{\alpha}_s \dot{\delta}_s + \dot{v}_{it}, \quad (1)$$

where $\dot{\delta}_s := \delta_s - T^{-1} \sum_{l=1}^T \delta_l$; $\delta_l = \mathbb{I}\{t=l\}$. $\dot{\delta}_s = \delta_s - T^{-1}$, as $\sum_{l=1}^T \delta_l = 1$ for all t . Thus, (1) can be rewritten using time dummy variables, δ_s , instead of time-demeaned time dummy variables, $\dot{\delta}_s$, as

$$\dot{y}_{it} = \dot{x}'_{it}\theta + \dot{\alpha}_1 + \sum_{s=2}^T \tilde{\alpha}_s \delta_s + \dot{v}_{it}, \quad (2)$$

where $\dot{\alpha}_1 := -T^{-1} \sum_{s=2}^T \tilde{\alpha}_s$.

(2) is precisely the regression equation being estimated by method 2 (include constant term; $T-1$ time dummy variables, δ_s). Defining $\dot{\alpha}_s := \dot{\alpha}_1 + \tilde{\alpha}_s$ for $s = 1, 2, \dots, T$, (2) can be rewritten as

$$\dot{y}_{it} = \dot{x}'_{it}\theta + \sum_{s=1}^T \dot{\alpha}_s \delta_s + \dot{v}_{it}, \quad (3)$$

because $\dot{\alpha}_1 + \sum_{s=2}^T \tilde{\alpha}_s \delta_s = \dot{\alpha}_1 \delta_1 + \sum_{s=2}^T \dot{\alpha}_s \delta_s$.

(3) is the regression equation estimated by method 1 (no constant term; T time dummy variables, δ_s).

Combining $\dot{\alpha}_1 = -T^{-1} \sum_{s=2}^T \tilde{\alpha}_s$ with $\dot{\alpha}_s = \dot{\alpha}_1 + \tilde{\alpha}_s$ implies $\sum_{t=1}^T \dot{\alpha}_t = \dot{\alpha}_1 + \sum_{t=2}^T \dot{\alpha}_t = \dot{\alpha}_1 + \sum_{t=2}^T (\dot{\alpha}_1 + \tilde{\alpha}_t) = \dot{\alpha}_1 + (T-1)\dot{\alpha}_1 - T\dot{\alpha}_1 = 0$.

The conversion between $\dot{\alpha}_s$ and $\tilde{\alpha}_s$ terms is similar to the transformation used in [Suits \(1984, p. 178\)](#), but applied to a model with no constant term.

Lemma 2. With unbalanced data, method 1 does not guarantee that $\sum_{t=1}^T \hat{\alpha}_t = 0$.

Proof. Consider a special case with no covariates and $T = 2$ as an illustration. The corresponding regression equation is

$$\dot{y}_{it} = \dot{\alpha}_1 \delta_1 + \dot{\alpha}_2 \delta_2 + \dot{v}_{it},$$

or equivalently, $\dot{y}_{i1} = \dot{\alpha}_1 \delta_1 + \dot{v}_{i1}$ and $\dot{y}_{i2} = \dot{\alpha}_2 \delta_2 + \dot{v}_{i2}$.

The least-squares estimators of $\dot{\alpha}_1$ and $\dot{\alpha}_2$ are $\hat{\alpha}_s = N_s^{-1} \sum_{i \in \mathcal{I}_s} (y_{i,s} - \bar{y}_i)$ for $s = 1, 2$, where \mathcal{I}_s is the set of units observed in period s ; N_s is the number of elements in \mathcal{I}_s ; $\bar{y}_i := T_i^{-1} \sum_{t \in \tau_i} y_{it}$; τ_i is the set of periods in which unit i is observed; T_i is the number of elements in τ_i . Then, $\hat{\alpha}_1 + \hat{\alpha}_2 =: A - B$, where $A := N_1^{-1} \sum_{i \in \mathcal{I}_1} y_{i,1} + N_2^{-1} \sum_{i \in \mathcal{I}_2} y_{i,2}$, and $B := N_1^{-1} \sum_{i \in \mathcal{I}_1} \bar{y}_i + N_2^{-1} \sum_{i \in \mathcal{I}_2} \bar{y}_i$.

When the panel is balanced, $N_1 = N_2 = N$, $\mathcal{I}_1 = \mathcal{I}_2 = \{1, 2, \dots, N\}$, and $T_i = T = 2$ for all i . Then, $A = B = T\bar{y}$, where $\bar{y} := (N_1 + N_2)^{-1} (\sum_{i \in \mathcal{I}_1} y_{i,1} + \sum_{i \in \mathcal{I}_2} y_{i,2}) = (NT)^{-1} (\sum_{i=1}^N \sum_{t=1}^T y_{it})$, so that $\hat{\alpha}_1 + \hat{\alpha}_2 = 0$. In general, however, with unbalanced data this zero-sum is not guaranteed: a counter-example is the dataset

$$\{y_{it}\} = \begin{bmatrix} 1 & 2 \\ 3 & . \\ 4 & 5 \end{bmatrix},$$

which has $A = 6 + \frac{1}{6} \neq B = 6 + 1.5 \neq T\bar{y} = 6$.

Lemma 3. Method 3 can be used on unbalanced data while ensuring that $\sum_{t=1}^T \hat{\alpha}_t = 0$.

Proof. By construction, method 3 estimates $T - 1$ terms, $\hat{\alpha}_t$ for $t = 2, 3, \dots, T$, then computes $\hat{\alpha}_1 = -T^{-1} \sum_{t=2}^T \hat{\alpha}_t$ and $\hat{\alpha}_t = \hat{\alpha}_1 + \hat{\alpha}_t$ for $t = 2, 3, \dots, T$, which ensures that $\sum_{t=1}^T \hat{\alpha}_t = 0$.

Other comments. The unmodified GFE model estimate obtains the time profiles arising from interacting group identity with a set of T time dummy variables, analogous to using method 1 in the $G = 1$ case. In the modified procedure's parameter update step, the algorithm interacts the group identity with $T - 1$ time-demeaned time dummy variables, generating $G(T - 1)$ estimates of relative effects $\tilde{\alpha}_{gt} := \dot{\alpha}_{gt} - \dot{\alpha}_{g,1}$; this is analogous to method 3 for $G = 1$. As the GFE algorithm requires GT estimates of the $\dot{\alpha}_{gt}$ to compute the sum of squared residuals across all i and t , it is necessary to perform the conversion step from the $T - 1$ estimates of the $\tilde{\alpha}_{gt}$ to T estimates of the $\dot{\alpha}_{gt}$, for each of the G time profiles.

2 Robustness checks

This section explores the sensitivity of the main results to changes in data composition and estimation methodology.

2.1 Data composition

The first robustness check determines whether the results depend materially on using a balanced subsample of each fund's data. It uses the same model as the main results, but the data is filtered down to retain a fully balanced sample, leaving $N = 8274$ units in the sample.

Covariate effects

Figure 1 plots covariate effect estimates for different values of G using the fully balanced subsample. Like the dataset used for the main results in the paper, the fully balanced subsample supports a seven-group model using the selection method in the paper.

Time profiles

Figure 2 plots the time profiles for $G = 4-9$ using the fully balanced subsample. Figure 3 shows the time profiles for $G = 7$, with element-wise confidence intervals computed using standard error estimates derived from the fixed- T variance estimate formula. While the numerical values differ, the economic interpretation of these results is similar to the interpretation of the main results in the paper.

2.2 Estimation methodology

2.2.1 Number of starting values

The number of possible allocations of N units into G groups is G^N , and solutions found by the GFE procedure depend on starting values for the algorithm (Bonhomme & Manresa, 2015); hence, as N and G increase, the GFE procedure is more likely to find a local, rather than global, optimum. This may require an increasing number of randomly selected starting values for the algorithm to adequately explore the solution space, if individual runs become trapped in regions around local optima.

To test the sensitivity of the main results to the choice of 1000 starting values, Figure 4 provides the estimated group time profiles from the equivalent estimation using 1 million starting values. With 1000 starting values, the objective function value is 2673.732, while with 1 million starting values the value is 2673.716. This change in the sum of squared errors across 107,935 data points is small, suggesting there is little gained from running the estimation procedure for more than 1000 starting values; the following paragraphs investigate whether there are any economically meaningful differences in the results with 1 million starting values compared to the main results.

The time profiles are nearly identical to those from the main results in the paper. The largest absolute difference in any pair of corresponding time profile value estimates is approximately 1.49×10^{-3} . With 1 million starting values, using the group labels as in the main results in the paper, group 4 contains four more people, group 7 has one person less and group 5 has three fewer people, compared to the run with 1000 starting values.

Table 1 also provides the covariate effect estimates for the estimation with 1 million starting values. The estimates and standard errors are identical to those in the main results to three decimal places. The largest difference in estimated effect magnitudes is approximately 2.87×10^{-4} , for the coefficient on the log minimum drawdown rate variable. These results suggest that the economic interpretation of the main results in the paper are robust to the number of starting values used; however, it is still possible that there exists a more optimal solution with

Figure 1: Fully balanced subsample – Point estimates and 95% confidence intervals for partial effects of log minimum drawdown rate and log account balance covariates on log regular drawdown rate, controlling for group-level time-varying unobservable heterogeneity assuming $G = 1, 2, \dots, 16$. Shaded regions denote confidence intervals constructed using standard errors derived from fixed- T variance estimate formula.

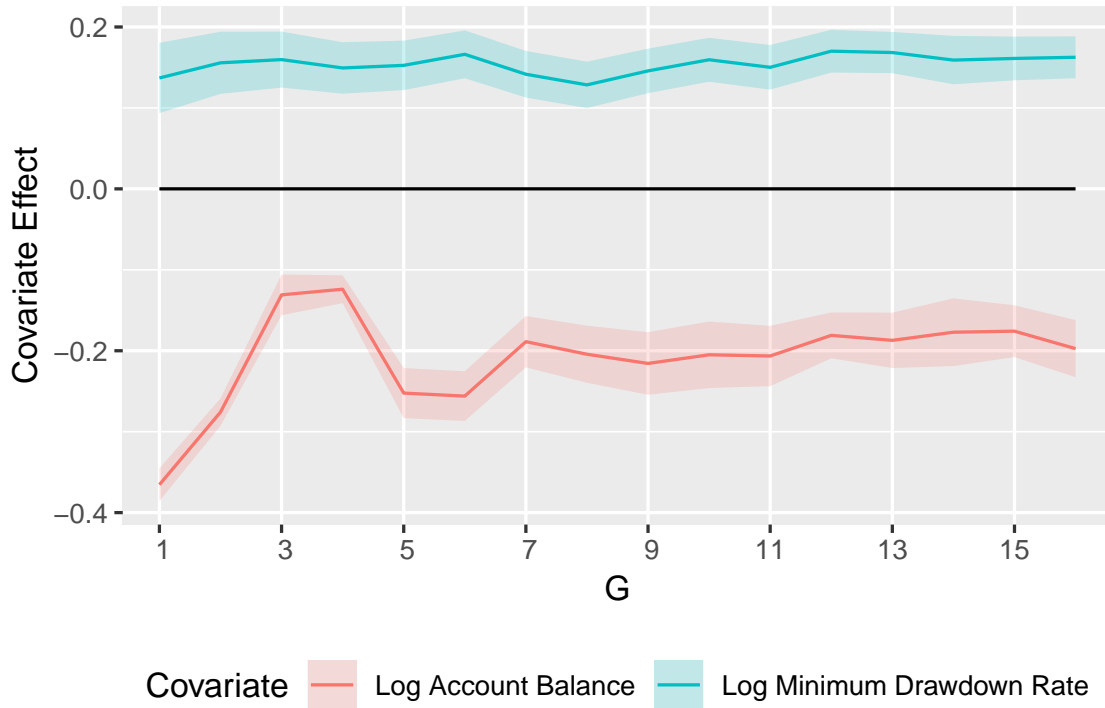


Figure 2: Fully balanced subsample – Point estimates for effects of group-level time-varying unobservable heterogeneity on log regular drawdown rates assuming $G = 4, 5, \dots, 9$. Estimated time-demeaned group time profiles shifted to begin at 0 on the vertical axis.

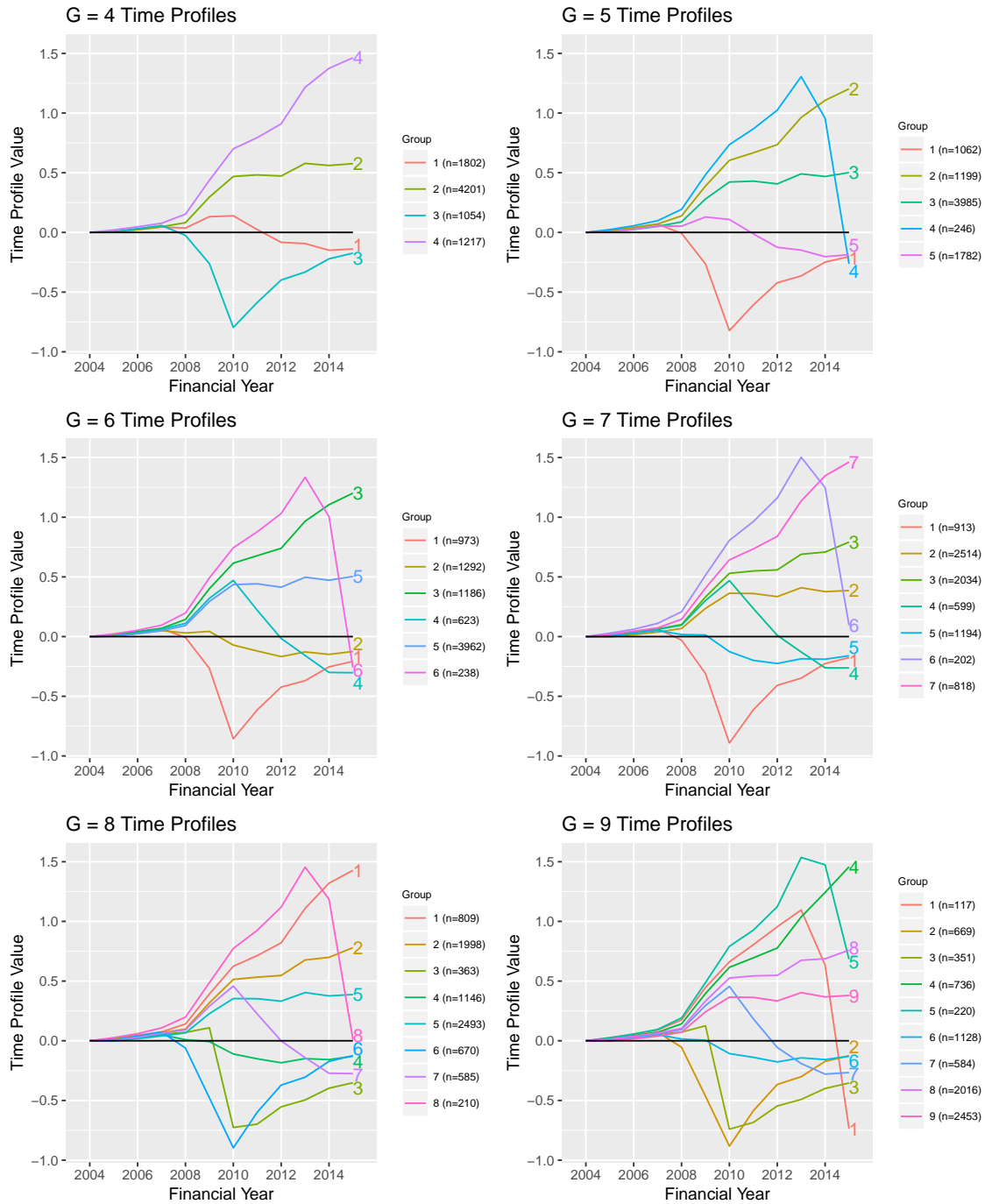


Figure 3: Fully balanced subsample – Point estimates and 95% confidence intervals from analytical formula for effects of group-level time-varying unobservable heterogeneity on log regular drawdown rates assuming $G = 7$. Shaded regions denote 95% element-wise confidence intervals constructed using standard errors derived from fixed- T variance estimate formula. Time-demeaned group time profiles shifted to begin at 0 on the vertical axis.

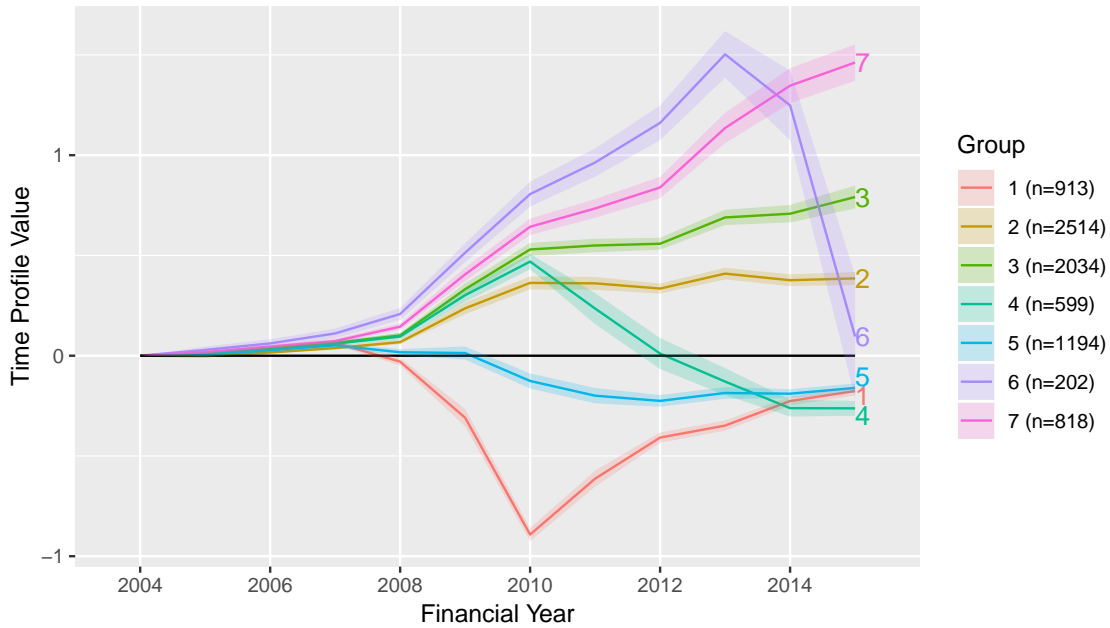
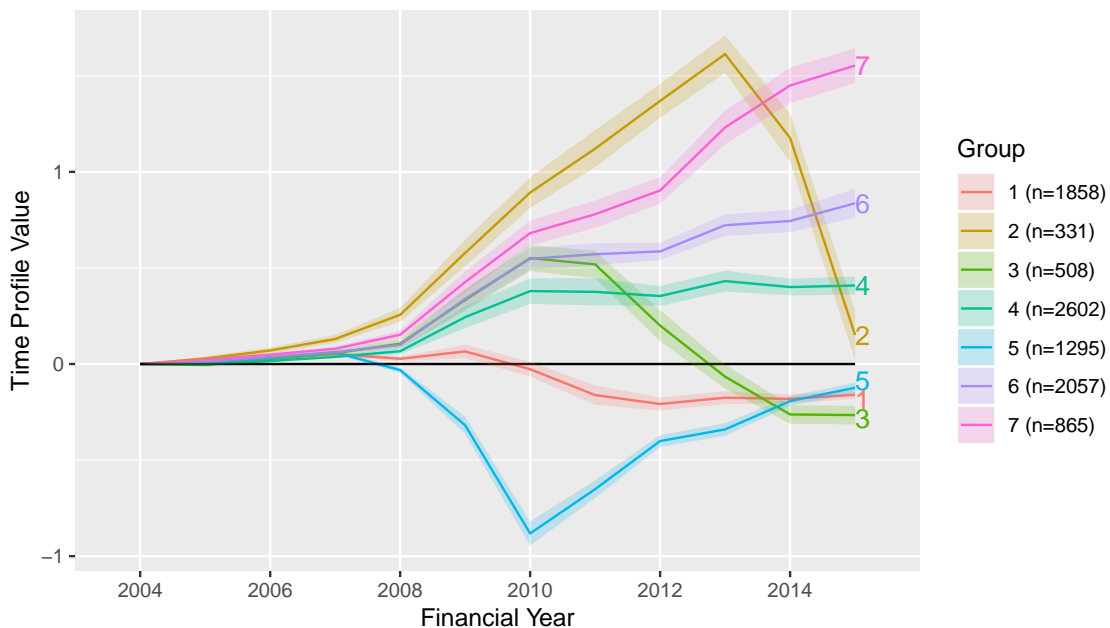


Figure 4: One million starting values – Point estimates and 95% confidence intervals from analytical formula for effects of group-level time-varying unobservable heterogeneity on log regular drawdown rates assuming $G = 7$. Shaded regions denote 95% element-wise confidence intervals derived from fixed- T variance estimate formula. Time-demeaned group time profiles shifted to begin at 0 on the vertical axis.



materially different results for the covariate effects or time profiles that was not found using 1 million starting values.

2.2.2 Unmodified estimation procedure

The paper uses a modified estimation method for unbalanced data, having the property that for $G = 1$, the results align precisely with those obtained by running a standard two-way fixed-effects regression model. Comparison output is presented here, using the unmodified algorithm to test the sensitivity of the main results in the paper to this alternative procedure.

Figure 5 shows how the covariate effect estimates evolve with G . Overall, the results for the log account balance variable appear almost identical to those in the main results. Although the results for the log minimum drawdown rate differ more significantly in magnitude to those in the main results, their economic implications are similar.

Figure 6 presents time profile point estimates for $G = 4, 5, \dots, 9$. Figure 7 shows the time profile plot for $G = 7$, including 95% element-wise confidence intervals constructed using standard errors derived from the fixed- T variance estimate formula. The plots show that the time profiles obtained from both estimation strategies are similar.

Figure 8 shows the time profile plot for $G = 1$, with axes identical to the corresponding time profile plot in the main results section of the paper. Comparing the plots reveals that the point estimates differ depending on the algorithm used, and the economic interpretations of time effects around financial year 2008 are different. Using the unmodified procedure suggests a small downward effect in 2008 followed by a gradual rise, while this initial drop is absent in the corresponding plot created using the modified algorithm in the paper.

3 Simulation exercise

This section uses simulation evidence to argue for the validity of the GFE procedure in applications with data resembling the superannuation dataset. It also uses the proposed method for matching labels between estimations to investigate how standard errors derived from the fixed- T variance estimate formula and the bootstrap compare to the simulated standard errors estimated across simulations.

Table 1: One million starting values – Point estimates and 95% confidence intervals for partial effects of log minimum drawdown rate and log account balance covariates on log regular drawdown rate, controlling for group-level time-varying unobservable heterogeneity assuming $G = 6$. Standard errors are derived from fixed- T variance estimate formula.

Covariate	Estimate (Standard Error)
Log Minimum Drawdown Rate	0.144 (0.0248)
Log Account Balance	-0.147 (0.0139)

Figure 5: Unmodified estimation procedure – Point estimates and 95% confidence intervals for partial effects of log minimum drawdown rate and log account balance covariates on log regular drawdown rate, controlling for group-level time-varying unobservable heterogeneity assuming $G = 1, 2, \dots, 16$. Shaded regions denote confidence intervals constructed using standard errors derived from fixed- T variance estimate formula.

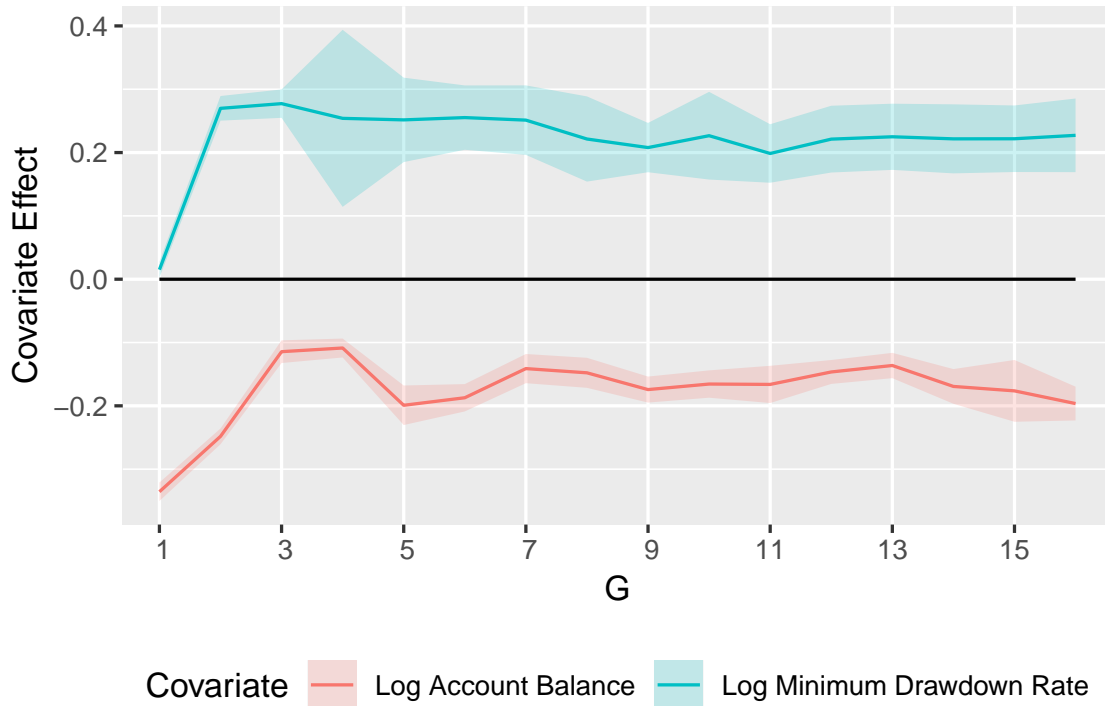


Figure 6: Unmodified estimation procedure – Point estimates for effects of group-level time-varying unobservable heterogeneity on log regular drawdown rates assuming $G = 4, 5, \dots, 9$. Estimated time-demeaned group time profiles shifted to begin at 0 on the vertical axis.

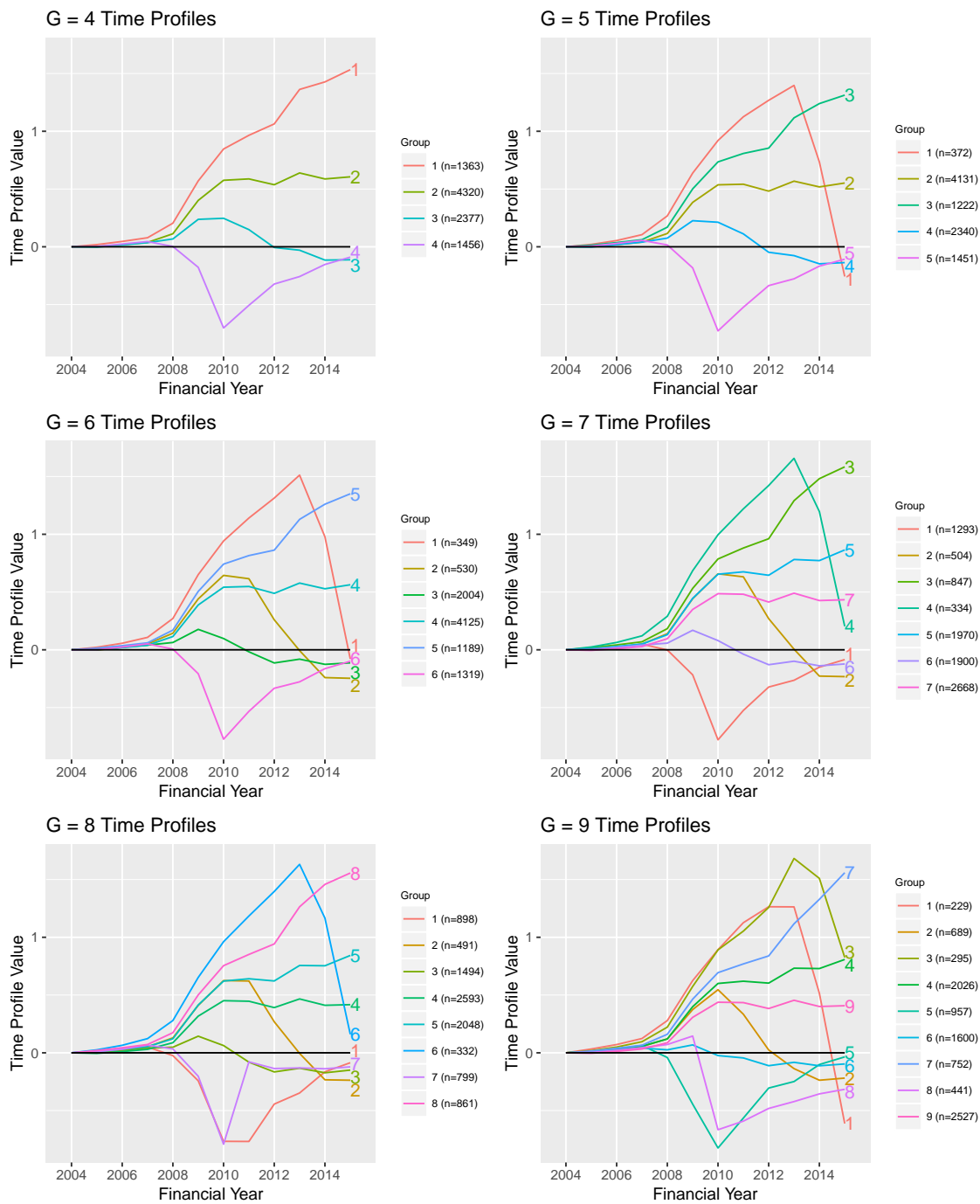


Figure 7: Unmodified estimation procedure – Point estimates and 95% confidence intervals from analytical formula for effects of group-level time-varying unobservable heterogeneity on log regular drawdown rates assuming $G = 7$. Shaded regions denote 95% element-wise confidence intervals constructed using standard errors derived from fixed- T variance estimate formula. Time-demeaned group time profiles shifted to begin at 0 on the vertical axis.

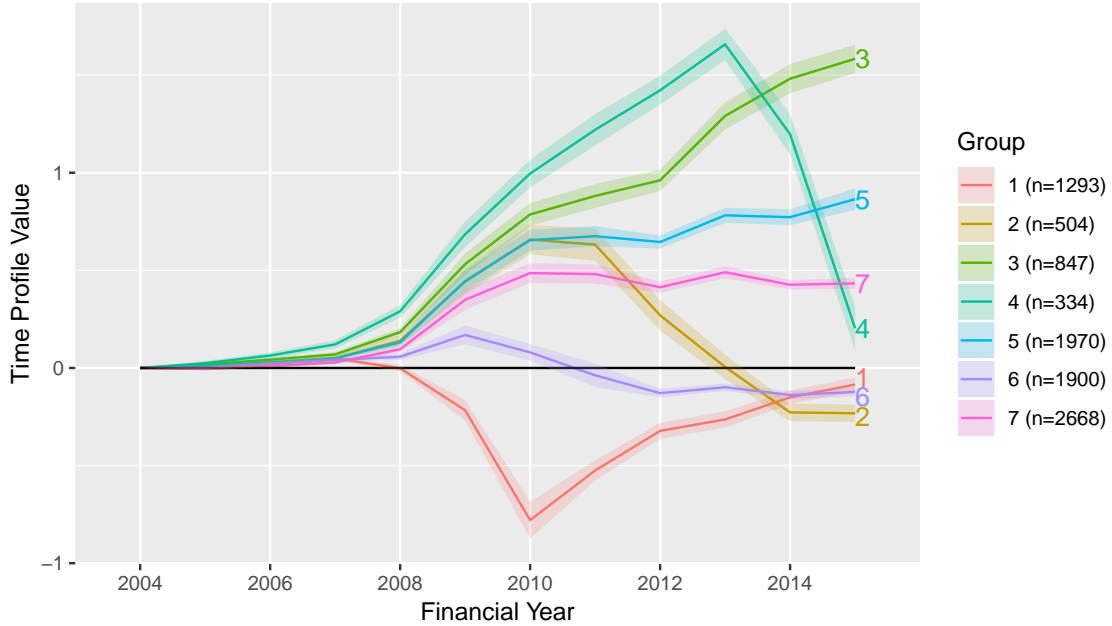
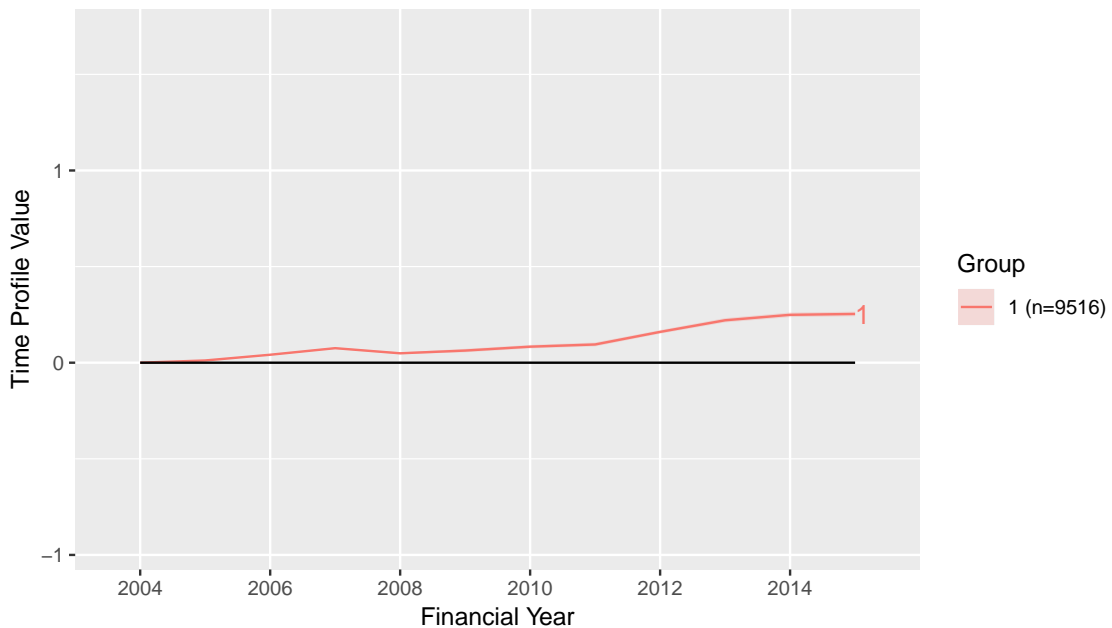


Figure 8: Unmodified estimation procedure – Point estimates and 95% confidence intervals from analytical formula for effects of group-level time-varying unobservable heterogeneity on log regular drawdown rates assuming $G = 1$. Shaded regions (indistinguishable from point estimates in plot) denote 95% element-wise confidence intervals constructed using standard errors derived from fixed- T variance estimate formula. Time-demeaned group time profiles shifted to begin at 0 on the vertical axis.



3.1 Simulation methodology

Creating the simulated datasets and a framework for analysing the results are now described.

3.1.1 Generating simulated data

Consider the data generating process (DGP)

$$\dot{y}_{it}^* := \dot{x}_{it}^{*\prime} \hat{\theta} + \hat{\alpha}_{git} + \dot{v}_{it}^*, \quad (4)$$

where:

- $\dot{x}_{it}^* = (\dot{x}_{1,it}^*, \dot{x}_{2,it}^*)'$ is a column vector of simulated covariate values for unit i at time t ;
- $\hat{\theta}$ and $\hat{\alpha}_{git}$ are the GFE estimates for the covariate effects and time-demeaned group time profiles from the main results in the paper, respectively;
- the simulated covariates have mean zero and there is no time-constant individual-specific fixed effect – that is, the generated data resembles the true data after time-demeaning;
- $\dot{x}_{k,it}^* \sim N(0, \hat{\sigma}_{\dot{x}_k}^2)$, where $\hat{\sigma}_{\dot{x}_k}^2$ is the sample variance of all values of the $\dot{x}_{k,it}$, for $k = 1, 2$;
- $\dot{v}_{it}^* \sim N(0, \hat{\sigma}_{\dot{v}}^2)$, where $\hat{\sigma}_{\dot{v}}^2$ is the sample variance of the empirical residuals $\hat{v}_{it} := \dot{y}_{it} - \dot{x}_{it}^{*\prime} \hat{\theta} - \hat{\alpha}_{git}$;
- $\dot{x}_{k,it}^*$ are generated using a method that induces correlation between the time profile values $\hat{\alpha}_{git}$ and the covariates $\dot{x}_{k,it}^*$, for $k = 1, 2$; this approximates the correlation observed in the data. The details of this are given below.

A simulation exercise using data simulated from (4) with the $\dot{x}_{k,it}^*$ uncorrelated with $\hat{\alpha}_{git}$ would be unfaithful to the challenges involved in estimating the model on the original data. Recall that the GFE method allows for arbitrary correlation between the covariates and the unobserved grouped fixed effects. Moreover, in the absence of correlation between $\dot{x}_{k,it}^*$ and $\hat{\alpha}_{git}$, a standard two-way fixed-effects regression of \dot{y} on the \dot{x} -es directly obtains unbiased estimates $\hat{\theta}$. Thus, recovering accurate estimates using the simulated data is unrealistically easy if the covariates are uncorrelated with the time profiles.

A realistic exercise simulates correlation between the covariates and the time profiles to match that observed in the data. Using the data to estimate the correlation statistics $\hat{\rho}_{k,g}$, for all (k, g) , allows a flexible correlation structure. The $\hat{\rho}_{k,g}$ values are the correlations between values of $\dot{x}_{k,it}^*$ and values of $\hat{\alpha}_{git}$; i.e., $\hat{\rho}_{k,g}$ is the correlation between the value of covariate k and the value contributed to the dependent variable by individual i 's group time profile. The $\hat{\rho}_{k,g}$ are estimated for all (k, g) by:

1. filtering the observed data to keep only records where $g_i = g$;
2. computing the sample correlation statistic between the observed values of $\dot{x}_{k,it}^*$ and corresponding estimated values of $\hat{\alpha}_{git}$; call this value $\hat{\rho}_{k,g}$.

Having estimated the correlation statistics, the aim is to generate Gaussian random variables $\dot{x}_{k,it}^*$ which have correlation $\hat{\rho}_{k,g}$ with the $\hat{\alpha}_{git}$. The following procedure induces this correlation structure, treating the model estimates of $\hat{\alpha}_{gt}$ for $(g, t) \in \{1, 2, \dots, G\} \times \{1, 2, \dots, T\}$ as if

they had been drawn from a Gaussian distribution. For all $(k, i, t) \in \{1, 2\} \times \{1, 2, \dots, N\} \times \{1, 2, \dots, T\}$:

1. set $W_{1,kit} = \hat{\alpha}_{g_i t} / \hat{\sigma}_\alpha$, where $\hat{\sigma}_\alpha$ is estimated using the sample standard deviation of the set of $G \times T$ estimated values $\hat{\alpha}_{gt}$;
2. draw $W_{2,kit} \sim N(0, 1)$;
3. set $W_{3,kit} = \hat{\rho}_{k, g_i} W_{1,kit} + \sqrt{1 - \hat{\rho}_{k, g_i}^2} W_{2,kit}$;
4. set $\hat{x}_{k, it}^* = \hat{\sigma}_{\hat{x}_k} W_{3,kit}$, where $\hat{\sigma}_{\hat{x}_k}$ is the sample standard deviation of all observed values of covariate \hat{x}_k .

The error term $\hat{v}_{it}^* \sim N(0, \hat{\sigma}_v^2)$, and (4) gives the simulated values of the dependent variable \hat{y}^* . The GFE procedure with $G = 7$ is then run on a large number of simulated datasets. Comparing the GFE estimation results to the DGP values checks the validity of the GFE procedure applied to this setting and the code implementing the method.

3.1.2 Framework for interpreting results

The simulation exercise investigates the following properties of the GFE estimator:

1. Whether the GFE procedure applied to a known DGP, constructed from the results of applying the GFE procedure to the superannuation dataset, estimates the DGP accurately in simulated datasets whose dimensions are the same as in the superannuation dataset.
2. The closeness of the confidence intervals derived from the fixed- T variance estimate formula to the ‘simulated’ confidence intervals—the intervals obtained by matching time profile estimates across a large number of simulated datasets and observing the empirical spread of estimates.
3. The closeness of the simulated confidence intervals to the bootstrap confidence intervals—the intervals obtained by matching time profile estimates across a large number of bootstrap samples drawn from the first simulated dataset and observing the empirical spread of the estimates.

The following steps are used to generate the simulation results:

1. $M = 1000$ datasets are generated independently from the DGP, each with $N = 9516$ units and covering $T = 12$ time periods. The GFE procedure is then run on each of these using 1000 random starting values for each estimation, and the standard errors are obtained from the fixed- T variance estimate formula.
2. Using the resulting set of M estimates of $\hat{\theta}$ and $\hat{\alpha} := \{\hat{\alpha}_{gt}\}_{(g,t) \in \{1,2,\dots,G\} \times \{1,2,\dots,T\}}$ as samples $\{\hat{\theta}^{(m)}\}_{m=1}^M$ and $\{\hat{\alpha}^{(m)}\}_{m=1}^M$ from the sampling distributions of the estimators, simulated standard errors and 95% element-wise confidence intervals are estimated.
3. All bootstrap results are obtained by creating $B = 1000$ bootstrap replicate datasets using the method outlined in the methodology section of the paper—except that here the first simulated dataset is treated as the source dataset for the bootstrap sampling. The GFE procedure with $G = 7$ is then run on each of the resulting bootstrap replicate

datasets. The bootstrap results that follow are different to the results obtained in the main results section of the paper, which use the observed data as the source dataset for bootstrap sampling.

4. Estimated time profiles are compared to the DGP time profiles after shifting all time profiles to begin at 0.

3.2 Results

For the first property listed in Section 3.1.2, the input values used for the DGP are compared to those estimated using the GFE procedure on the first simulated dataset. Figure 9 shows this comparison for the time profiles; Table 2 compares the covariate effects numerically. The results are close and suggest that the GFE procedure recovers the parameters of the DGP with a high degree of accuracy.

Figure 10 summarises the distribution of time profile estimates across all 1000 simulated datasets. The 95% element-wise confidence interval bounds represent the empirical 2.5 and 97.5 percentiles of each estimated value. The tightness of these confidence intervals around the DGP values suggests that in most simulated datasets, the time profile estimates are numerically close to the true values, and economically indistinguishable—meaning the interpretations of the time profiles are the same. The DGP time profile values for group 7 tend to be close to the upper bounds of the simulated empirical 95% intervals, and for the terminal time period, are slightly above the upper bound.

Table 3 makes the corresponding comparison for the covariate effects. The simulated confidence intervals surround the DGP values; however, for both covariates, the DGP estimates are relatively close to the upper bounds of the intervals.

For the second property listed in Section 3.1.2, Figure 10 is compared to Figure 11. Figure 11 shows time profile estimates and 95% element-wise confidence intervals constructed from standard errors derived from the fixed- T variance estimate formula, where the input data is the first simulated dataset. The plots are nearly indistinguishable up to group relabelling, suggesting that the fixed- T variance estimate formula applied to the first simulated dataset estimates the true standard errors with reasonable precision. Table 4 gives a similar comparison for the covariate effects, and has the same interpretation.

As with the previous comparison, all 1000 simulated datasets are considered next, by comparing the empirical distribution of estimated standard errors—derived from the results of applying the fixed- T variance formula to 1000 simulated datasets—to the simulated standard errors—computed by calculating the sample standard deviation of parameter estimates across

Table 2: DGP covariate effects vs. first simulated dataset estimates.

	Log Minimum Drawdown Rate	Log Account Balance
DGP	0.1436	-0.1472
First simulated dataset	0.1445	-0.1490

Figure 9: DGP time profiles vs. first simulated dataset estimates. Red series represent DGP values, blue series are time profile estimates derived from the first simulated dataset. Time-demeaned group time profiles shifted to begin at 0 on the vertical axis.

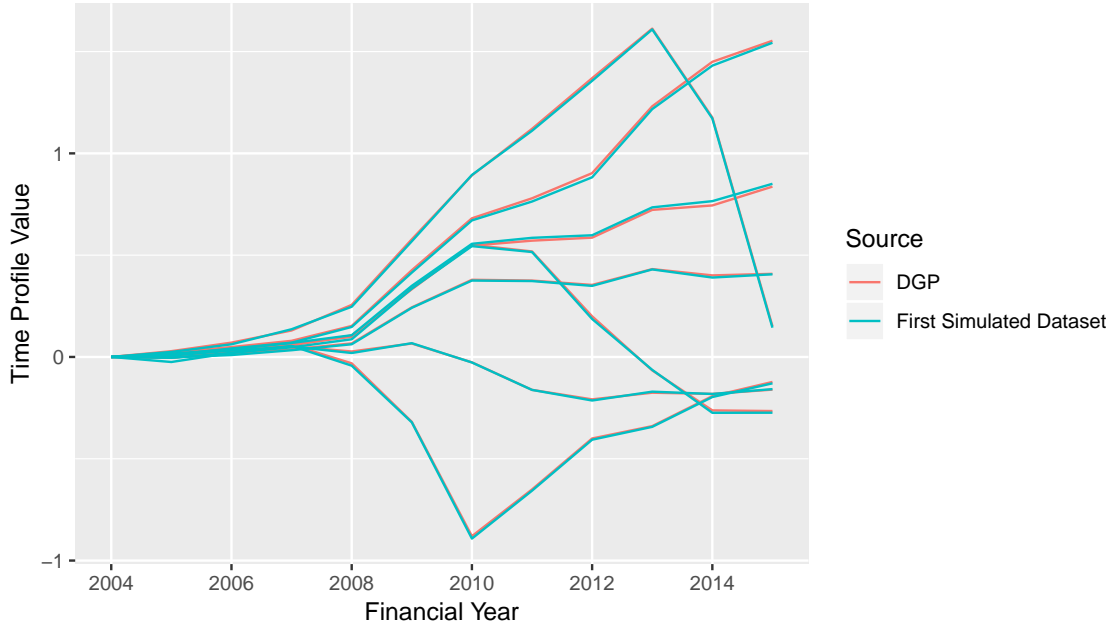


Figure 10: DGP time profiles and simulated 95% CIs. Time-demeaned group time profile values are the inputs to the DGP and here shifted to begin at 0 on the vertical axis. Shaded regions denote 95% element-wise confidence intervals computed from empirical percentiles of the shifted, time-demeaned group time profile estimates across 1000 simulated datasets.

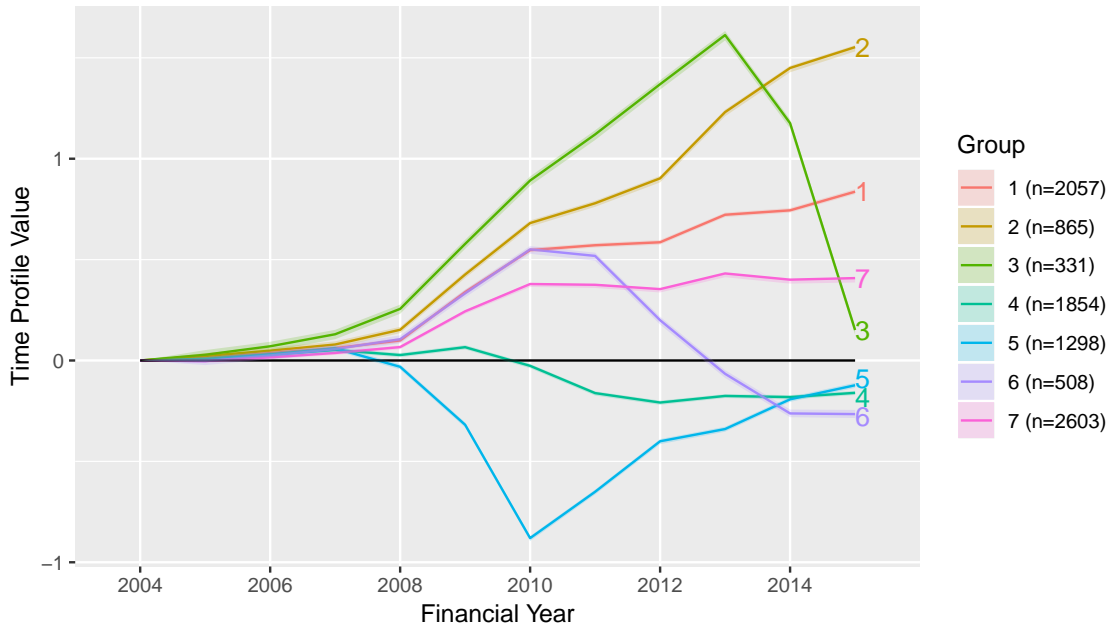


Table 3: DGP covariate effects and simulated 95% CIs.

	Log Minimum Drawdown Rate	Log Account Balance
DGP value	0.1436	-0.1472
Simulated 95% CIs	[0.1340, 0.1459]	[-0.1522, -0.1471]

Simulated 95% CI bounds represent empirical 2.5 and 97.5 percentiles of the estimated covariate effects across 1000 simulated datasets.

Figure 11: Time profile estimates from first simulated dataset, CIs from formula. Time-demeaned group time profile values from GFE estimation on first simulated dataset and shifted to begin at 0 on the vertical axis. Shaded regions denote 95% element-wise confidence intervals derived from fixed- T variance estimate formula.

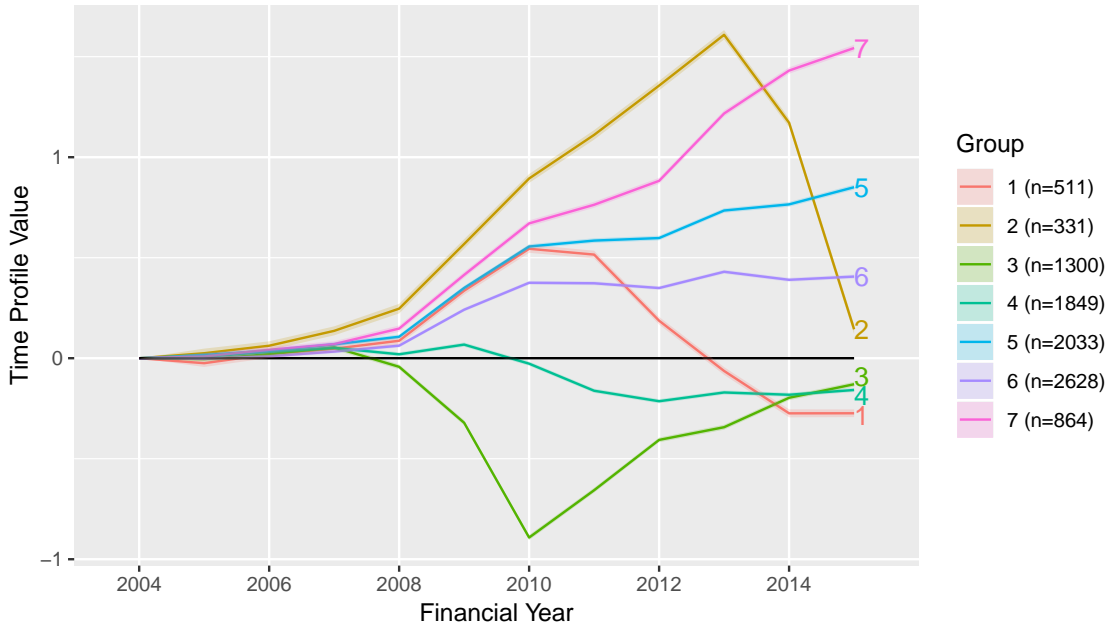


Table 4: Covariate effect estimates from first simulated dataset, CIs from formula.

	Log Minimum Drawdown Rate	Log Account Balance
Covariate Effect Estimate	0.1445	-0.1490
95% CI based on formula	[0.1415, 0.1475]	[-0.1515, -0.1465]

95% CIs derived from fixed- T variance estimate formula.

the 1000 simulated datasets. Table 5 provides the figure references for the standard error distribution plots by group of the time-demeaned group time profile values, shifted to begin at zero in the first time period, corresponding to the financial year ended 30 June 2004. For each group, the plots show the empirical distribution of the standard errors for estimates corresponding to financial years 2005 to 2015, inclusive. The group labels follow Figure 10, which shows the group time profiles with element-wise confidence intervals derived from the simulated standard errors. These are the same group labels presented in the figures for the main results in the paper. In general, the simulated standard error value is in an area of nontrivial density in the corresponding empirical standard error distribution.

Figure 12 provides the corresponding plots for standard errors of the covariate estimates. The fixed- T variance estimate formula tends to overestimate the true standard error for the first covariate; for the second covariate, the true standard error is more centrally located in the distribution of empirical standard errors.

Figures 10 and 13 are compared for the third property listed in Section 3.1.2. Figure 13 gives time profile estimates and 95% element-wise confidence intervals constructed from the empirical distribution of estimates across 1000 bootstrap replications, where the input data is the first simulated dataset. The results are again nearly indistinguishable up to group relabelling. This suggests that inference conducted using the bootstrap procedure gives almost identical results to that using the fixed- T variance estimate formula, which approximates the true standard errors well. Ideally, the bootstrap procedure would be performed on all 1000 simulated datasets, and the resulting distributions of bootstrap standard errors compared to the simulated standard errors, as done for the fixed- T variance estimate formula. However, computational constraints prevent this.

Considering the simulation evidence, the fixed- T variance estimate formula performs well in datasets simulated from the generating process implied by the GFE estimation results for the superannuation dataset. This suggests that if the GFE assumptions are satisfied, the analytical formula may be adequate in datasets of similar size to the superannuation dataset, not requiring the bootstrap procedure for inference on the parameter estimates. This is important as using our code to perform the bootstrap on the superannuation dataset is currently too computationally intensive to run on a standard machine; it requires access to a high-

Table 5: Lookup table – Standard error distributions for time profile estimates. Groups labelled as per Figure 10.

Group Label	Figure
1	18
2	19
3	20
4	21
5	22
6	23
7	24

Figure 12: Covariate effect analytical SE distributions across simulated datasets. Black lines plot the kernel density estimate for standard errors derived from the fixed- T variance estimate formula after estimating the GFE model on 1000 simulated datasets. Red vertical lines represent the value of the simulated standard error.

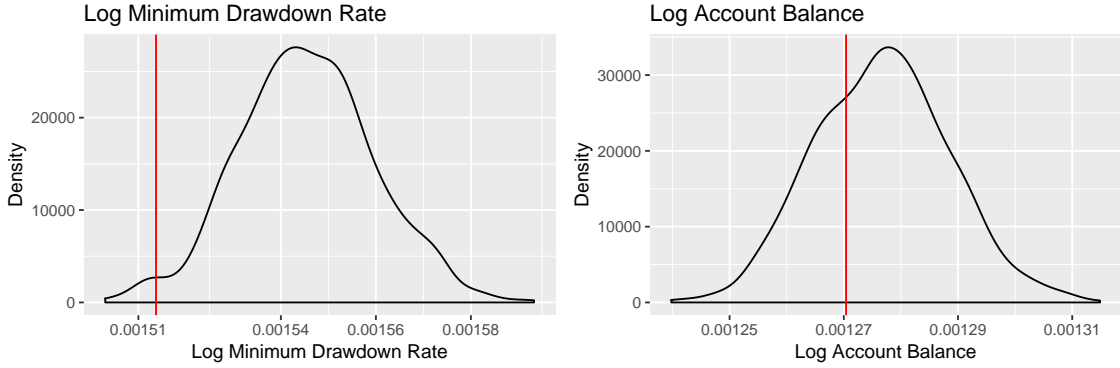
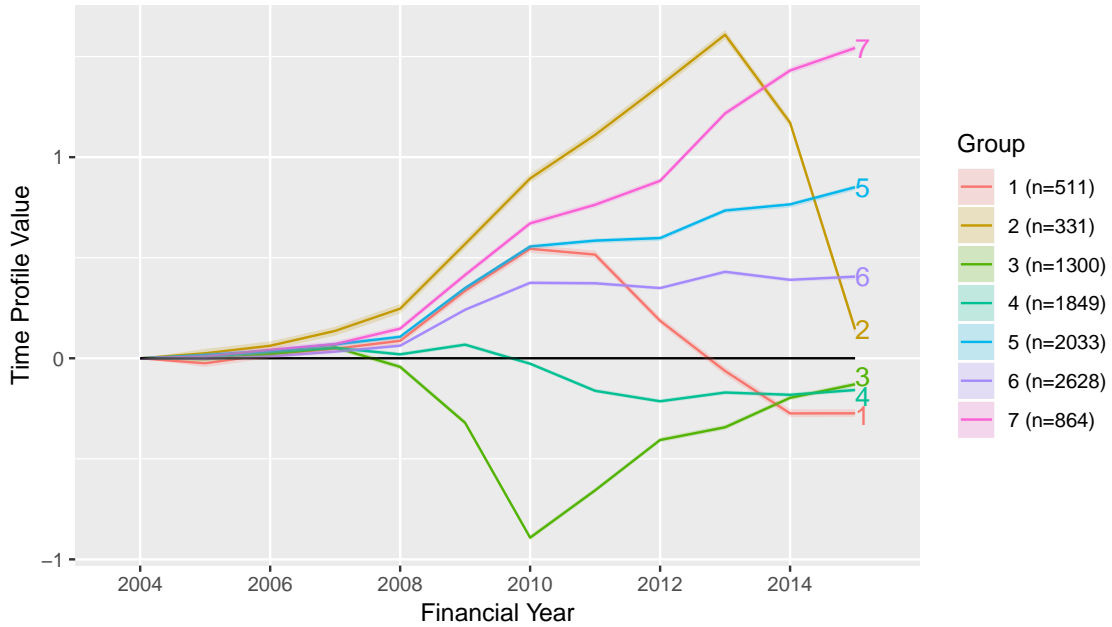


Figure 13: Time profile estimates from first simulated dataset, CIs from bootstrap. Results from point estimates aggregated over 1000 bootstrap replications using the first simulated dataset to generate bootstrap replicate datasets. Time-demeaned group time profile values from GFE estimation on first simulated dataset and shifted to begin at 0 on the vertical axis. Shaded regions denote 95% element-wise confidence intervals computed from empirical percentiles across 1000 bootstrap replications.



performance computing cluster. As for the bootstrap results on the simulated data, these suggest that the bootstrap may also perform comparably well; however, due to computational constraints, our implementation is unable to test this as rigorously as for the analytical formula.

4 Superannuation drawdowns dataset

4.1 More on covariate selection

Possible covariates for the analysis included in the dataset are limited to age, account balance and gender. From the available information, two derived covariates are also constructed: the minimum drawdown rate, and a crude estimate of an individual’s risk appetite over the observation period. For each person–year observation, the age of the member maps to the relevant minimum drawdown rate the retiree is constrained by, with concessional reductions in the rates applying to the 2009–2013 financial years.

As the risk appetite variable is only used descriptively, and does not enter into the model estimation, its preciseness does not affect the main results. Its construction involves observing movements in account balances and comparing these with the amounts drawn down and contributed to the funds by retirees. From this, ignoring administrative fees on the accounts, one can roughly estimate the return on assets. As the source data is at a monthly frequency, this return is computed monthly and then annualised; comparing it to the S&P/ASX 200 market index over matching time periods gives an approximate measure of sensitivity to market returns. Taking the magnitude of the average of these sensitivities then serves as a proxy for risk appetite.

Applying the within transformation—centering all variables around their time averages for each individual—prevents estimating the effect of any time-invariant covariates, which do not show within-individual variation; this includes gender as well as the constructed risk appetite variable. Thus, gender and risk appetite do not enter in the GFE estimation, although they are used to qualitatively characterise the groups that the GFE method finds in the data.

Furthermore, age is not included as a covariate because the focus is on estimating group effects for each time period; these time effects cannot easily be separated from the effect of ageing after within-transforming the data.

4.2 Exploratory data analysis

The remainder of this section presents a preliminary descriptive analysis of the dataset used to generate the main results.

4.2.1 Summary statistics

Table 6 summarises characteristics that vary across individuals but not time. The age at 31 December 2015 represents the individual’s cohort, equivalent to measuring a year-of-birth

variable. The median retiree in the sample was born in 1936, with more than 50% of the sample born in an interval capturing four years on either side.

The age at account opening is the age when the retiree initiates a phased withdrawal product and begins drawing down from the account. In the superannuation dataset, the median retiree was aged 64 when opening their account. In general, opening an account before age 65 requires an individual to cease employment.

The sex indicator variable equals 1 if the retiree is male, and 0 otherwise. The mean value of 0.56 represents the proportion of retirees in the sample that are male.

The risk appetite variable is a proxy for the returns in the account relative to the reference S&P/ASX 200 index. The median retiree earned approximately 46% of the index returns in the sample period, with 75% of the sample earning less than 55% of the index returns. This variable suggests that most retirees have asset mixes that are conservative or balanced, with few retirees seeking aggressive returns in these accounts.

Table 7 summarises the time-varying variables in the dataset. The regular drawdown rate is the dependent variable of interest. The median drawdown rate in the sample is 9% of the account balances annually, while the mean is 12%. In absolute terms, the median regular drawdown amount is \$4800 while the average is \$6436.

The ad-hoc drawdown indicator variable equals 1 if the retiree made an ad-hoc withdrawal from their account balance during a given financial year; its mean value of 0.07 indicates that 7% of the observations recorded contain an ad-hoc drawdown. An interpretation is that the average retiree in the sample makes an ad-hoc drawdown roughly once every 14 years. Conditional on making an ad-hoc drawdown, the median ad-hoc drawdown rate is 7% of the account balance at the start of the year, while the mean is 15%. In dollars, the median ad-hoc drawdown is \$4656 and the average is \$10,217.

Median account balances, as measured at the beginning of each financial year, are \$52,063, with roughly 50% of balances lying in the interval (\$30,000, \$87,000).

Table 6: Summary statistics – Time-invariant variables.

	Age at 31 December 2015	Age at Account Open	Sex: Male	Risk Appetite
Mean	79.4	63.57	0.56	0.41
SD	5.22	4.17	0.5	0.21
Median	79.78	64.23	1	0.46
Q1	76.37	60.9	0	0.25
Q3	83.03	65.39	1	0.54
Min	60.66	48.48	0	0
Max	101.46	85.44	1	1.88
Count	9516	9516	9516	9507

Table 7: Summary statistics – Time-varying variables.

	Regular Drawdown Rate	Regular Drawdown Amount	Ad-hoc Drawdown Indicator	Ad-hoc Drawdown Rate	Ad-hoc Drawdown Amount	Account Balance
Mean	0.12	6435.91	0.07	0.15	10,216.56	72,686.55
SD	0.12	6121.76	0.25	0.21	24,672.68	78,721.39
Median	0.09	4800	0	0.07	4655.9	52,063
Q1	0.07	2992	0	0.02	1132.33	30,532.5
Q3	0.12	7728	0	0.18	10,000	87,427
Min	0	1	0	0	1	1
Max	2	166,695	1	0.9	600,000	2,427,083
Count	107,935	107,975	108,717	7450	7454	108,635

4.2.2 Histograms

Figure 14 plots the histograms of the time-invariant covariates. Most notable is the spike around age 65 for the account open age distribution, corresponding to the age at which individuals can open a phased withdrawal account unconditionally. Also instructive are the multiple peaks in the risk appetite distribution, suggesting a bunching of retirees into distinct asset mix options.

Figure 15 plots the histograms for the time-varying variables, which show some evidence of ad-hoc drawdown rates bunching around several modes for the larger values.

5 Characterising groups in the seven-group model

The section provides summary statistics and histograms created for each of the estimated groups from the main results. This allows comparison of each of the groups’ characteristics against other groups, using the following set of tables and plots. Alternatively, it is possible to compare group-level characteristics against the aggregate sample, by comparing with the results in Section 4.2 of this Supplement. We also present panel plots to supplement those given in the paper. Throughout the section, group labels follow the main results section in the paper.

5.1 Summary statistics by group

5.1.1 Time-invariant variables

Table 8 lists table references for the summary statistics of the time-invariant variables by group.

5.1.2 Time-varying variables

Table 9 lists table references for the summary statistics of the time-varying variables by group.

5.2 Histograms by group

5.2.1 Time-invariant variables

Table 10 lists figure references for the histograms of the time-invariant variables by group.

Figure 14: Histograms – Time-invariant variables. These are graphical representations of the data summarised in Table 6.

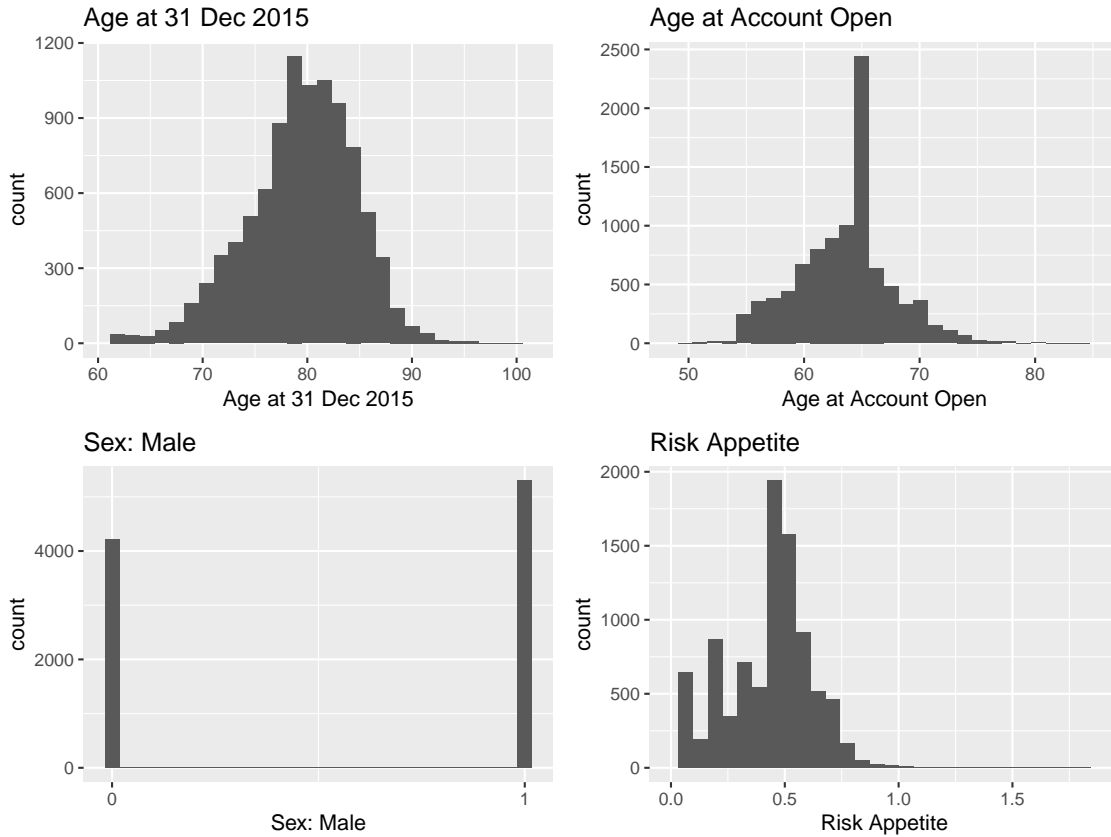


Table 8: Lookup table – Summary statistics for time-invariant variables by group. Group labels follow the main results section in the paper.

Group	Table
1	13
2	14
3	15
4	16
5	17
6	18
7	19

Table 9: Lookup table – Summary statistics for time-varying variables by group. Group labels follow the main results section in the paper.

Group	Table
1	20
2	21
3	22
4	23
5	24
6	25
7	26

Figure 15: Histograms – Time-varying variables. These are graphical representations of the data summarised in Table 7.

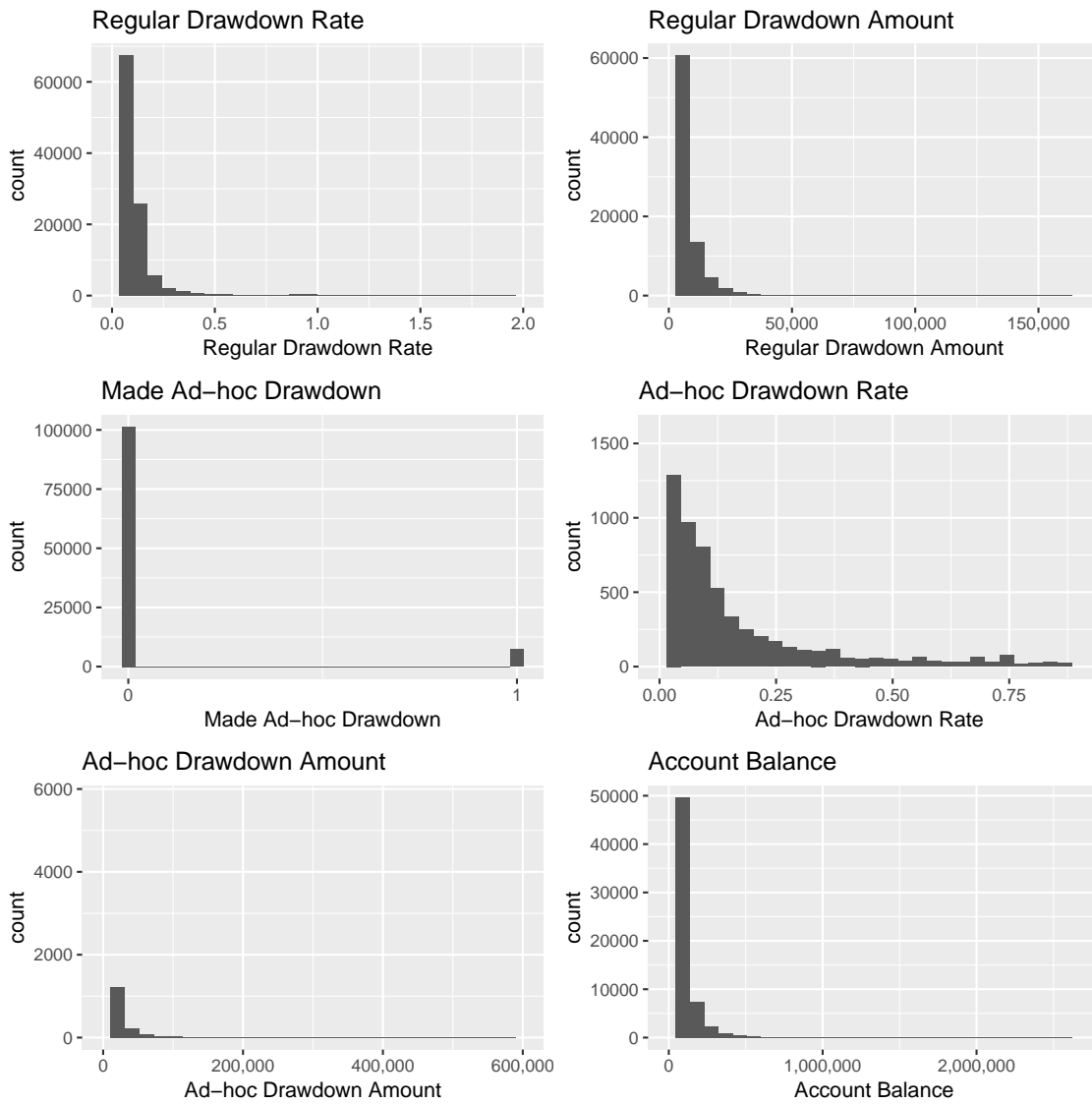


Table 10: Lookup table – Histograms of time-invariant variables by group. Group labels follow the main results section in the paper.

Group	Figure
1	25
2	26
3	27
4	28
5	29
6	30
7	31

5.2.2 Time-varying variables

Table 11 lists figure references for the histograms of the time-varying variables by group.

5.3 Time-demeaned panel plots by group

Table 12 lists figure references for time-demeaned panel plots by group. Each figure shows four variables after time-demeaning by unit: the log regular drawdown rate; the log regular drawdown dollar amount; the log account balance at the financial year start; composite residuals from the estimation. We define the composite residuals as $\hat{\alpha}_{g_{it}} + \hat{v}_{it} := y_{it} - x'_{it}\hat{\theta}$; a composite residual is the estimated group time profile value plus the model residual, obtained by subtracting the estimated effect of covariates from the dependent variable. The black line represents the estimated time-demeaned group time profile values $\hat{\alpha}_{gt}$. The composite residual plots provide information similar to that of a residual plot of \hat{v}_{it} , but also convey a sense of how large the estimated idiosyncratic unobserved component \hat{v}_{it} is compared to the estimated systematic unobserved component $\hat{\alpha}_{g_{it}}$.

6 Panel plots for the two-group model

Figures 16 and 17 show panel plots of time-demeaned variables for the two groups in the two-group model. Group labels in these plots follow the two-group model results in the paper.

Table 11: Lookup table – Histograms of time-varying variables by group. Group labels follow the main results section in the paper.

Group	Figure
1	32
2	33
3	34
4	35
5	36
6	37
7	38

Table 12: Lookup table – Time-demeaned (TD) panel plots by group. Group labels follow the main results section in the paper.

Group	Figure
1	39
2	40
3	41
4	42
5	43
6	44
7	45

Figure 16: $G = 2$ model – Group 1 time-demeaned (TD) panel plots. Account balances as at financial year start. The black series in the bottom-right panel represents estimated time-demeaned group time profile values.

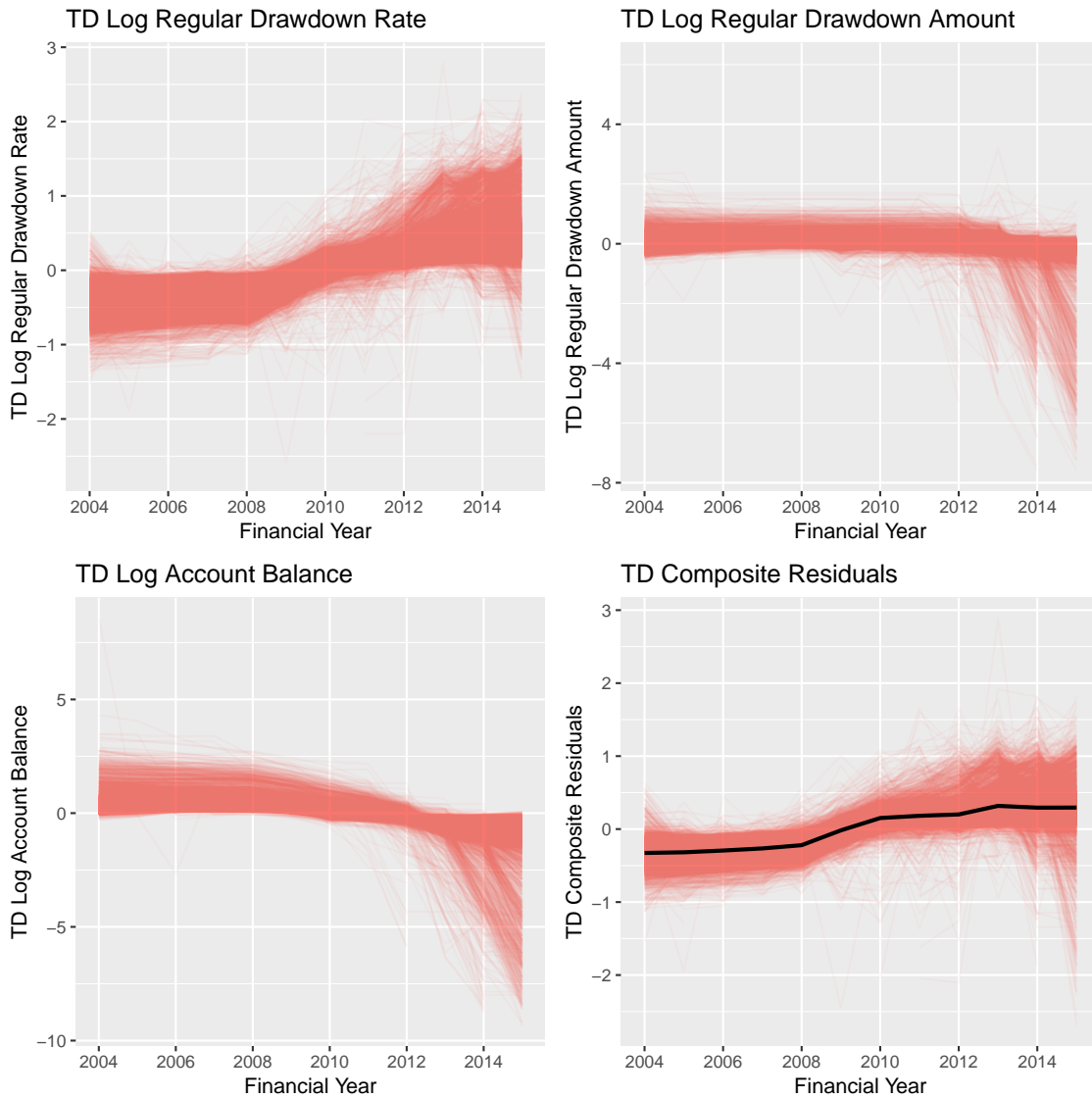


Figure 17: $G = 2$ model – Group 2 time-demeaned (TD) panel plots. Account balances as at financial year start. The black series in the bottom-right panel represents estimated time-demeaned group time profile values.

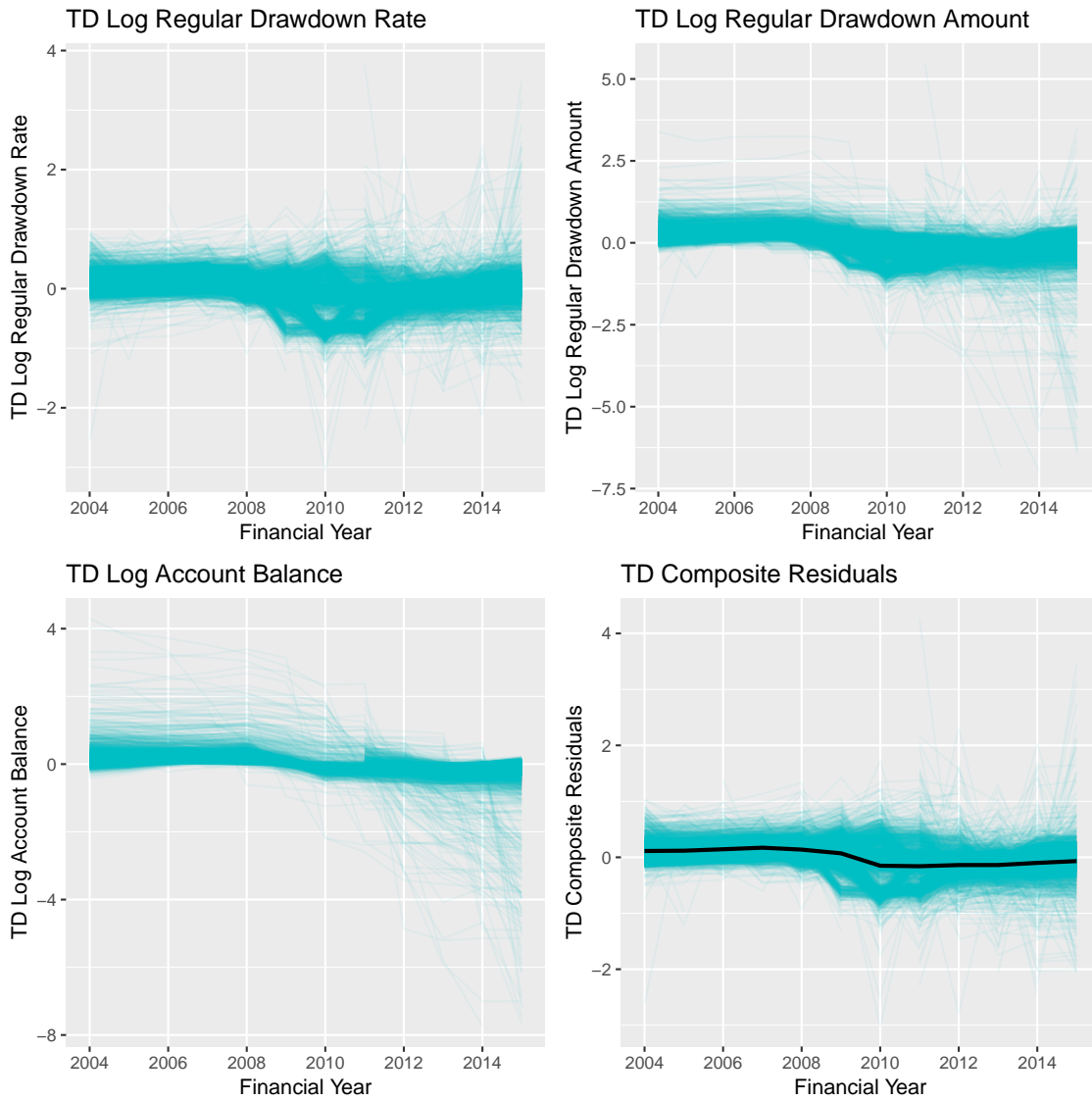


Table 13: Group 1 summary statistics – Time-invariant variables.

	Age at 31 Dec 2015	Age at Account Open	Sex: Male	Risk Appetite
Mean	81.53	64.67	0.62	0.43
SD	4.22	3.84	0.49	0.18
Median	81.76	65	1	0.46
Q1	78.87	62.69	0	0.34
Q3	84.57	66.67	1	0.54
Min	67.67	50.45	0	0
Max	94.7	80.22	1	0.92
Count	2057	2057	2057	2055

Table 14: Group 2 summary statistics – Time-invariant variables.

	Age at 31 December 2015	Age at Account Open	Sex: Male	Risk Appetite
Mean	80.03	63.36	0.62	0.41
SD	5.23	5	0.48	0.2
Median	79.41	63.67	1	0.46
Q1	76.42	59.82	0	0.24
Q3	83.54	65.57	1	0.54
Min	67.53	50.26	0	0.01
Max	96.23	81.78	1	1.02
Count	865	865	865	863

Table 15: Group 3 summary statistics – Time-invariant variables.

	age_at_31DEC15	age_at_account_open	sex_male	risk_appetite
Mean	81.75	64.66	0.69	0.35
SD	4.43	4.29	0.46	0.22
Median	81.39	64.94	1	0.4
Q1	79.24	61.93	0	0.17
Q3	83.88	65.74	1	0.5
Min	65.82	55.92	0	0
Max	99.87	85.44	1	1.52
Count	331	331	331	331

Table 16: Group 4 summary statistics – Time-invariant variables.

	Age at 31 December 2015	Age at Account Open	Sex: Male	Risk Appetite
Mean	78.17	63.54	0.51	0.44
SD	6.09	4.19	0.5	0.21
Median	78.93	64.1	1	0.47
Q1	74.25	60.79	0	0.31
Q3	82.57	65.46	1	0.57
Min	60.66	51.3	0	0
Max	97.06	79.79	1	1.59
Count	1854	1854	1854	1852

Table 17: Group 5 summary statistics – Time-invariant variables.

	Age at 31 December 2015	Age at Account Open	Sex: Male	Risk Appetite
Mean	78.12	63.92	0.49	0.47
SD	6.17	4.25	0.5	0.21
Median	78.8	64.35	0	0.49
Q1	73.35	61.48	0	0.35
Q3	82.77	65.93	1	0.6
Min	60.81	51.58	0	0
Max	101.46	81.91	1	1.88
Count	1298	1298	1298	1298

Table 18: Group 6 summary statistics – Time-invariant variables.

	Age at 31 December 2015	Age at Account Open	Sex: Male	Risk Appetite
Mean	78.19	63.16	0.53	0.45
SD	5.7	4.16	0.5	0.21
Median	78.99	63.78	1	0.48
Q1	74.56	60.5	0	0.34
Q3	82.34	65.29	1	0.58
Min	61.74	52.68	0	0
Max	94.21	76.01	1	1.09
Count	508	508	508	508

Table 19: Group 7 summary statistics – Time-invariant variables.

	Age at 31 December 2015	Age at Account Open	Sex: Male	Risk Appetite
Mean	78.97	62.56	0.54	0.35
SD	3.93	3.77	0.5	0.2
Median	79.08	63.06	1	0.39
Q1	76.49	60.15	0	0.22
Q3	81.83	65.02	1	0.5
Min	65.27	48.48	0	0
Max	92.5	78.32	1	0.88
Count	2603	2603	2603	2600

Table 20: Group 1 summary statistics – Time-varying variables.

	Regular Drawdown Rate	Regular Drawdown Amount	Ad-hoc Drawdown Indicator	Ad-hoc Drawdown Rate	Ad-hoc Drawdown Amount	Account Balance
Mean	0.13	6687.54	0.05	0.14	10434.4	60246.23
SD	0.07	5615.68	0.21	0.16	20751.13	56052.49
Median	0.11	5172	0	0.09	6000	44855
Q1	0.09	3360	0	0.05	3432	27314
Q3	0.15	7944	0	0.15	10013	73574.5
Min	0.01	1	0	0	1	1
Max	1.22	70800	1	0.9	500000	812479
Count	24638	24644	24684	1144	1145	24675

Table 21: Group 2 summary statistics – Time-varying variables.

	Regular Drawdown Rate	Regular Drawdown Amount	Ad-hoc Drawdown Indicator	Ad-hoc Drawdown Rate	Ad-hoc Drawdown Amount	Account Balance
Mean	0.25	6933.94	0.1	0.18	10224.05	46450.67
SD	0.23	5594.9	0.3	0.17	19495.22	47647.52
Median	0.15	5460	0	0.12	5000	33775
Q1	0.11	3372	0	0.06	2000	15689.5
Q3	0.3	8928	0	0.25	10075	62153.75
Min	0.01	2	0	0	1	1
Max	2	42000	1	0.9	277831	543370
Count	10344	10345	10372	1114	1115	10368

Table 22: Group 3 summary statistics – Time-varying variables.

	Regular Drawdown Rate	Regular Drawdown Amount	Ad-hoc Drawdown Indicator	Ad-hoc Drawdown Rate	Ad-hoc Drawdown Amount	Account Balance
Mean	0.34	6076.35	0.1	0.35	9789.94	33754.28
SD	0.3	6305.35	0.3	0.3	19162.35	46781.99
Median	0.2	4400	0	0.23	4013	19960
Q1	0.14	2291	0	0.09	42	5732.25
Q3	0.46	7481.25	0	0.6	10000	42861.5
Min	0	1	0	0	1	1
Max	1.38	48000	1	0.9	233305	632325
Count	3716	3716	3944	461	461	3914

Table 23: Group 4 summary statistics – Time-varying variables.

	Regular Drawdown Rate	Regular Drawdown Amount	Ad-hoc Drawdown Indicator	Ad-hoc Drawdown Rate	Ad-hoc Drawdown Amount	Account Balance
Mean	0.07	6412.78	0.09	0.11	8635.62	90976.64
SD	0.03	6524.65	0.29	0.2	25313.44	94553.22
Median	0.07	4588.91	0	0.02	2253.33	65456
Q1	0.06	2712	0	0.01	732.5	39864
Q3	0.08	7560	0	0.09	7500	104543
Min	0	30	0	0	1	15
Max	0.94	99768	1	0.9	430000	1573153
Count	19460	19472	19609	1831	1833	19597

Table 24: Group 5 summary statistics – Time-varying variables.

	Regular Drawdown Rate	Regular Drawdown Amount	Ad-hoc Drawdown Indicator	Ad-hoc Drawdown Rate	Ad-hoc Drawdown Amount	Account Balance
Mean	0.06	5898.44	0.11	0.11	9308.75	99415.18
SD	0.04	6219.52	0.31	0.19	26711.86	103532.05
Median	0.06	4201.49	0	0.03	2565.83	71760
Q1	0.05	2310	0	0	622.93	43445.75
Q3	0.07	7094.75	0	0.09	8705.42	115423.25
Min	0	10	0	0	3	53
Max	0.75	109320	1	0.9	600000	1514586.47
Count	13184	13192	13294	1403	1403	13286

Table 25: Group 6 summary statistics – Time-varying variables.

	Regular Drawdown Rate	Regular Drawdown Amount	Ad-hoc Drawdown Indicator	Ad-hoc Drawdown Rate	Ad-hoc Drawdown Amount	Account Balance
Mean	0.1	6377.06	0.11	0.21	13530.6	73469.07
SD	0.08	5853.41	0.31	0.27	32379.36	71795.16
Median	0.08	4800	0	0.09	5000	53776
Q1	0.07	2670	0	0.02	1159.84	30503
Q3	0.11	8060	0	0.31	13318.59	89727
Min	0	1	0	0	1	1
Max	1.57	86688.13	1	0.9	455548	781753.8
Count	5437	5438	5592	606	606	5585

Table 26: Group 7 summary statistics – Time-varying variables.

	Regular Drawdown Rate	Regular Drawdown Amount	Ad-hoc Drawdown Indicator	Ad-hoc Drawdown Rate	Ad-hoc Drawdown Amount	Account Balance
Mean	0.09	6366.74	0.03	0.16	12575.79	73117.21
SD	0.03	6367.71	0.17	0.2	26520.99	76839.21
Median	0.09	4764	0	0.09	6000	53267.5
Q1	0.07	3036	0	0.04	3000	33820
Q3	0.11	7416	0	0.18	12000	87103.25
Min	0.02	12	0	0	31	13
Max	0.92	166695	1	0.9	520802	2427083
Count	31156	31168	31222	891	891	31210

Figure 18: Group 1 time profile analytical SE distributions across simulated datasets. Black lines plot the kernel density estimate for standard errors derived from the fixed- T variance estimate formula after estimating the GFE model on 1000 simulated datasets. Red vertical lines represent the value of the simulated standard error.

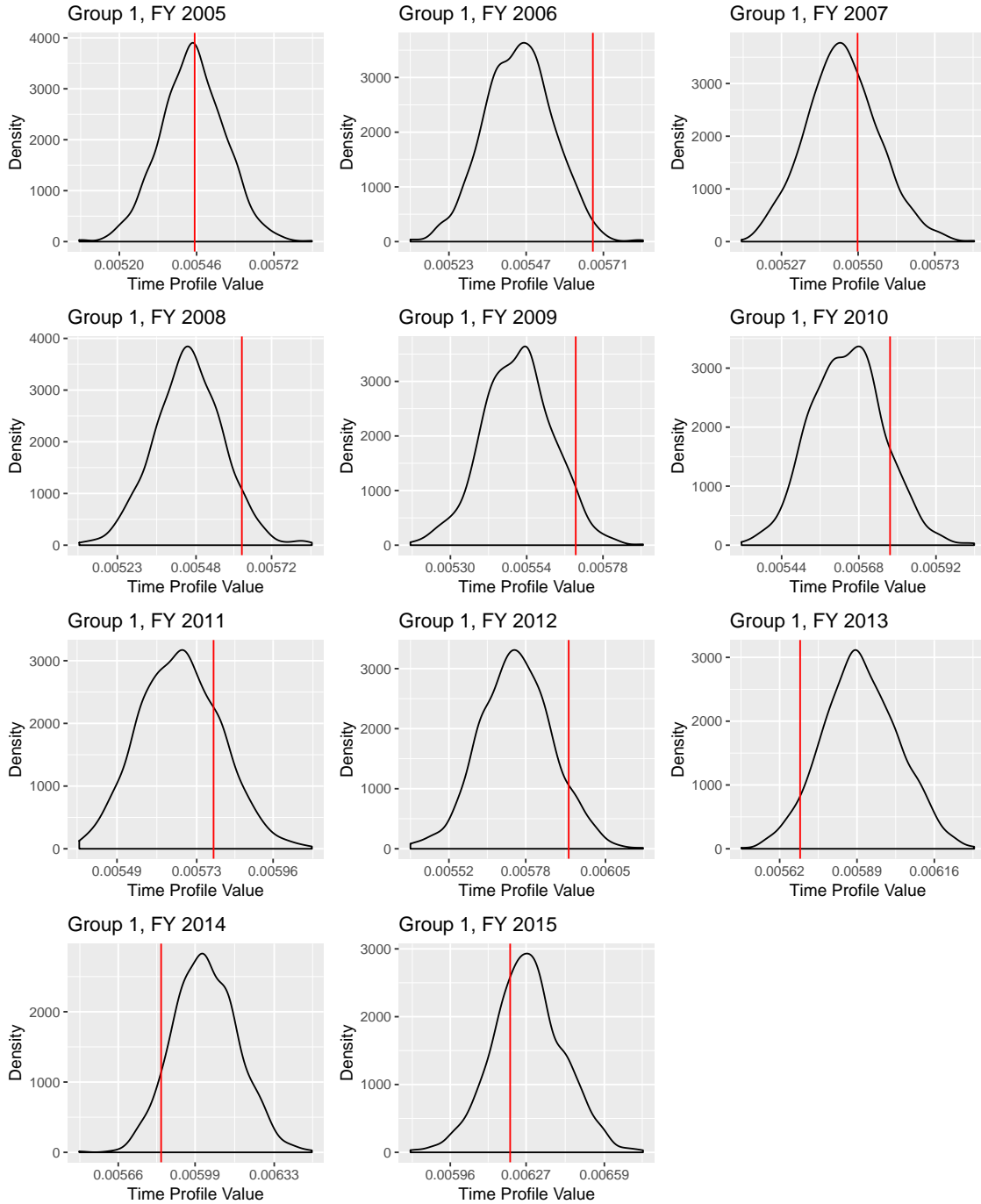


Figure 19: Group 2 time profile analytical SE distributions across simulated datasets. Black lines plot the kernel density estimate for standard errors derived from the fixed- T variance estimate formula after estimating the GFE model on 1000 simulated datasets. Red vertical lines represent the value of the simulated standard error.

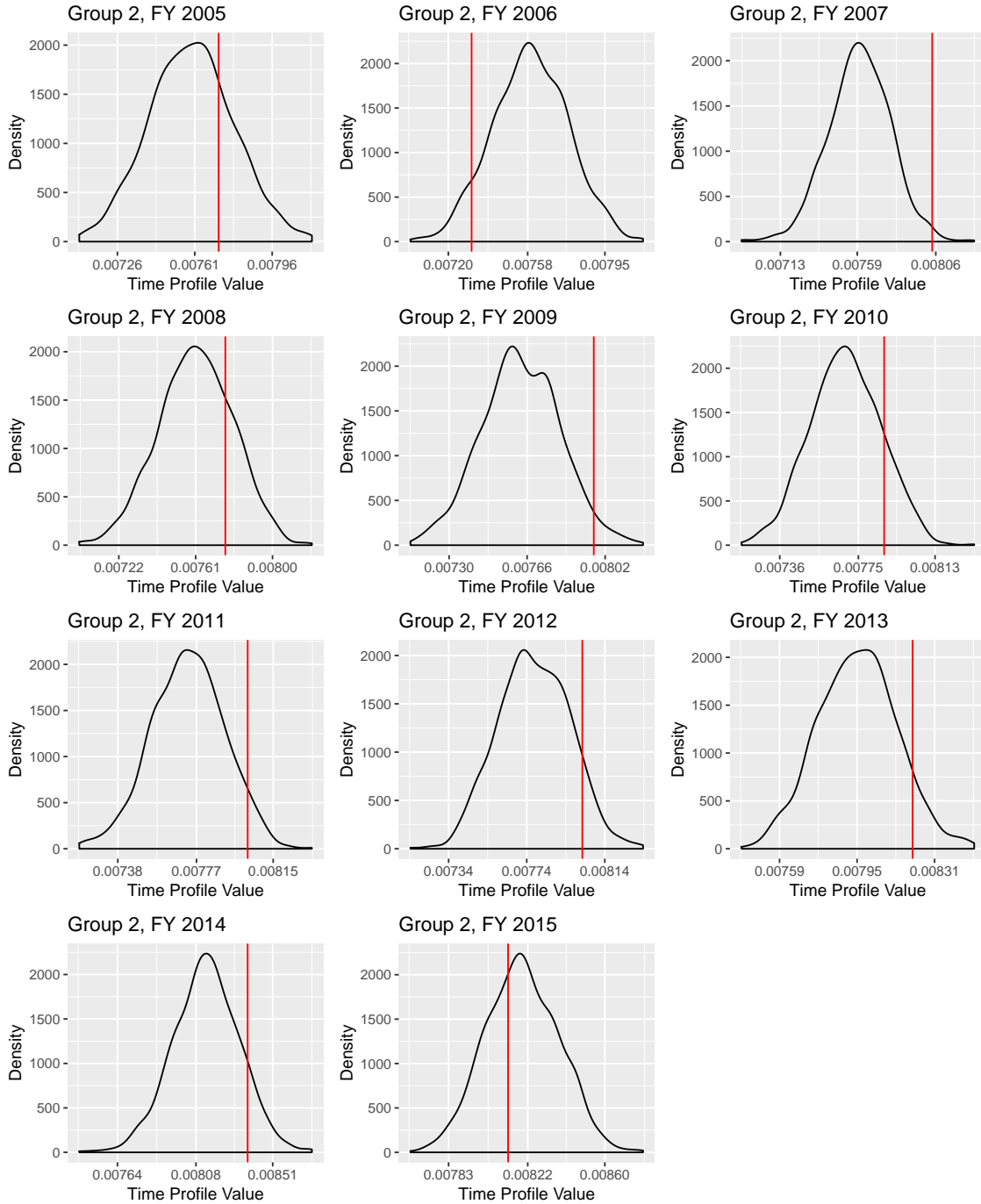


Figure 20: Group 3 time profile analytical SE distributions across simulated datasets. Black lines plot the kernel density estimate for standard errors derived from the fixed- T variance estimate formula after estimating the GFE model on 1000 simulated datasets. Red vertical lines represent the value of the simulated standard error.

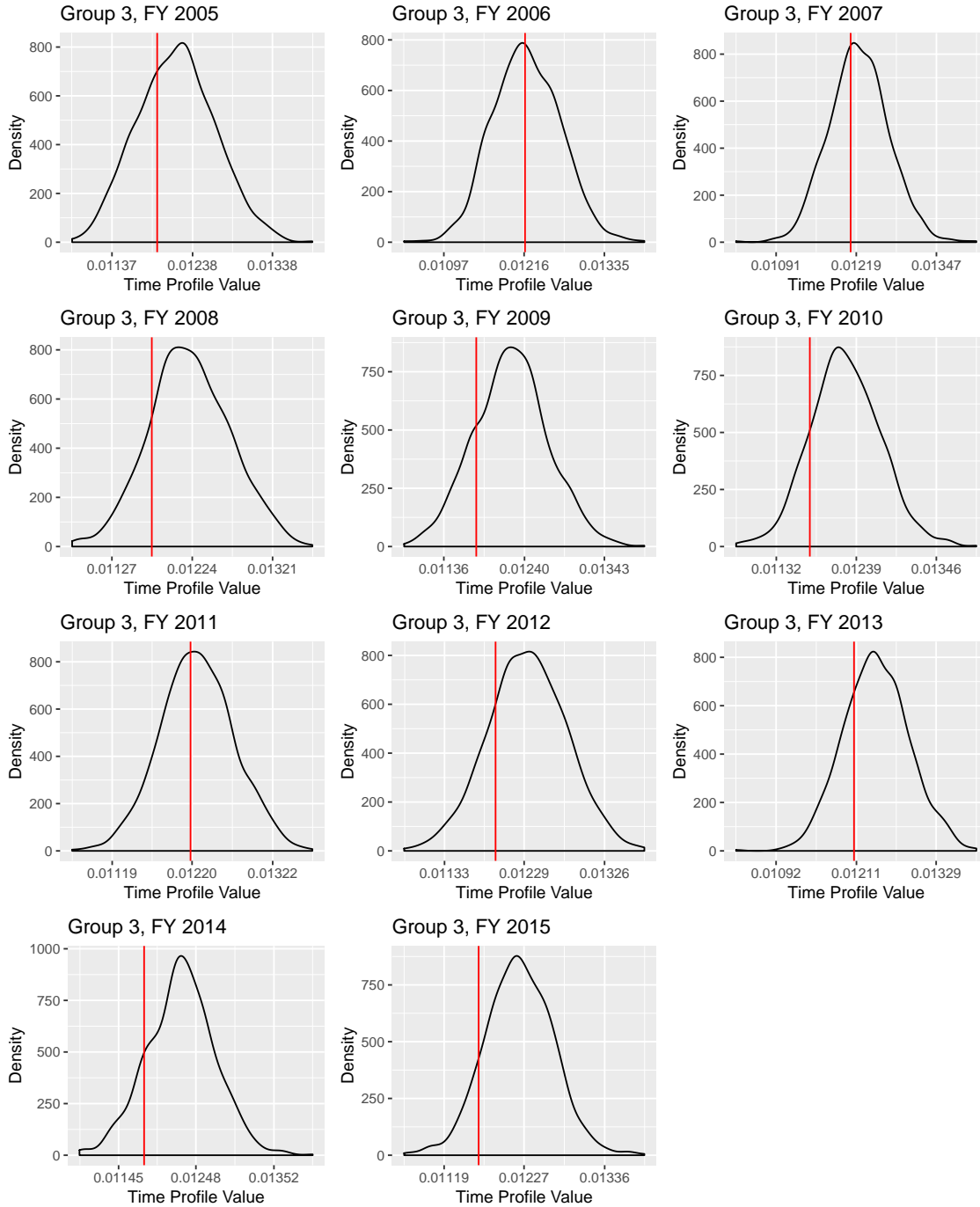


Figure 21: Group 4 time profile analytical SE distributions across simulated datasets. Black lines plot the kernel density estimate for standard errors derived from the fixed- T variance estimate formula after estimating the GFE model on 1000 simulated datasets. Red vertical lines represent the value of the simulated standard error.

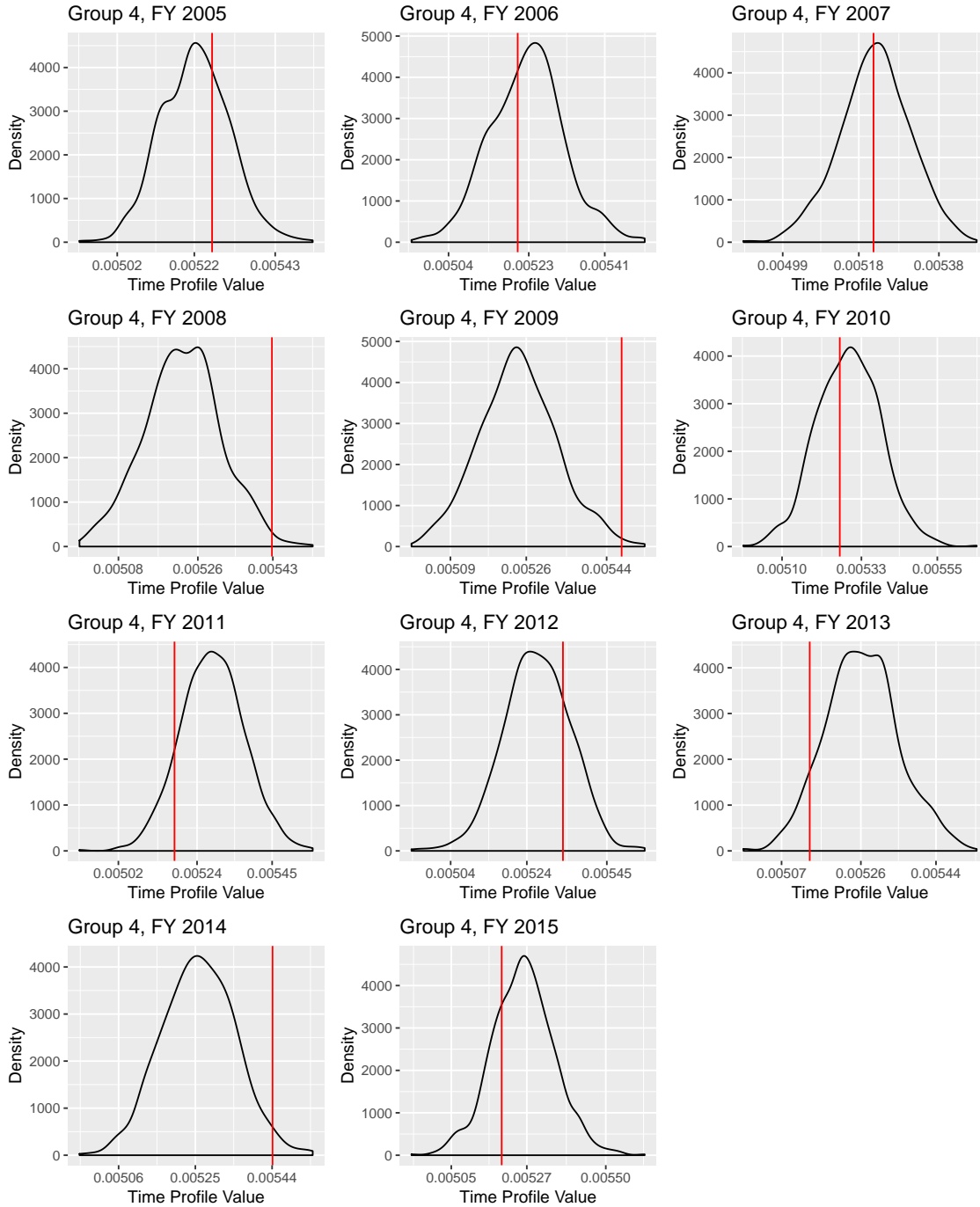


Figure 22: Group 5 time profile analytical SE distributions across simulated datasets. Black lines plot the kernel density estimate for standard errors derived from the fixed- T variance estimate formula after estimating the GFE model on 1000 simulated datasets. Red vertical lines represent the value of the simulated standard error.

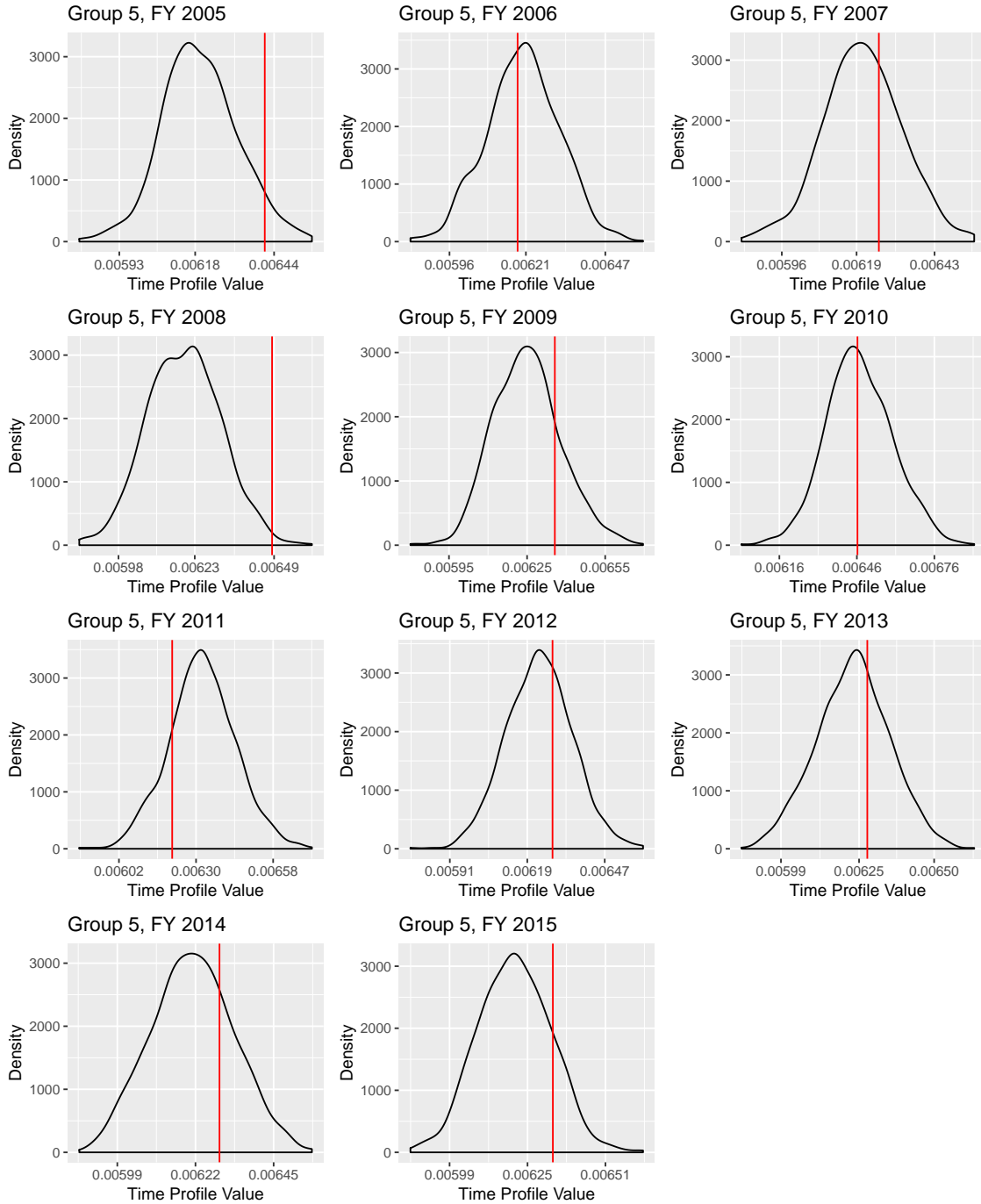


Figure 23: Group 6 time profile analytical SE distributions across simulated datasets. Black lines plot the kernel density estimate for standard errors derived from the fixed- T variance estimate formula after estimating the GFE model on 1000 simulated datasets. Red vertical lines represent the value of the simulated standard error.

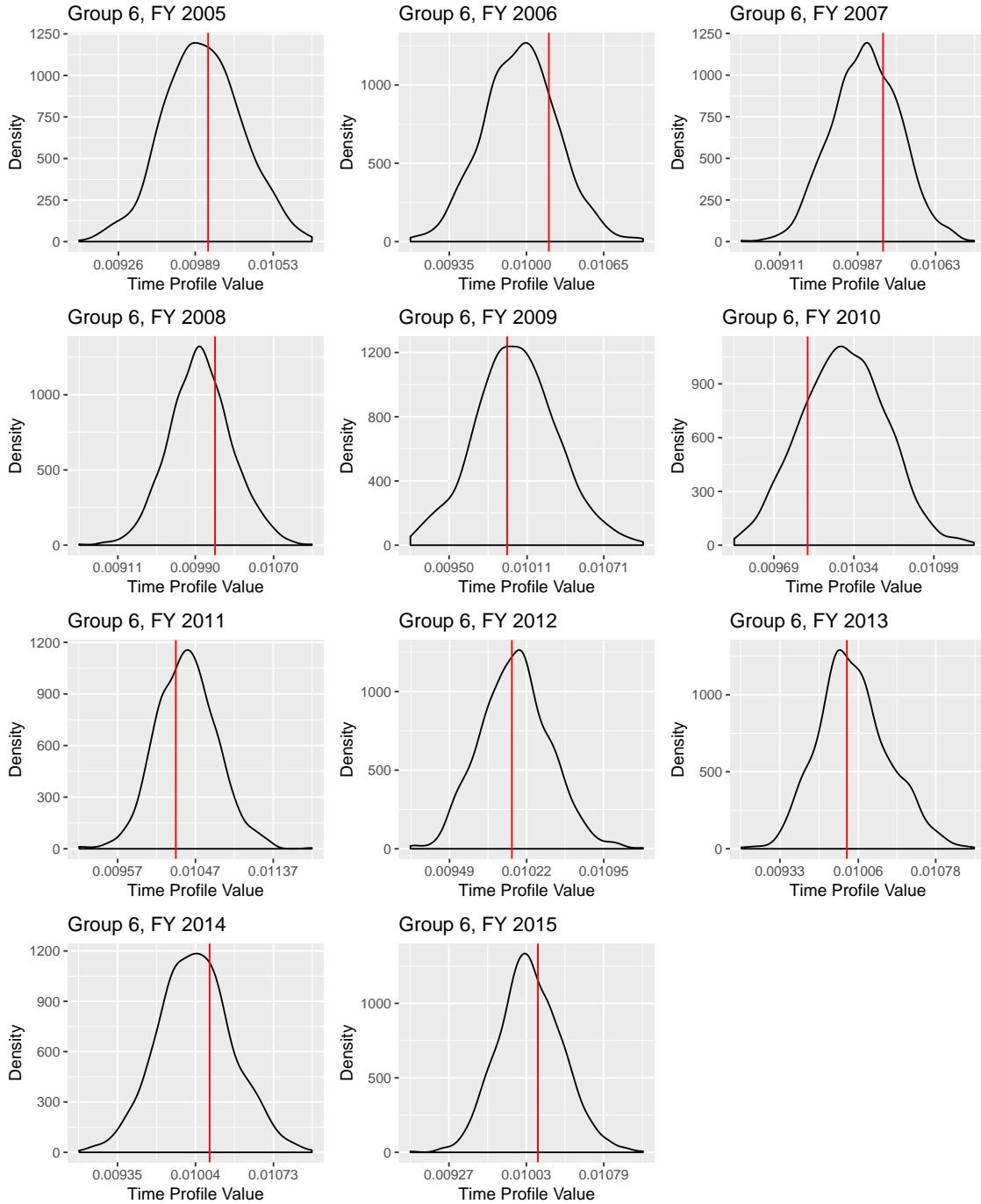


Figure 24: Group 7 time profile analytical SE distributions across simulated datasets. Black lines plot the kernel density estimate for standard errors derived from the fixed- T variance estimate formula after estimating the GFE model on 1000 simulated datasets. Red vertical lines represent the value of the simulated standard error.

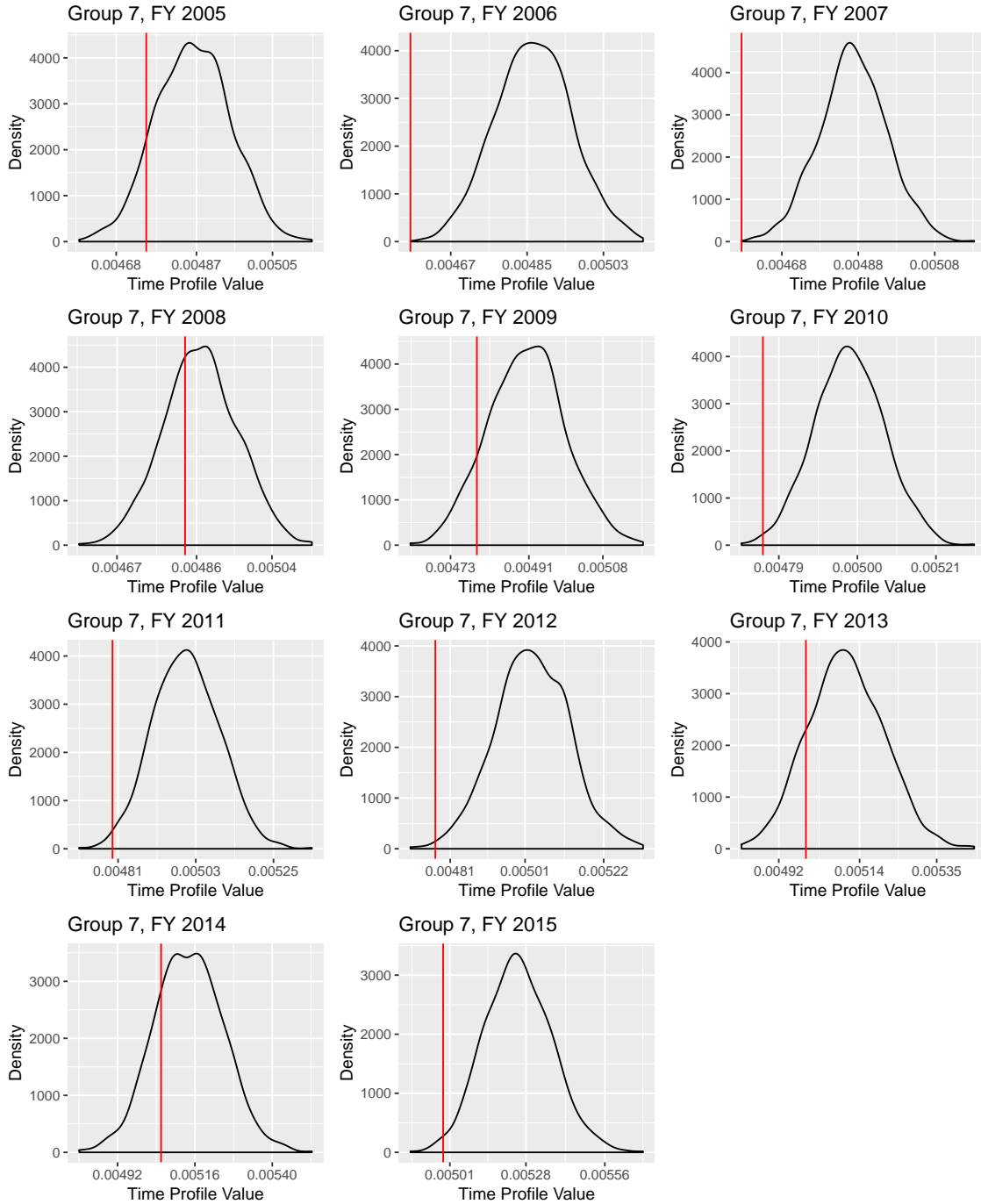


Figure 25: Group 1 histograms – Time-invariant variables.

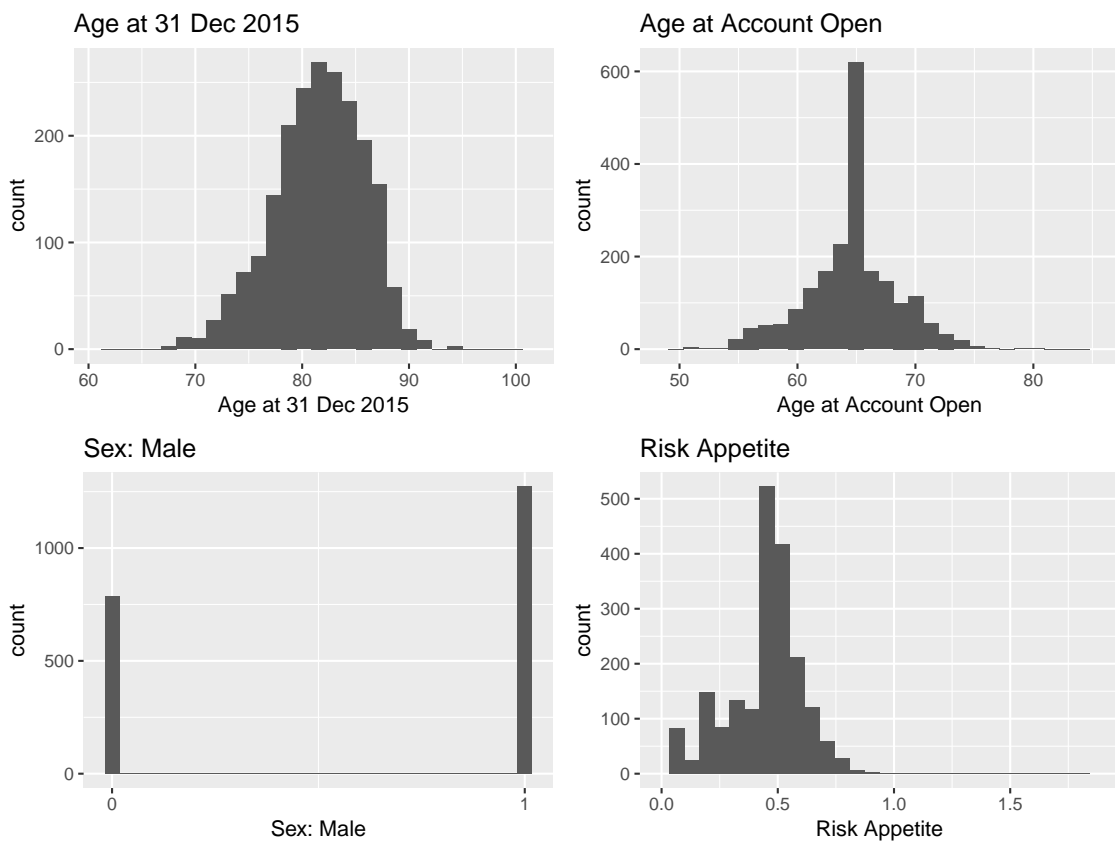


Figure 26: Group 2 histograms – Time-invariant variables.

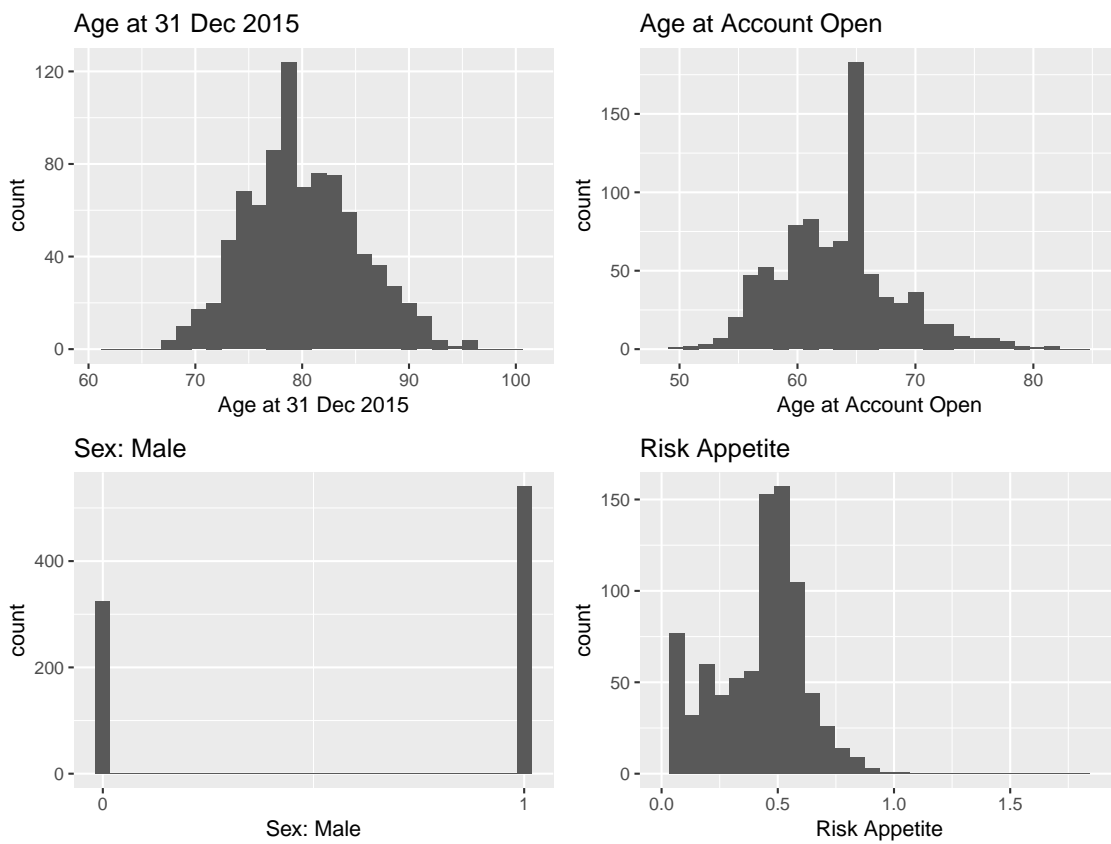


Figure 27: Group 3 histograms – Time-invariant variables.

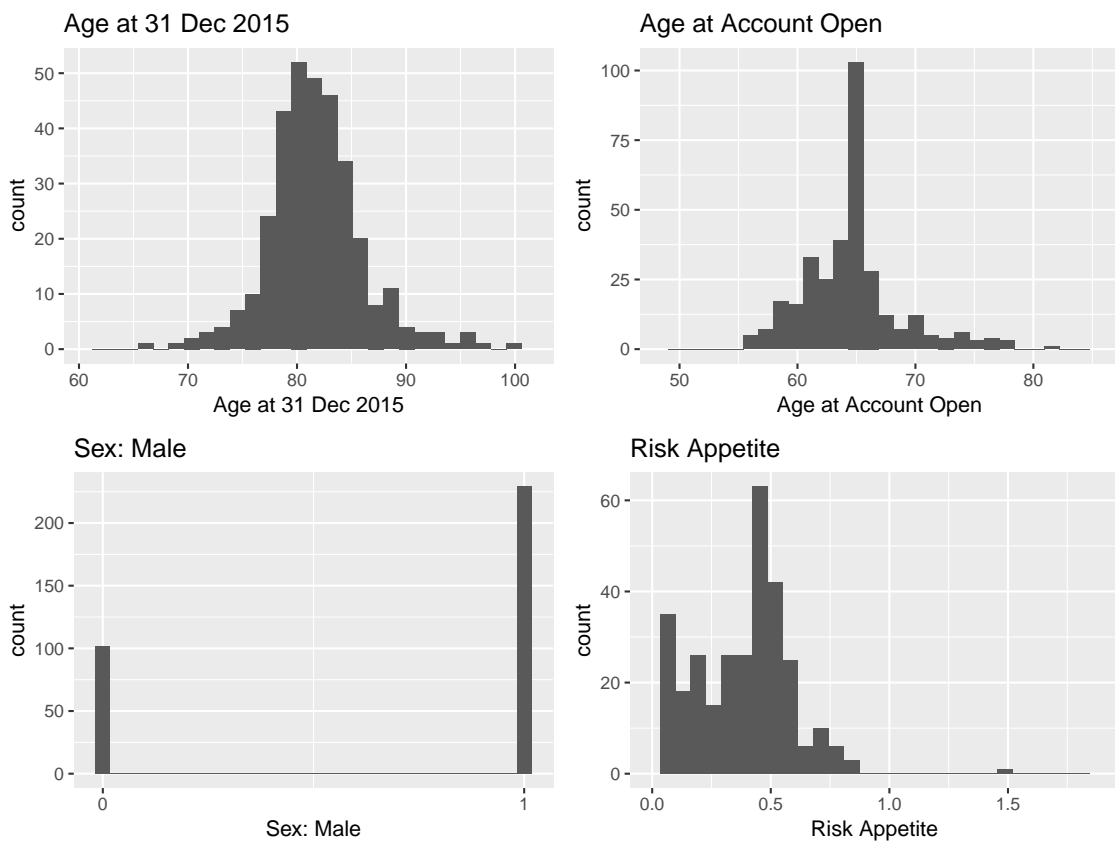


Figure 28: Group 4 histograms – Time-invariant variables.

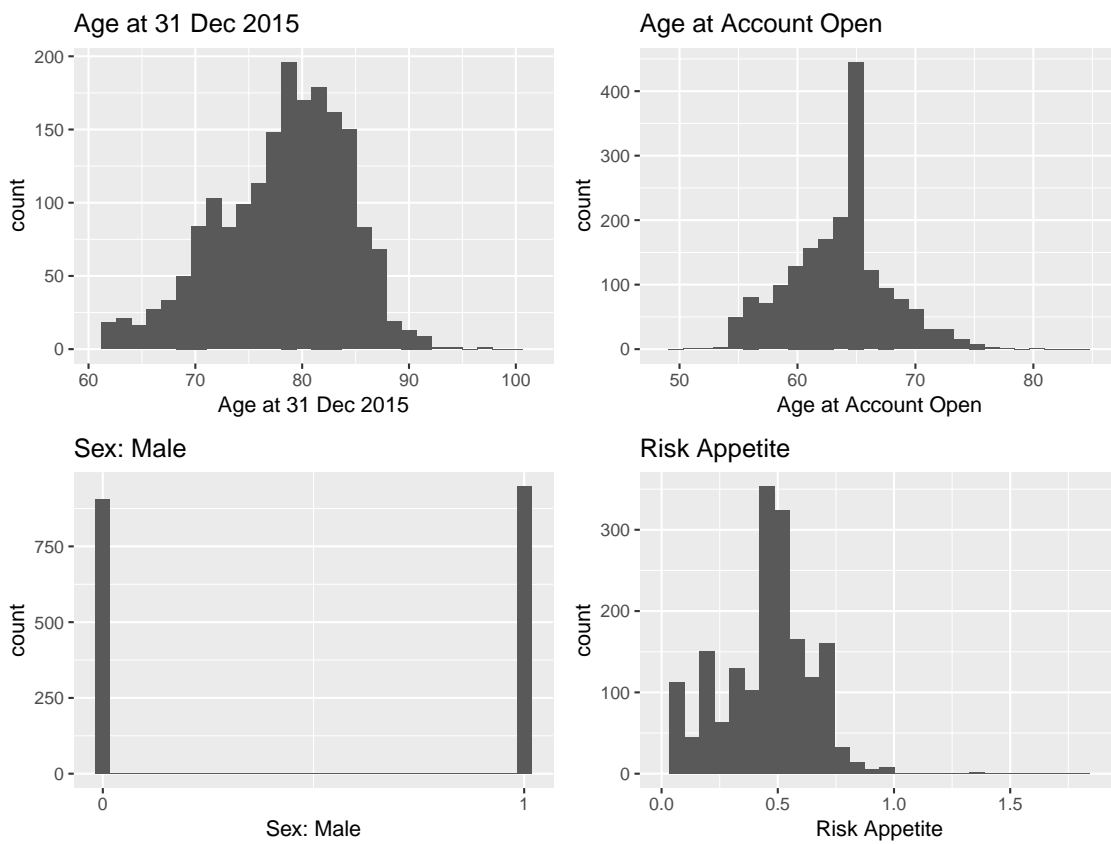


Figure 29: Group 5 histograms – Time-invariant variables.

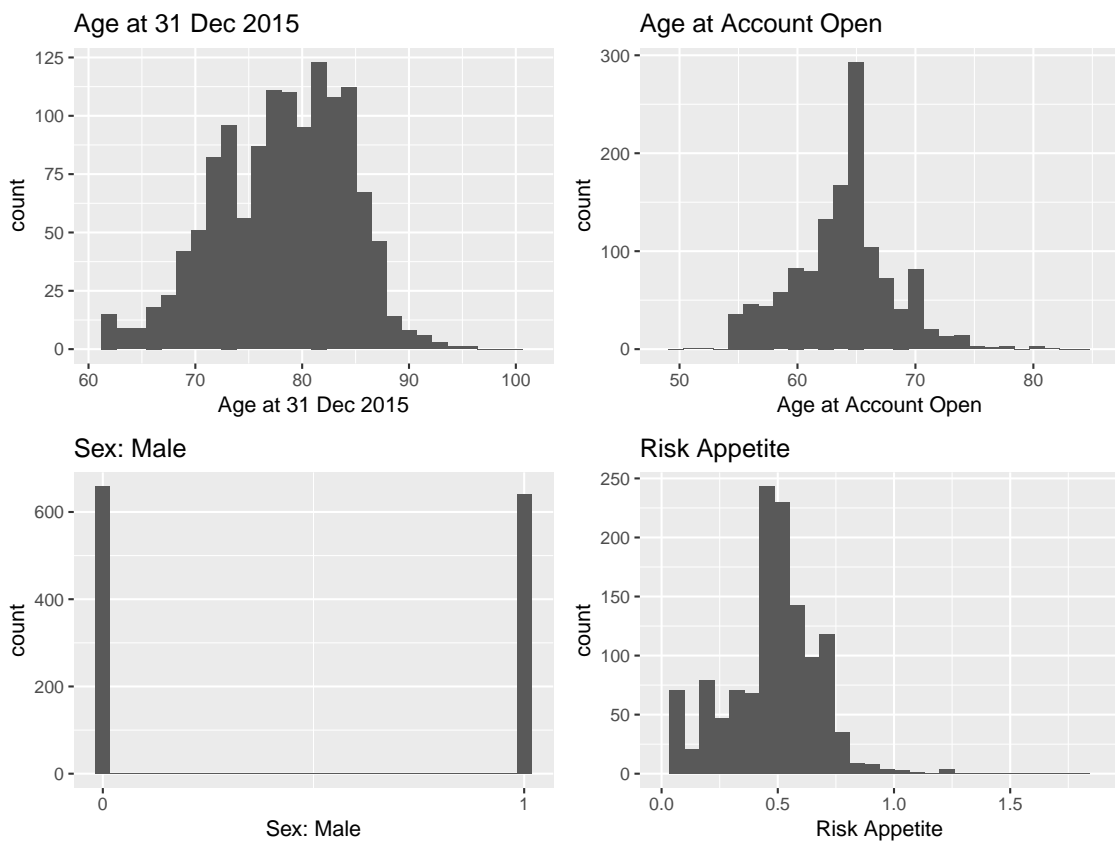


Figure 30: Group 6 histograms – Time-invariant variables.

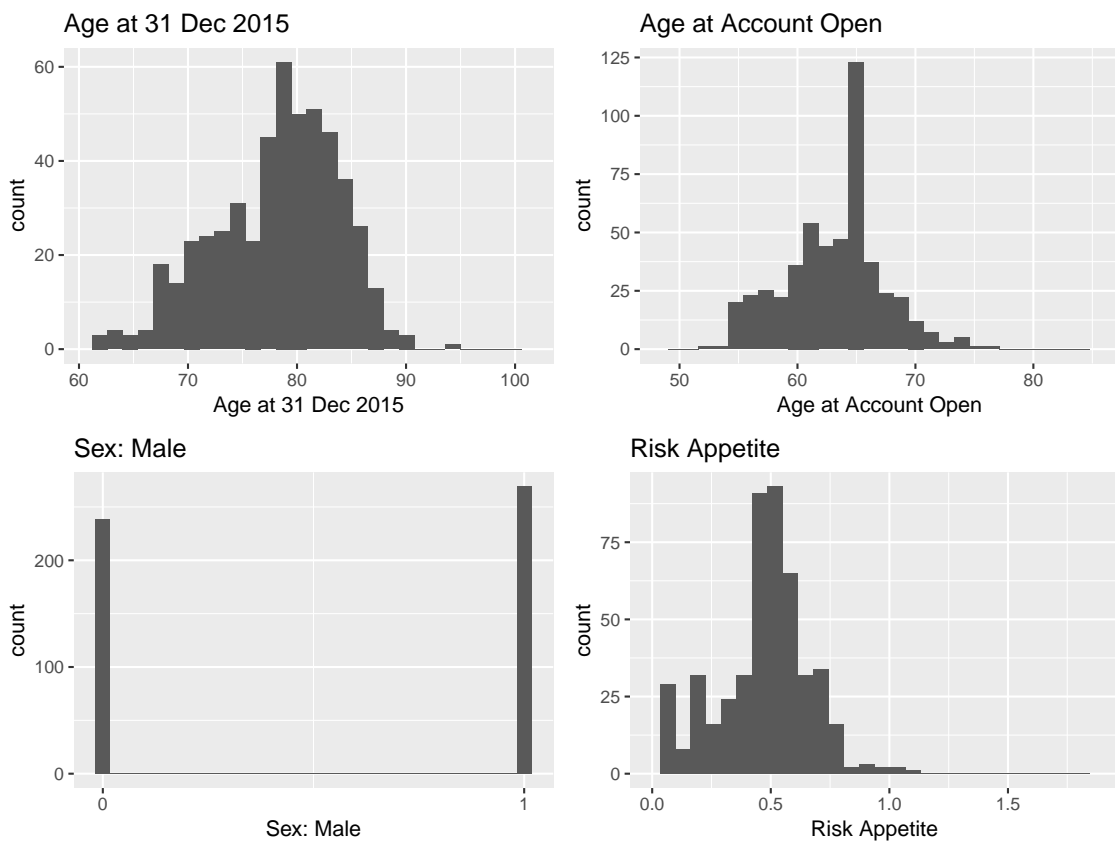


Figure 31: Group 7 histograms – Time-invariant variables.

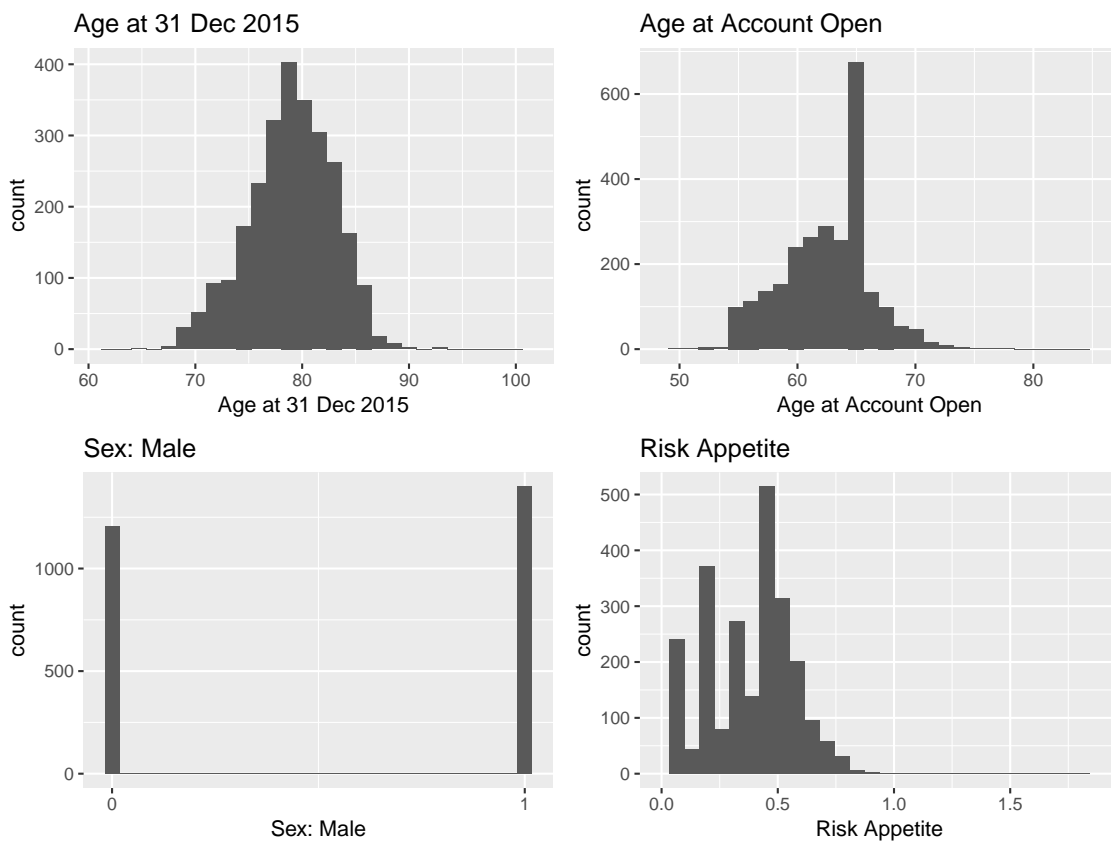


Figure 32: Group 1 histograms – Time-varying variables.

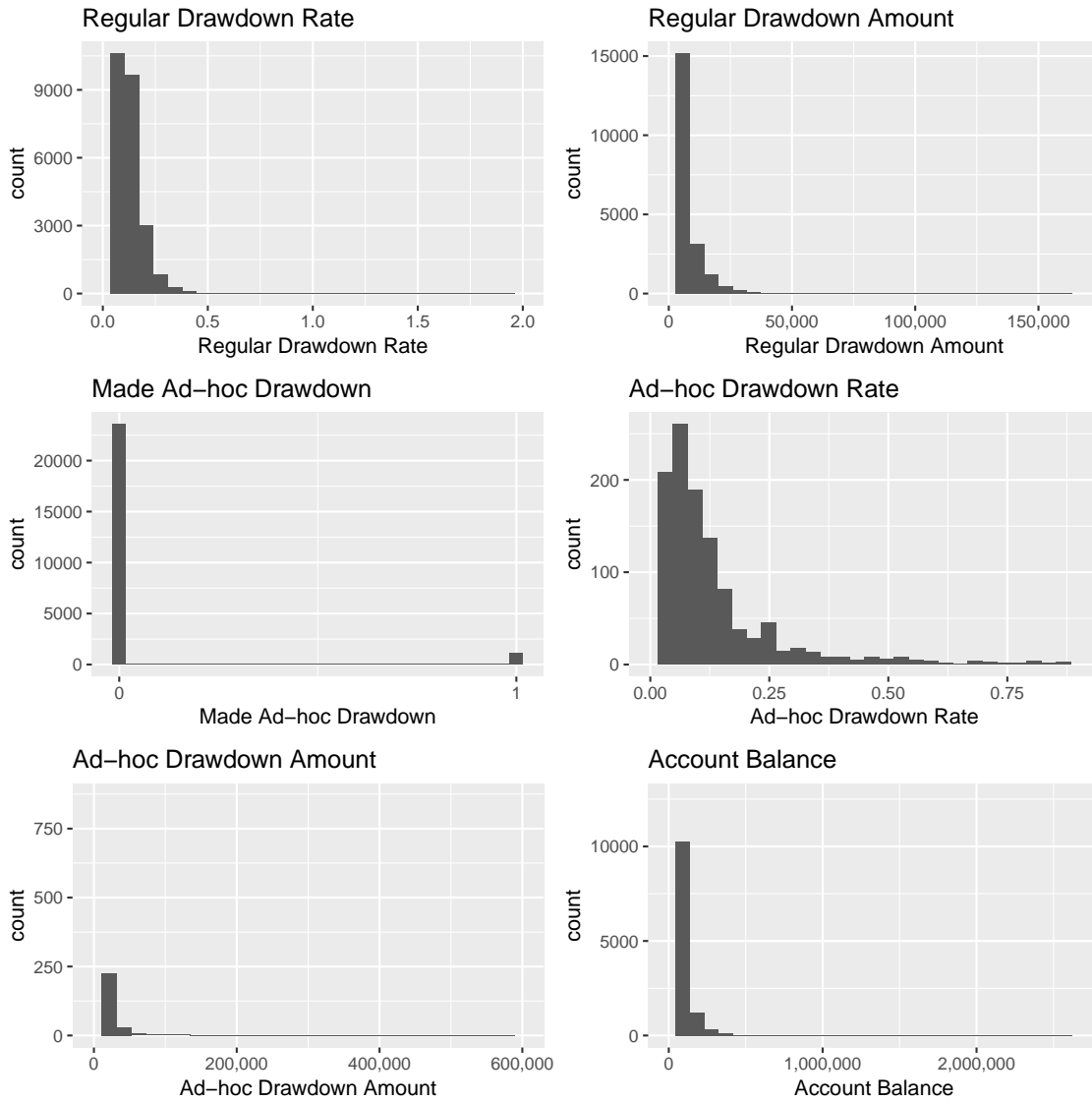


Figure 33: Group 2 histograms – Time-varying variables.

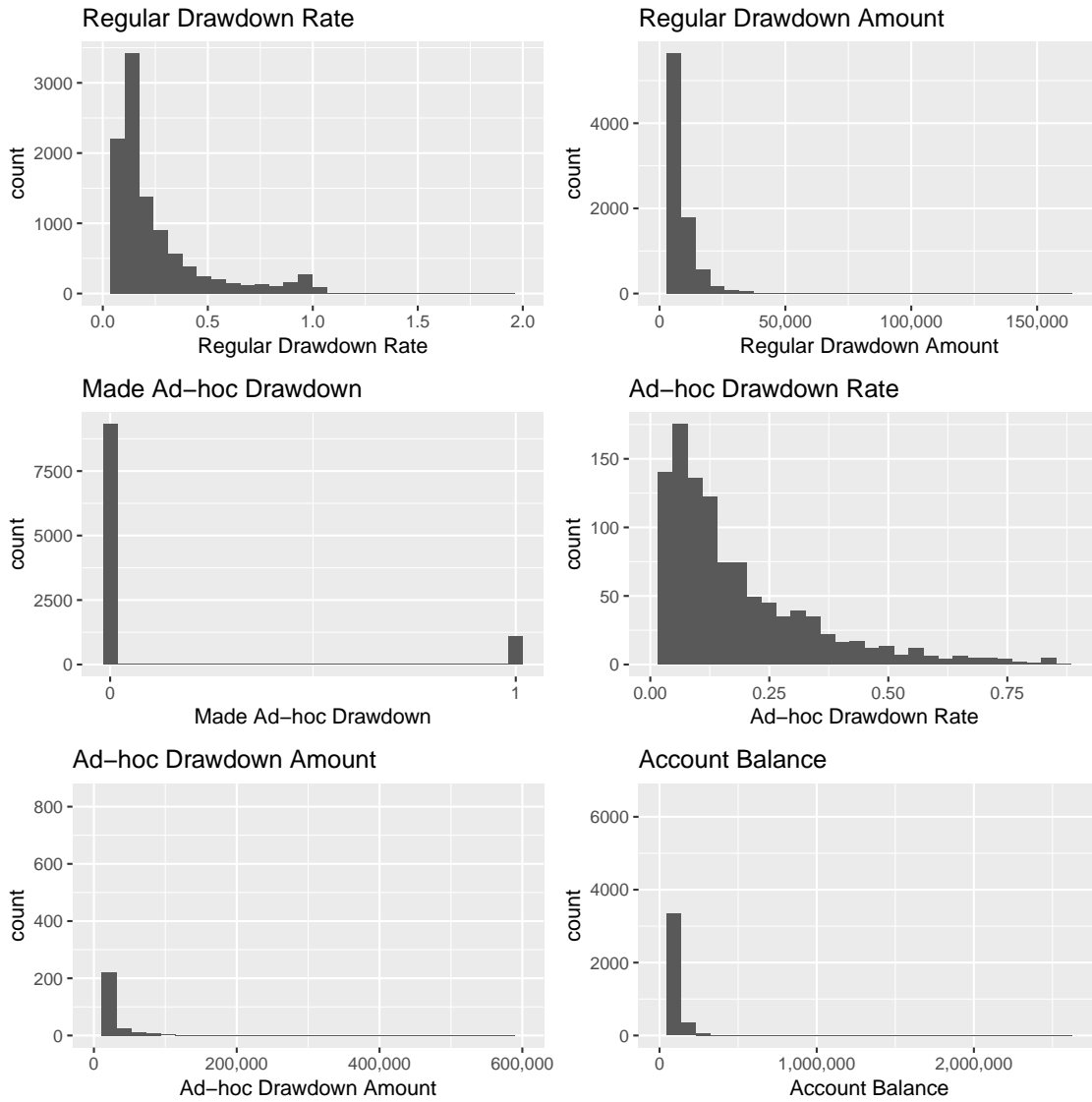


Figure 34: Group 3 histograms – Time-varying variables.

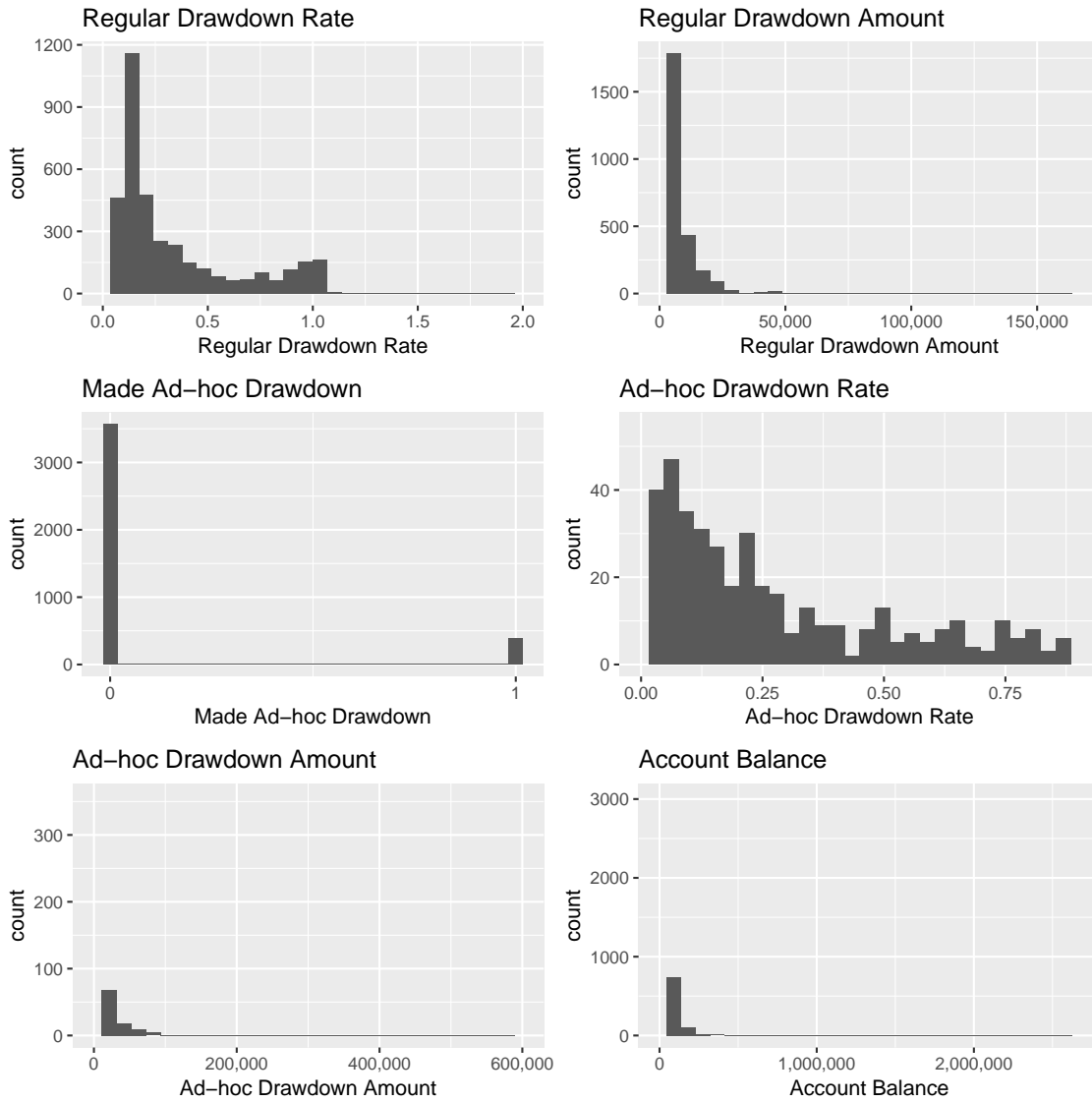


Figure 35: Group 4 histograms – Time-varying variables.

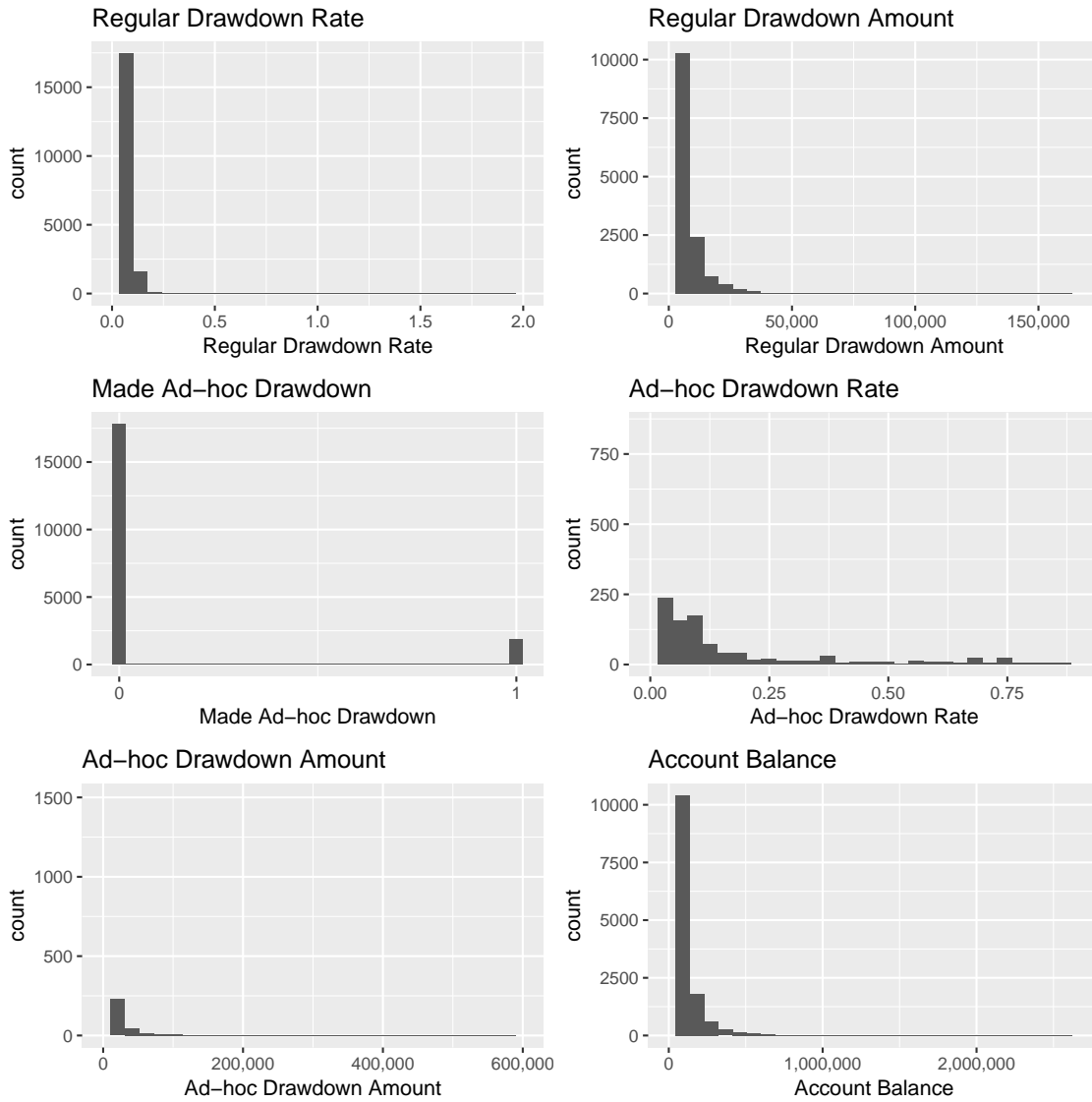


Figure 36: Group 5 histograms – Time-varying variables.

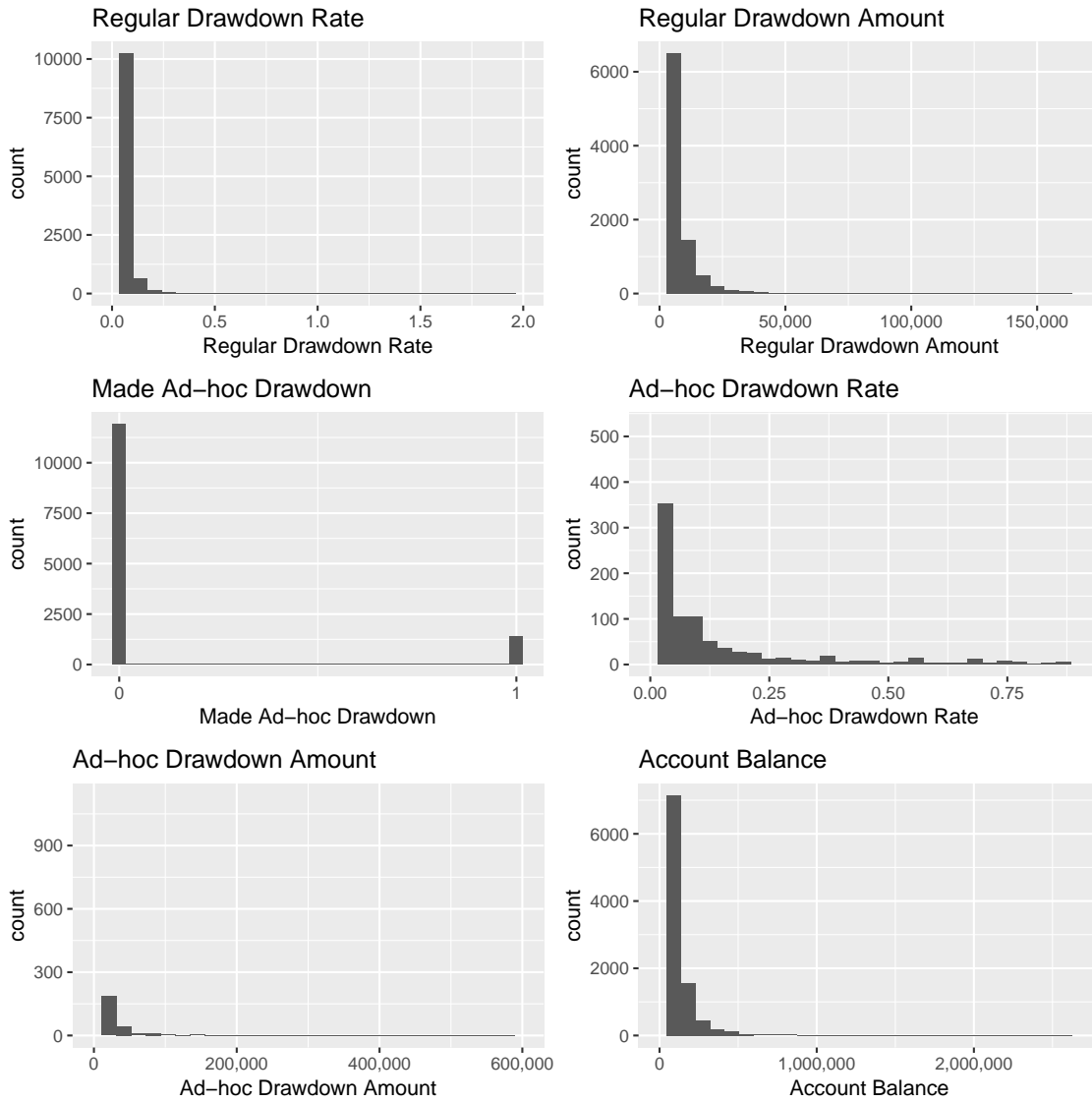


Figure 37: Group 6 histograms – Time-varying variables.

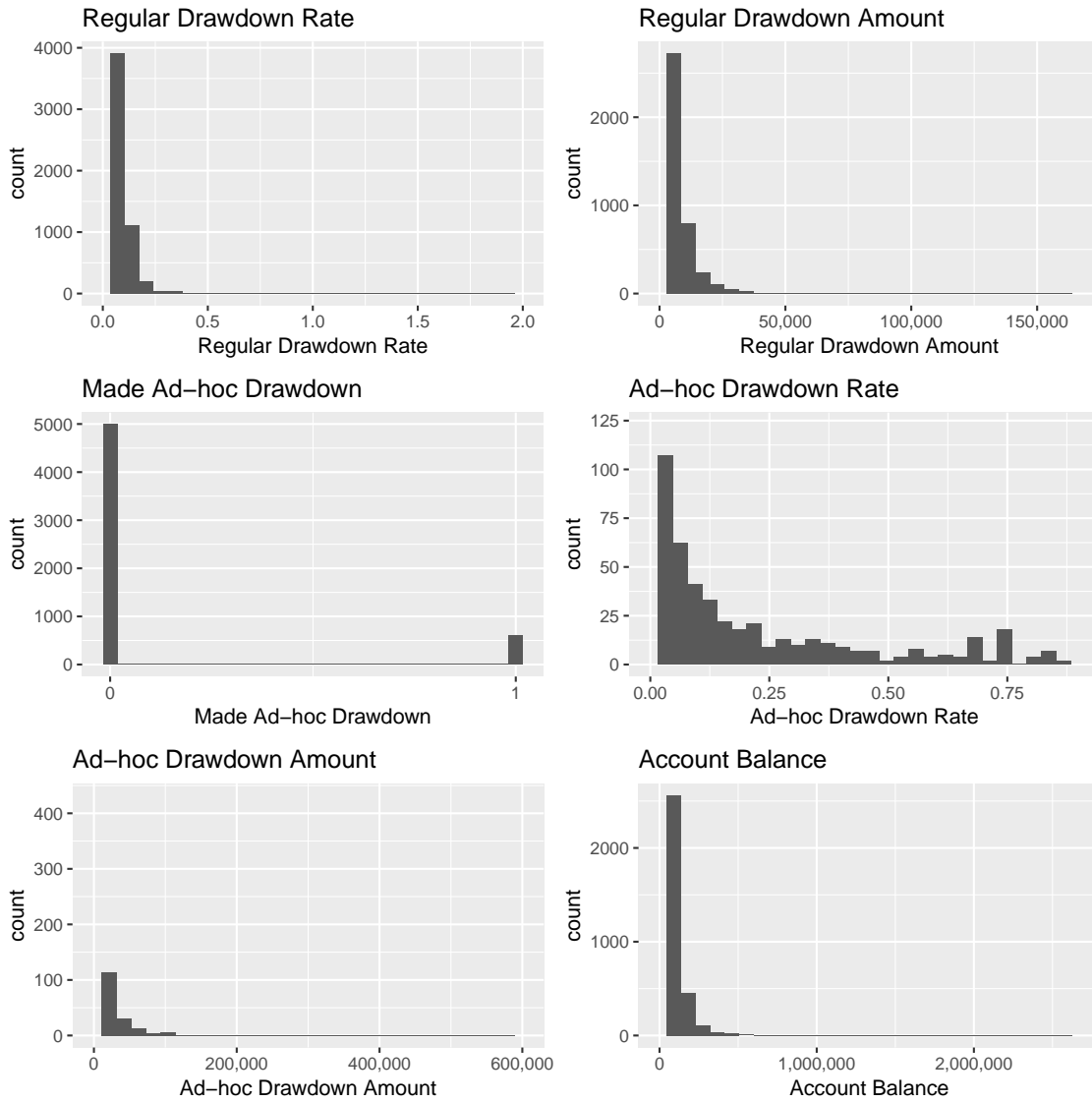


Figure 38: Group 7 histograms – Time-varying variables.

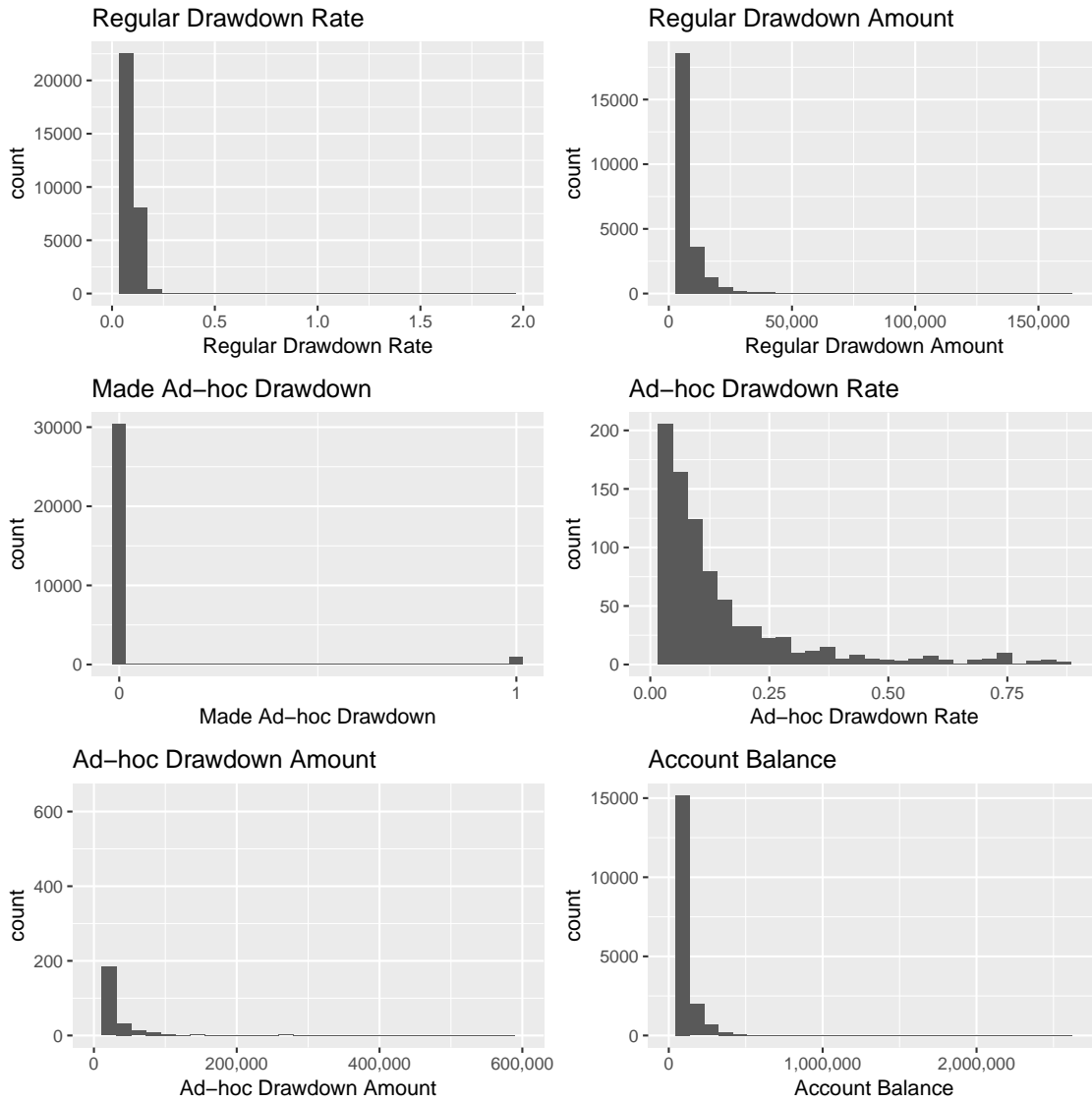


Figure 39: $G = 7$ model – Group 1 time-demeaned (TD) panel plots. Account balances as at financial year start. The black series in the bottom-right panel represents estimated time-demeaned group time profile values.

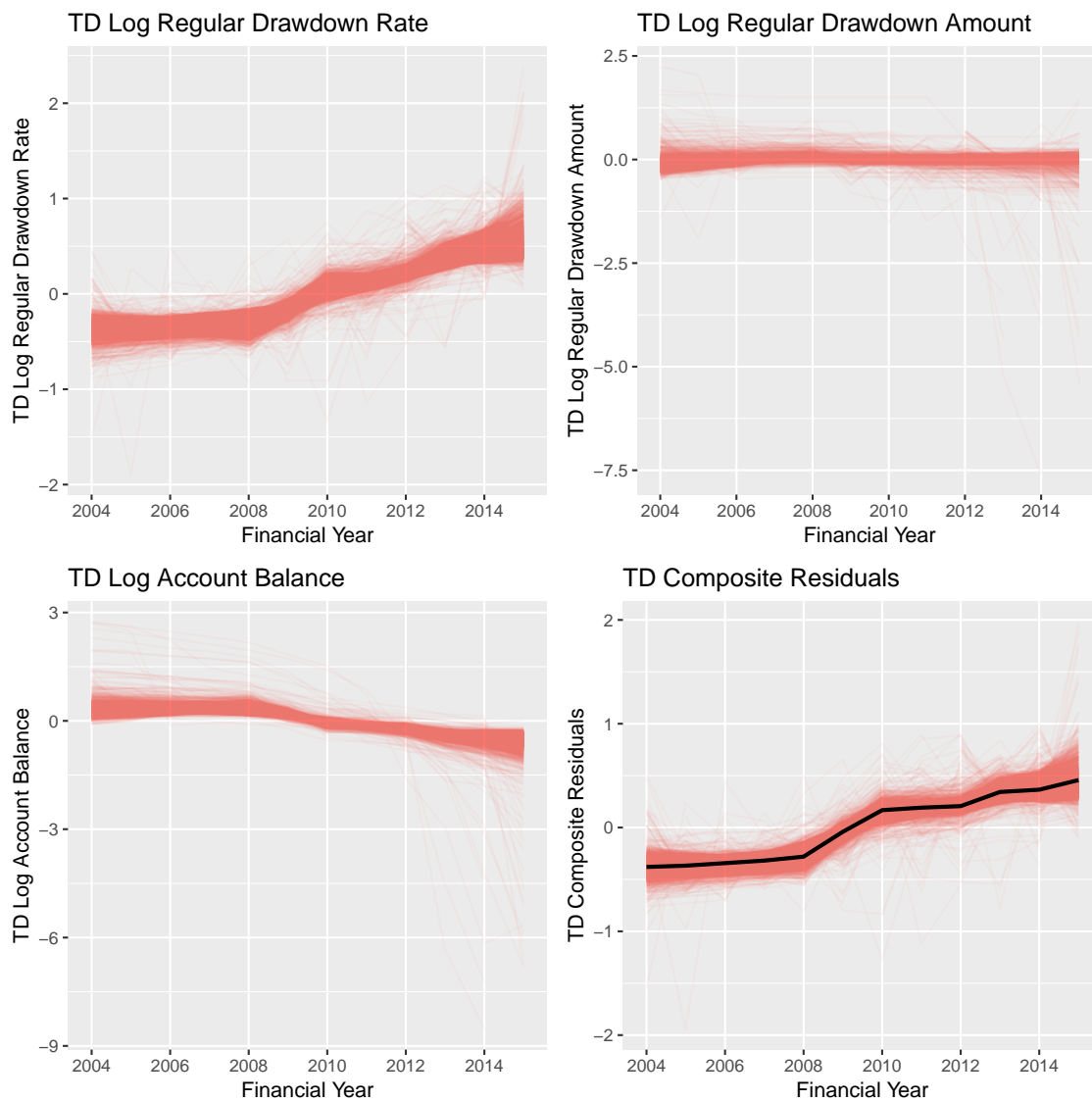


Figure 40: $G = 7$ model – Group 2 time-demeaned (TD) panel plots. Account balances as at financial year start. The black series in the bottom-right panel represents estimated time-demeaned group time profile values.

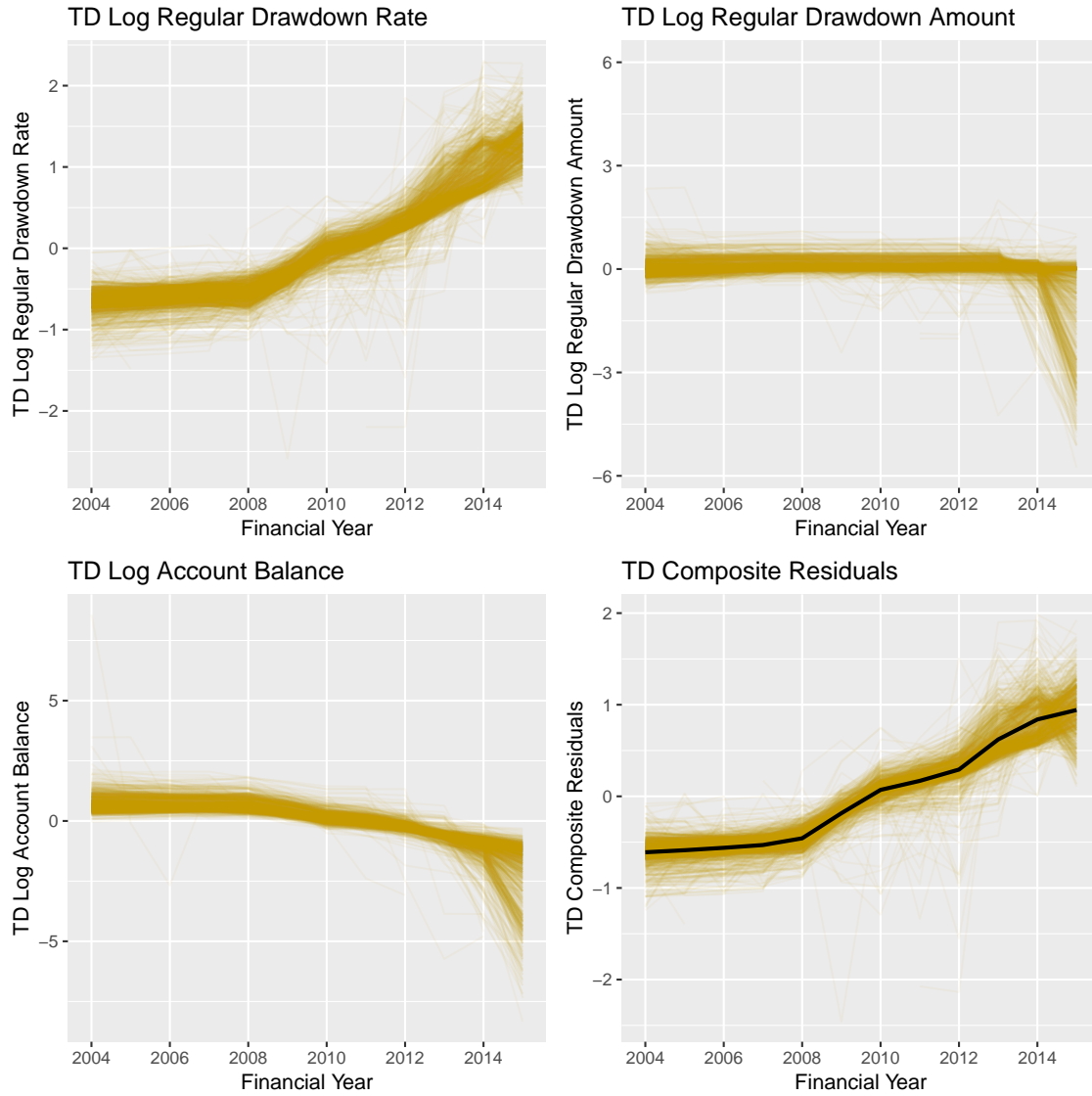


Figure 41: $G = 7$ model – Group 3 time-demeaned (TD) panel plots. Account balances as at financial year start. The black series in the bottom-right panel represents estimated time-demeaned group time profile values.

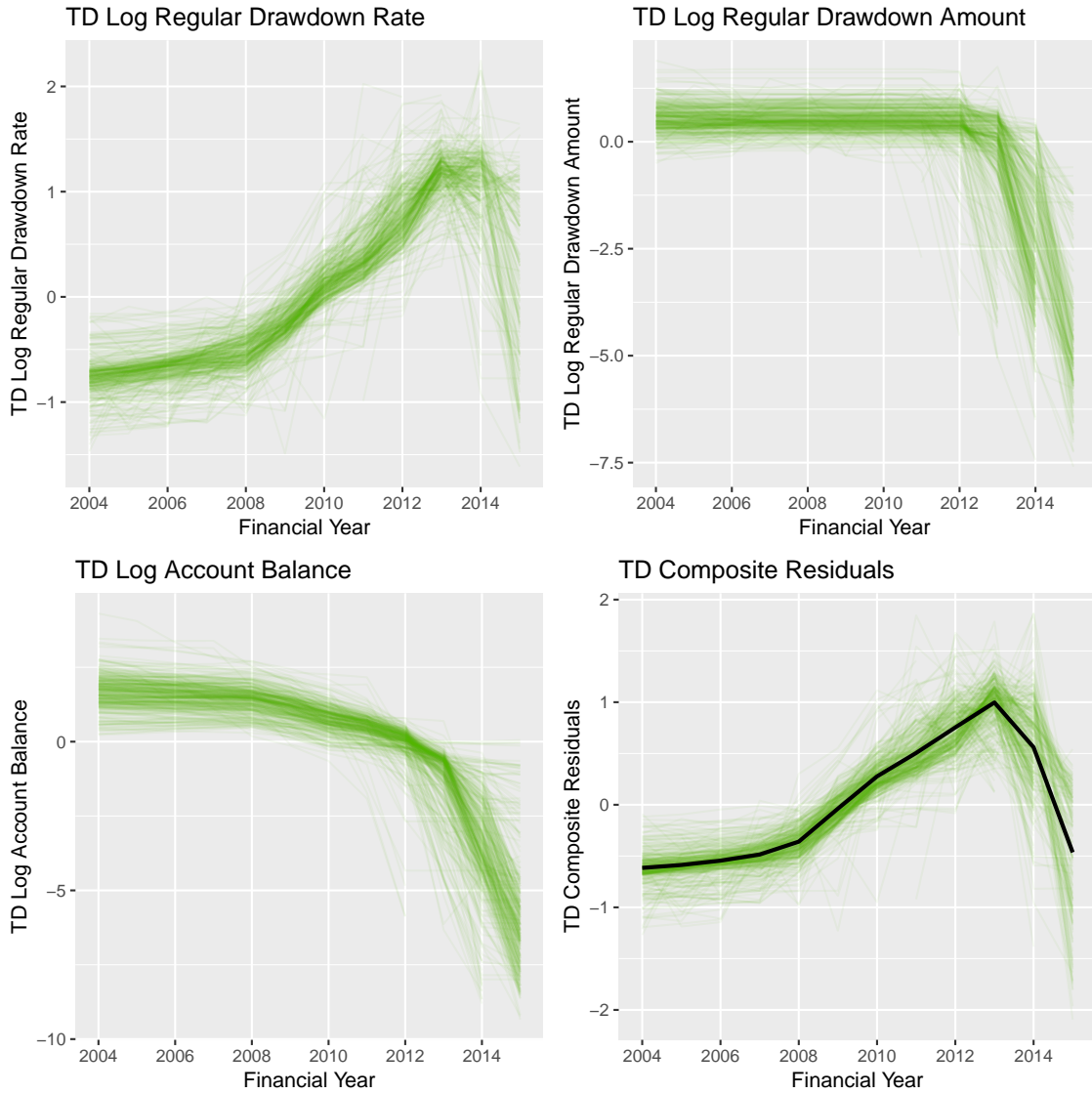


Figure 42: $G = 7$ model – Group 4 time-demeaned (TD) panel plots. Account balances as at financial year start. The black series in the bottom-right panel represents estimated time-demeaned group time profile values.

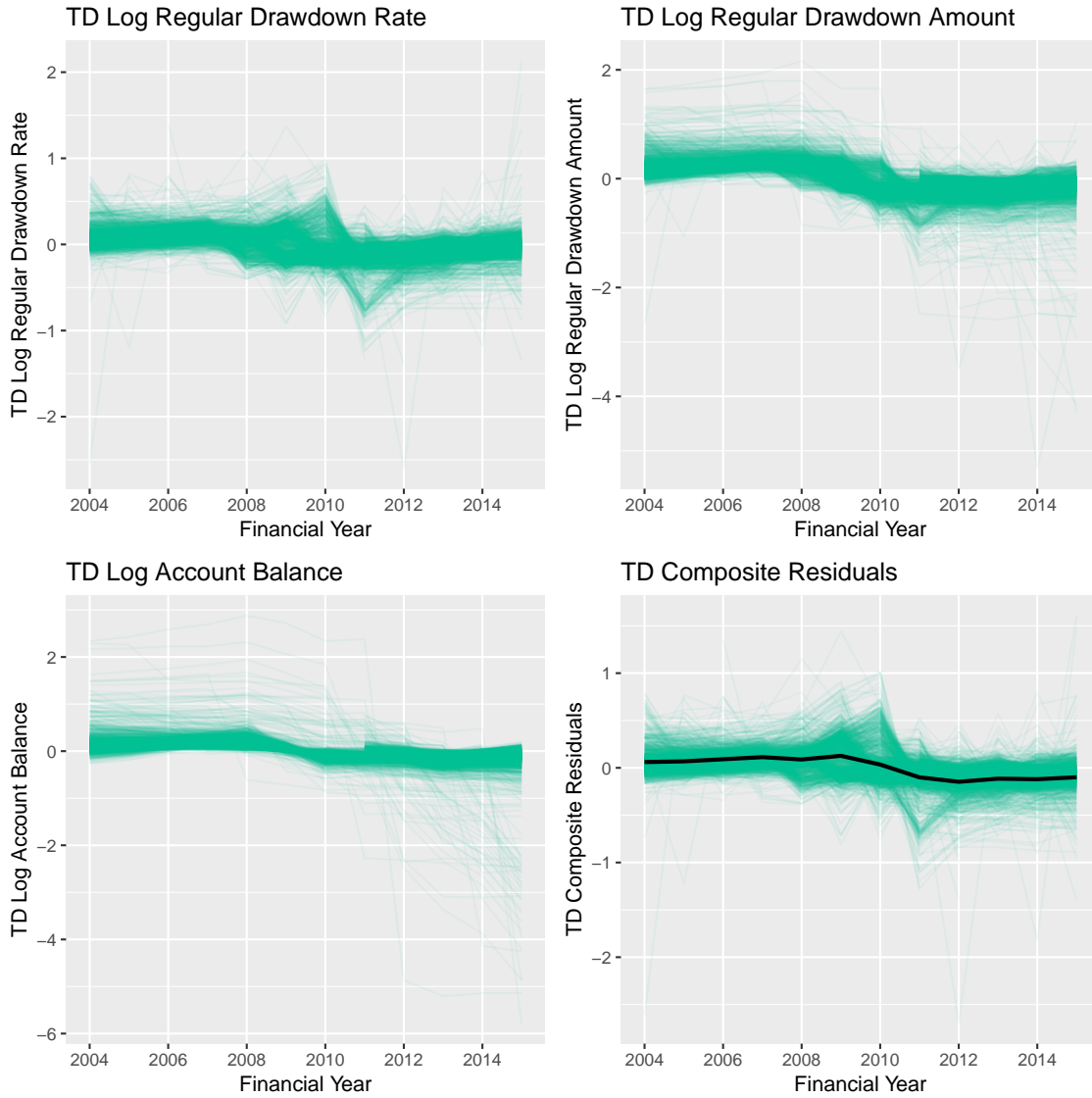


Figure 43: $G = 7$ model – Group 5 time-demeaned (TD) panel plots. Account balances as at financial year start. The black series in the bottom-right panel represents estimated time-demeaned group time profile values.

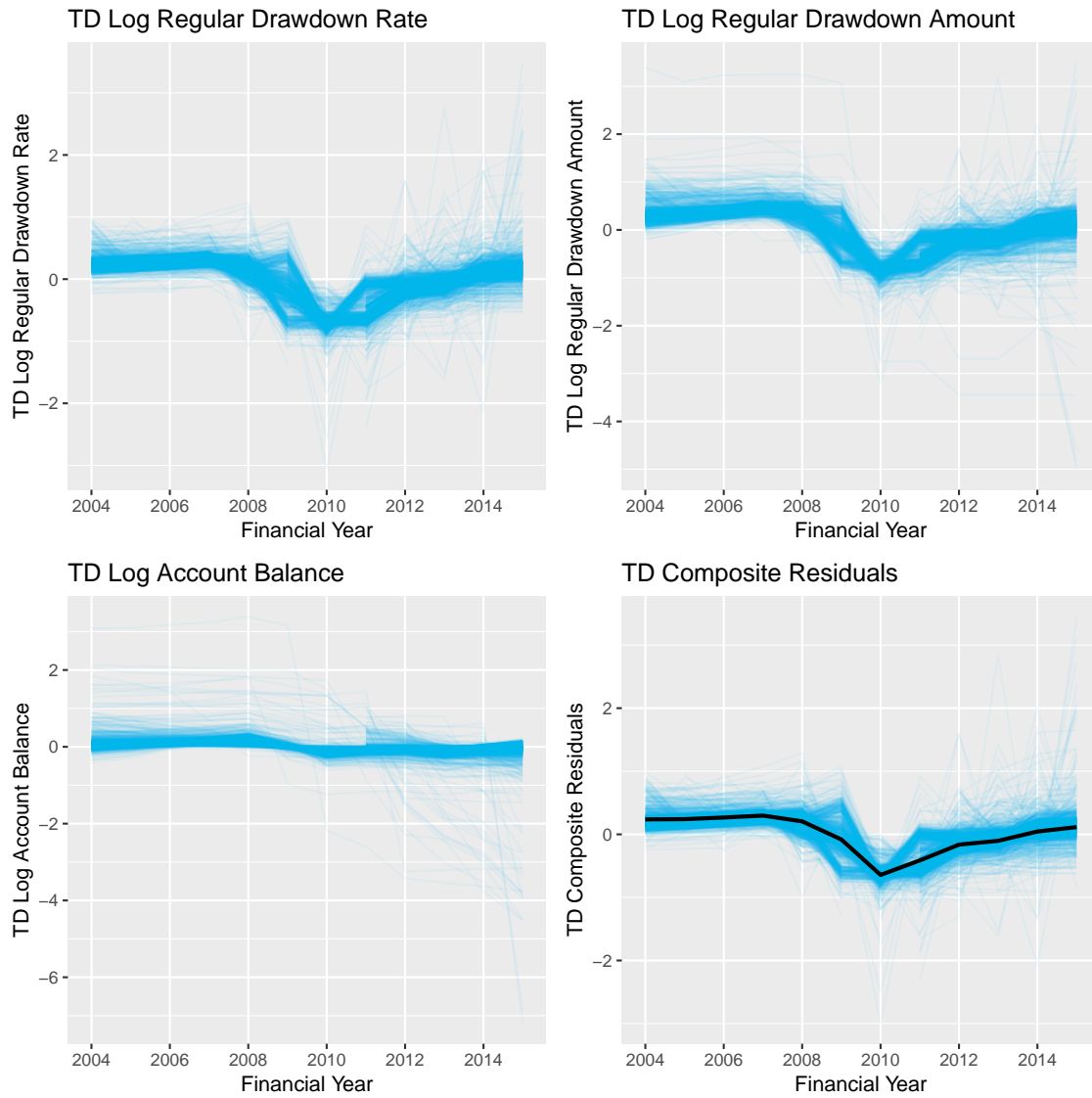


Figure 44: $G = 7$ model – Group 6 time-demeaned (TD) panel plots. Account balances as at financial year start. The black series in the bottom-right panel represents estimated time-demeaned group time profile values.

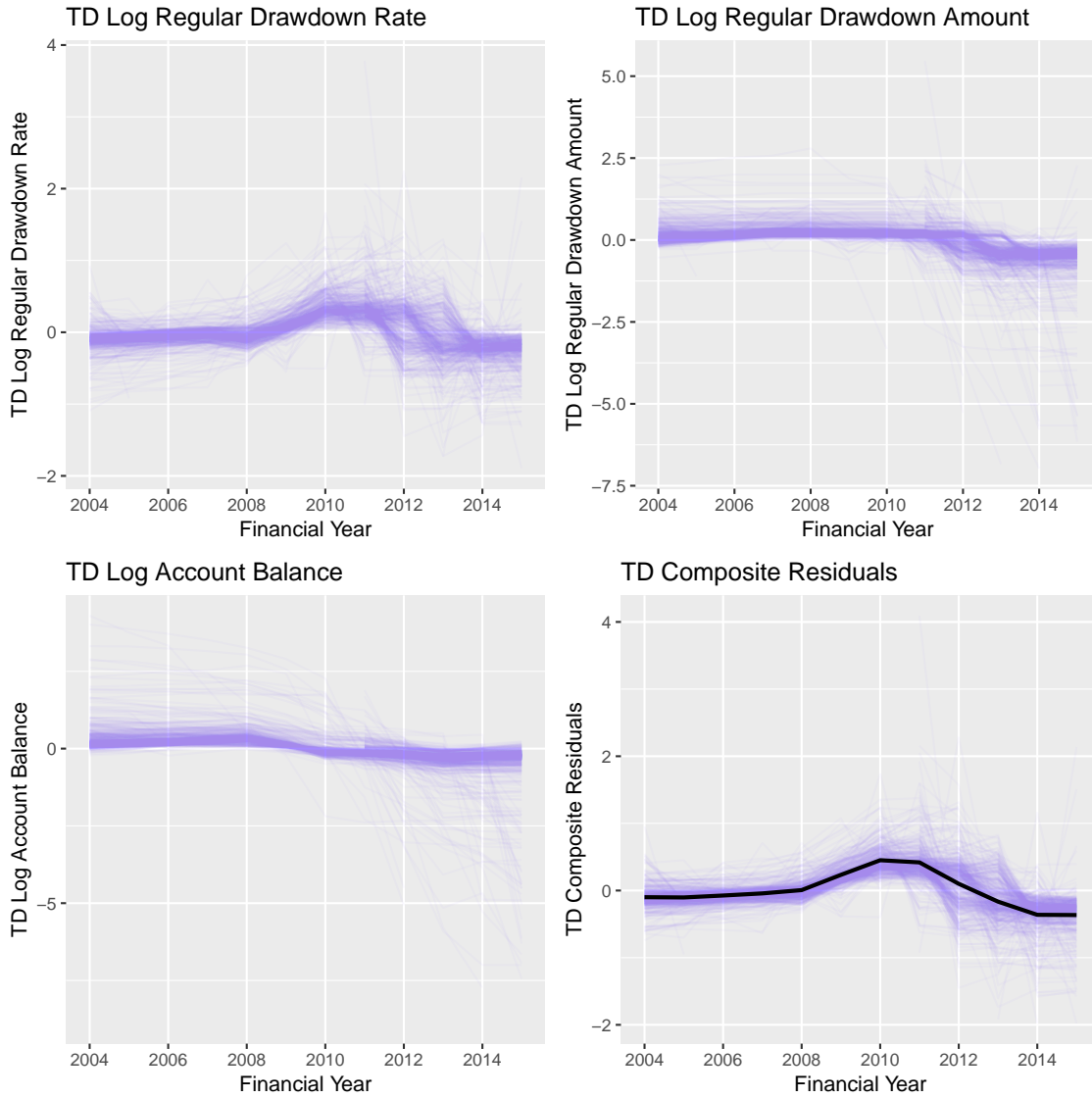
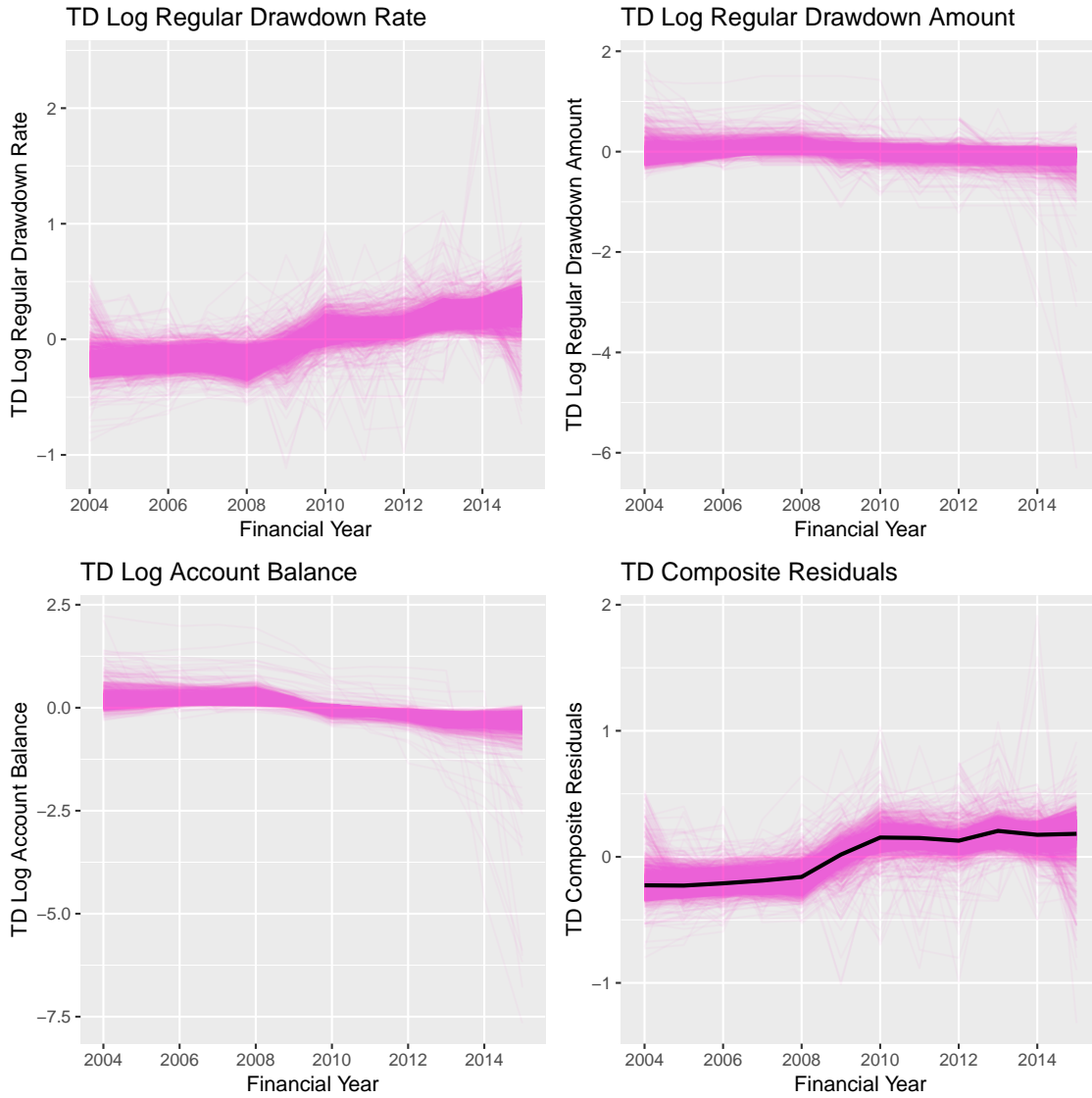


Figure 45: $G = 7$ model – Group 7 time-demeaned (TD) panel plots. Account balances as at financial year start. The black series in the bottom-right panel represents estimated time-demeaned group time profile values.



References

- Bonhomme, S., & Manresa, E. (2015). Grouped patterns of heterogeneity in panel data. *Econometrica*, *83*, 1147–1184. doi: 10.3982/ECTA11319
- Suits, D. B. (1984). Dummy variables: Mechanics v. interpretation. *The Review of Economics and Statistics*, *66*, 177–180. doi: 10.2307/1924713